ORNL/TM-2017/480

Mercury Remediation Technology Development for Lower East Fork Poplar Creek—2017 Progress Report

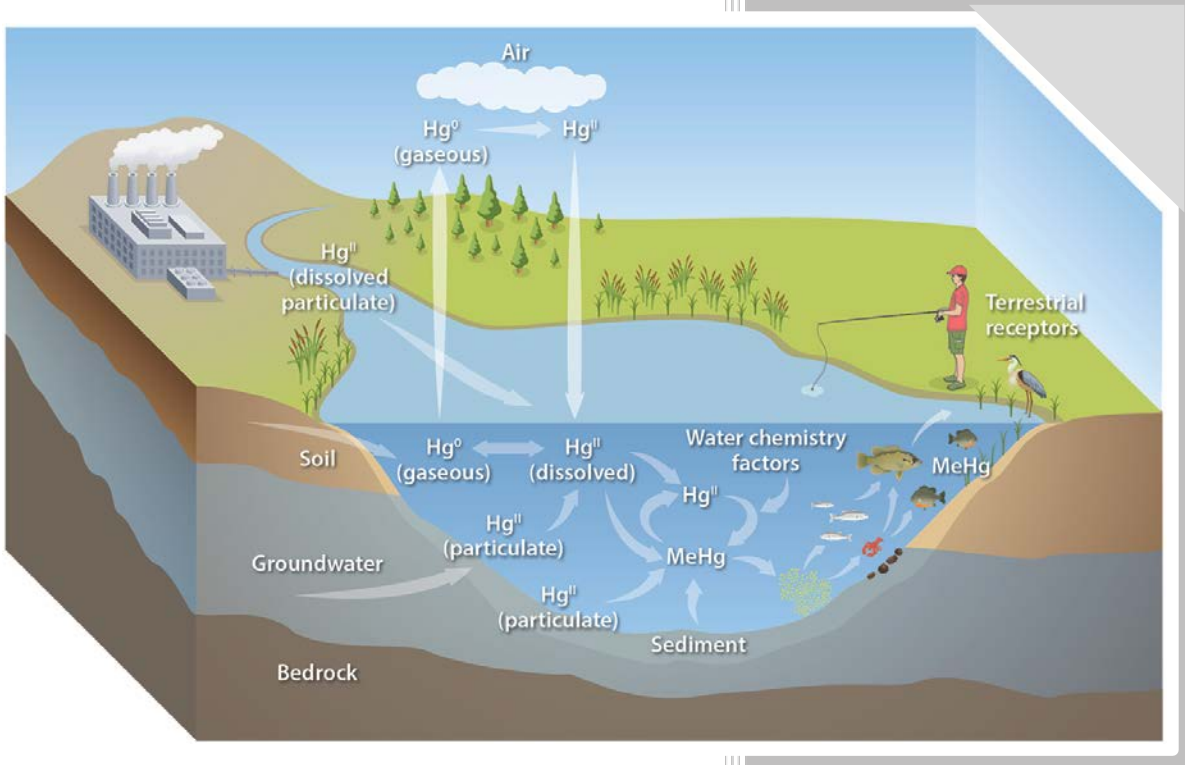

July 2018

Approved for public release.
Distribution is unlimited.

OAK RIDGE NATIONAL LABORATORY
MANAGED BY UT-BATTELLE FOR THE US DEPARTMENT OF ENERGY

ORNL/TM-2017/480

Environmental Sciences Division

MERCURY REMEDIATION TECHNOLOGY DEVELOPMENT FOR LOWER EAST FORK POPLAR CREEK — 2017 PROGRESS REPORT

Project Lead
Mark J. Peterson

Task 1—Soil and Groundwater Source Control
Melanie Mayes *(Task Lead)*
Alex Johs
Leroy Goñez Rodriguez
Christopher DeRolph
Eric Pierce

Task 2—Surface Water and Sediment Manipulation
Scott Brooks *(Task Lead)*
David Watson
Katherine Muller
Todd Olsen
Kenneth Lowe

Task 3—Ecological Manipulation
Teresa Mathews *(Task Lead)*
Ryan McManamay
John Smith
Jesse Morris
Michael Jones

Date Published: July 2018

Prepared for
URS | CH2M Oak Ridge, LLC (UCOR)
Oak Ridge, TN 37831

Prepared by
OAK RIDGE NATIONAL LABORATORY
Oak Ridge, TN 37831-6283
managed by
UT-BATTELLE, LLC
for the
US DEPARTMENT OF ENERGY
under contract DE-AC05-00OR22725

CONTENTS

LIST OF FIGURES

LIST OF TABLES

ACRONYMS AND ABBREVIATIONS

ACW	artificial creek water
AEL	Aquatic Ecology Laboratory
AFRI	Applied Field Research Initiative
BGS	below ground surface
BMAP	Biological Monitoring and Abatement Program
BrCl	bromine chloride
$CaBr_2$	calcium bromide
$CaCl_2$	calcium chloride
Chloramine T	N-chloro-*p*-toluenesulfonamide
COP	canola oil polysulfide
D	downstream
DFBA	difluorobenzoic acid
DI	deionized
DO	dissolved oxygen
DOC	dissolved organic carbon
DOE	US Department of Energy
EDX	energy dispersive x-ray
EFK	East Fork Poplar Creek kilometer
EFPC	East Fork Poplar Creek
EM	Environmental Management
EPA	US Environmental Protection Agency
FY	fiscal year
HCl	hydrogen chloride
Hg	mercury
Hg(II)	mercury cation
$HgCl_2$	mercuric chloride
HgD	dissolved mercury
Hg-NOM	mercury–natural organic matter
HgS	mercuric sulfide
HgT	total mercury
HRD	historical release deposit
I	inland
K_d	sorbent:water partition coefficient
LEFPC	lower East Fork Poplar Creek
MeHg	methylmercury
MeHgD	dissolved methylmercury
MeHgT	total methylmercury
MMHg	monomethylmercury
MSIPP	Minority Serving Institutions Partnership Program
NOM	natural organic matter
OF	outfall
ORNL	Oak Ridge National Laboratory
ORWTF	Oak Ridge Wastewater Treatment Facility
PCOP	porous canola oil polysulfide
Phenol red	phenolsulfonphthalein
RPCOP	reduced porous canola oil polysulfide
RSI	Restoration Services Inc.
S	stream

SEM	scanning electron microscopy
SGD	somatic growth dilution
$SnCl_2$	stannous chloride
SR-NOM	Suwannee River aquatic natural organic matter
SUVA	specific ultraviolet absorbance
TD	technology development
TRL	technology readiness level
TSS	total suspended solids
U	upstream
UCOR	URS | CHM2 Oak Ridge LLC
UEFPC	upper East Fork Poplar Creek
UV	ultraviolet
UV-Vis	ultraviolet–visible spectroscopy
WEMA	West End Mercury Area
Y-12	Y-12 National Security Complex

1. INTRODUCTION

Mercury (Hg) remediation is a high priority for the US Department of Energy (DOE) Oak Ridge Office of Environmental Management, especially at and near the Y-12 National Security Complex (Y-12) where historical Hg use has resulted in contaminated buildings, soils, and downstream surface waters. To address Hg contamination of East Fork Poplar Creek (EFPC), DOE has adopted a phased, adaptive management approach to remediation, which includes Hg treatment actions at Y-12 in the short-term and research and technology development (TD) to evaluate longer-term solutions in the downstream environment (US Department of Energy 2014).

The current Hg TD priorities in Oak Ridge were developed as part of significant strategic planning efforts beginning in 2014. The initial strategic planning efforts involved multiple meetings and workshops engaging DOE management, site contractors, scientists and engineers, and local stakeholders such as the US Environmental Protection Agency (EPA), Tennessee Department of Environment and Conservation, and Site Specific Advisory Board. An outcome of the strategic planning efforts was the two foundational DOE documents *Strategic Plan for Mercury Remediation* and *Mercury Technology Development Plan*. From the beginning, an adaptive management approach to TD activities was adopted such that plans could change as new knowledge became available. Therefore, in FY 2017 both documents were in the process of being revised and updated. Five important planning reports were issued over the 2014–2017 period that provide the basis for the long-term remediation strategy in Oak Ridge and the TD activities described herein:

1. *Strategic Plan for Mercury Remediation at the Y-12 National Security Complex, Oak Ridge, Tennessee* (2014, DOE/OR/01-2605&D2; 2017 draft revision in progress). Provides the overall remediation roadmap for Hg remediation at Y-12.

2. *Mercury Technology Development Plan for Remediation of the Y-12 Plant and East Fork Poplar Creek* (2014, DOE/ORO-2489; 2017 draft revision in progress). Highlights the priorities for Hg TD in Oak Ridge.

3. *Mercury Remediation Technology Development for Lower East Fork Poplar Creek* (2015; ORNL/SPR-2014/645). Provides the overall strategy for Hg TD activities in lower EFPC (LEFPC).

4. *Technology Plan to Address the EM Mercury Challenge*. DOE headquarters 2016 report that summarizes the overall approach to the DOE Environmental Management (EM) Hg challenge at Oak Ridge and Savannah River.

5. *Mercury Remediation Technology Development for Lower East Fork Poplar Creek—FY 2016 Progress Report* (ORNL/TM-2016/494). Provides Hg TD progress for 2016 and 2017 plans for LEFPC.

This report provides the most recent findings from the LEFPC research and TD activities that support in part the Hg TD plan, with a focus on FY 2017 activities. The goal of LEFPC TD is to develop strategies and technologies that could lead to new options for Hg remediation in LEFPC.

LEFPC research and TD activities to date have emphasized understanding Hg transport and fate processes in the EFPC system as an important precursor to the development of targeted remedial technologies. This approach and prioritization are consistent with the adaptive management paradigm and DOE technology readiness level (TRL) guidelines. A major emphasis of TD studies in 2017 was on field characterization and obtaining a watershed-scale understanding. Task 1, Soil and Groundwater Source Control, focuses on

addressing downstream Hg sources to the creek (especially floodplain and bank soils) and groundwater. Task 2, Surface Water and Sediment Manipulation, centers on potential manipulation of instream processes, including the many water and sediment chemistry factors that affect Hg methylation. Task 3, Ecological Manipulation, investigates methods to manipulate the food chain at both lower and higher levels of organization to decrease Hg concentrations in fish. Together, the three study tasks focus on manipulating the key factors that affect Hg concentrations in fish: the amount of inorganic Hg available to the ecosystem, conversion of inorganic Hg to methylmercury (MeHg), and bioaccumulation of MeHg through the food web.

2. TASK 1: SOIL AND GROUNDWATER SOURCE CONTROL

2.1 OVERVIEW

Legacy Hg contamination in creek bank soils accounts for most of the annual export of Hg from the EFPC watershed. Approximately 85% of the Hg inventory is associated with floodplain soils contained in the 18 km reach of LEFPC immediately downstream of Y-12 (Southworth et al. 2013). Soil particles enriched in legacy Hg eroding from the creek bank contribute to concentrations in the water column and sediments and provide a source for instream production of MeHg.

Until recently, however, the bank soils were never systematically characterized for total Hg and MeHg concentrations or their spatial variability. Considerable progress was made in FY 2014–16, with four major field campaigns for determination of Hg, MeHg, and bulk soil characteristics. Frequent but spatially variable outcroppings of a dark-colored historical release deposit (HRD) were identified in the 6 km immediately downstream of Y-12, and it became clear that the HRD was much more widespread than previously believed. The HRD is now known to constitute the majority of high Hg and MeHg observations in all creek bank soils, and it is concentrated around the National Oceanic and Atmospheric Administration facility and the former Bruner's Market between Adams Road and Louisiana Avenue. However, the role of erosion is not yet effectively incorporated into the team's findings. Gaps remain in understanding how Hg in creek bank soil makes its way into EFPC waters, as well as what happens to that Hg once it is liberated from the creek banks.

A variety of laboratory-scale batch tests confirmed that less than 0.025% of the total Hg in the solid phase was released from the HRD soils. Although 0.025% seems low, the concentrations observed in lab-scale batch experiments are up to 12,000 ng Hg/L. In partnership with the Applied Field Research Initiative Program (AFRI), scanning electron microscopy with energy dispersive x-rays conclusively identified the form of Hg in the HRD soils as very small aggregates of Hg sulfide. It is now suspected that the mechanism for release is dissolution, and enough data now likely exist to enable predictions of Hg speciation in water over the next year. Sequential extractions confirmed that >80% of the Hg in the HRD and all creek bank soils are resistant to release. Although this is encouraging, the liberated concentrations from lab-scale experiments are still several orders of magnitude higher than concentrations found in EFPC.

Therefore, new studies involving columns packed with the HRD soils were designed to determine the rate and extent of Hg release. Early results suggest that the extent of re-adsorption inside the columns might be significant because eluted Hg concentrations are an order of magnitude lower than those observed in the batch tests. However, it appears that Hg is still persistently released. Various hydrological tests were performed in the columns, and researchers suspect that the hydraulic conditions of soil aggregates do not limit the release of Hg. However, when the aggregates are broken, around 32% more Hg is released from the soils. Future work will focus on the extent of Hg release and will be coupled with downstream columns consisting of engineered sorbents to test the extent and rate of removal by the sorbents. The batch and column efforts have yet to include MeHg, but MeHg will be a target analyte in the FY 2018 column experiments.

Sorbent technologies are considered as a means to limit the release of mobile Hg species from creek banks, floodplain soils, and sediments in EFPC. Laboratory-scale batch experiments conducted in previous years focused primarily on the characterization of potential sorbent materials and the role of Hg speciation. In collaboration with Flinders University, Australia, researchers studied how Hg complexation with natural organic matter (NOM) affects the performance of the novel sorbent canola oil polysulfide (COP). In FY 2017, researchers began to transition from batch experiments to column experiments to evaluate parameters that will inform future remediation engineering efforts. This first set of column

experiments aimed to determine hydraulic properties and physical characteristics of engineered sorbent materials. Preliminary data from experiments with EFPC water suggests a role for Hg associated with fine particulates. A key focus in FY 2018 will be to evaluate removal efficiencies under field-relevant conditions.

The groundwater work has now resulted in a solid 1.5 years of mostly continuous water table elevation, temperature, and conductivity data in the three groundwater wells and one stream water well at each of the three locations along EFPC. There are 11 manual sampling events for MeHg, Hg, pH, iron and sulfur redox couples, dissolved organic carbon (DOC), anions, and cations. As expected, the stream water data show that the Hg concentrations in surface water decrease as a function of stream length, whereas the MeHg concentrations increase. Both Hg and MeHg continue to be the highest in groundwater at East Fork Poplar Creek kilometer (EFK) 18.7 (the former Bruner's Market location) where the HRD is prominently exposed. Most groundwater samples from all locations show evidence of low redox conditions (i.e., reduced iron and sulfide). Low redox conditions would be required for methylation of Hg to occur in groundwater, but researchers do not have direct evidence of methylation in groundwater. However, MeHg concentrations are consistently higher in groundwater than in surface water, which suggests groundwater MeHg production is possible. There is significant seasonal variation, with Hg in groundwater varying approximately twofold, whereas MeHg varies three- to fourfold. Overall, the results in FY 2017 were similar to those in FY 2016. The vadose zone monitoring of the HRD layer at EFK 18.7 was enhanced beyond monitoring the moisture of the creek bank. Two additional sites in the floodplain were established to monitor for temperature, moisture content, and oxygen content. All sites have instrumentation installed above, within, and below the HRD. Results continue to show that the HRD layer remains wet for long periods, but early results of oxygen content show significant oxygen levels in the HRD. Future groundwater monitoring is likely to be limited with the focus of future investigations on better understanding of the HRD and its links with bank soil leaching and erosion processes, especially in the Bruner's Market area.

In the coming year, conceptual and quantitative understanding will be forthcoming about the role of the HRD on vadose zone and groundwater Hg and MeHg concentrations and the potential for release from the solid phase. Efforts will shift to compiling information into conceptual models and finding links among soils, sediments, groundwater, and biota. The testing of strategies for removal of Hg and MeHg in waters using sorbents will move into the forefront.

2.2 CREEK BANK SOILS

2.2.1 Field-Scale Investigations of Creek Bank Soils

In FY 2017 the focus of this subtask was to evaluate and interpret the results of previous sampling activities of creek bank soils and stream bank sediments from FY 2014 to 2016. The HRD constitutes by far the highest concentrations in the entire system (Figure 2-1). There are 778 analyses of Hg in stream bank soils, with a mean of 126 mg Hg/kg soil (mg/kg hereafter), median of 18 mg/kg, minimum of 0.03 mg/kg, and maximum of 4,690 mg/kg (Figure 2-2a). There are 252 analyses of MeHg in stream bank soils, with a mean of 5 ng Hg/g soil (ng/g hereafter), median of 3 ng/g, minimum of 0.01 ng/g, and a maximum of 60 ng/g (Figure 2-2b). Both datasets include results from Southworth et al. (2013). The combined Hg and MeHg datasets provide an unprecedented understanding of the distribution of Hg and MeHg in the stream bank soils of EFPC downstream of Y-12.

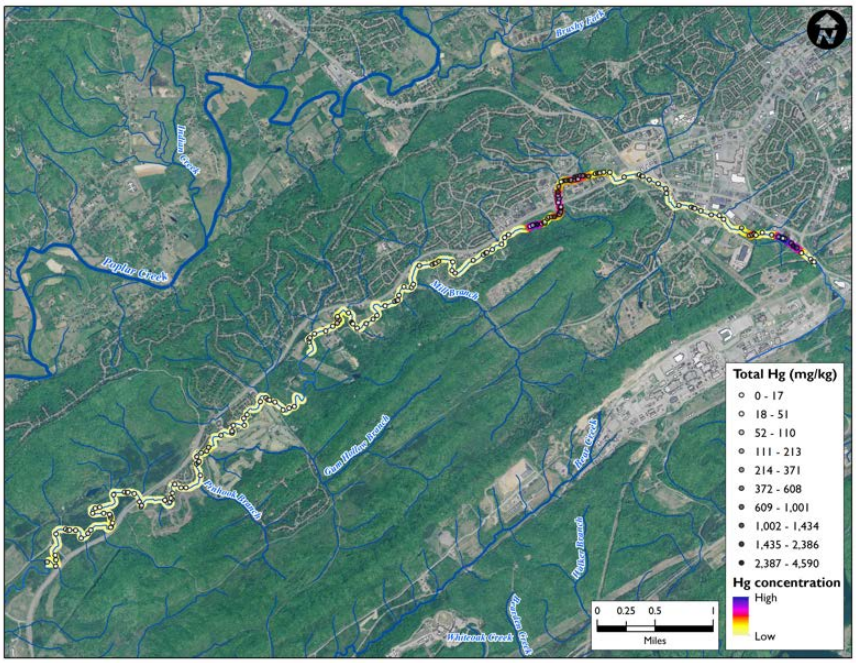

Figure 2-1. Spatial distribution of the concentrations of total Hg in EFPC stream bank soils.

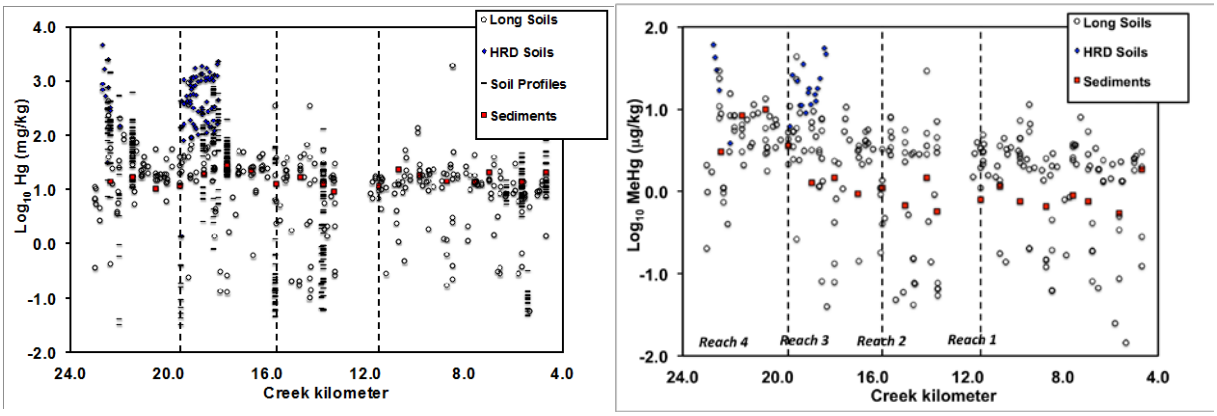

Figure 2-2. Spatial distribution of (a) total Hg and (b) MeHg concentrations (log_{10}) in stream bank soils and bulk streambed sediments. Different sampling activities are represented—longitudinal soil samplings in 2014 and 2015 (Long), HRD soil sampling, vertical and horizontal soil profiles (data from creek kilometers 22.4, 21.5, 17.6, 13.7, 5.6, and 4.7 from Southworth et al. 2013), and streambed sediment sampling.

Oak Ridge National Laboratory (ORNL) has informally sectioned EFPC into four subwatersheds and has identified four stream "reaches" associated with each subwatershed. Reach 4 starts at Station 17 at Y-12 and represents the most upstream location, whereas Reach 1 represents the most downstream location (Table 2-1). Reaches 4 and 3 encompass the HRD zones and had significantly higher Hg concentration (n = 240, p = 2.5E-11) in comparison with Reaches 2 and 1. For example, the interquartile range (i.e., the 25th to 75th percentile) of the HRD sampling activity (n = 86) was 185 and 1,037 mg/kg, respectively, with a median and maximum of 429 and 4,590 mg/kg. The interquartile range of Hg from both longitudinal stream bank soil surveys (n = 281) was 7.67 and 24.92 mg/kg, respectively, with a median and maximum of 15.52 and 941 mg/kg. Therefore, the HRD soils have one to two orders of magnitude higher Hg concentrations than the rest of the creek bank soils. They seem to outcrop in an area around 2 km in length, and the thickness of the layer is 18 inches at its greatest. The HRD is therefore confined to

Reaches 4 and 3, and these reaches can be considered the most important diffuse source of Hg loading to the stream (Figure 2-2a). The relatively low Hg concentrations from EFK 22 to 20 are linked to highly disturbed soils associated with urbanization, concrete-lined channels, and riprap-enclosed stream banks in the main commercial development zone of the city of Oak Ridge. Outside of Reaches 4 and 3, Hg concentration was relatively uniform.

Table 2-1. LEFPC reach designations

Reach	Start (EFPC km)	End (EFPC km)
1	0.0	11.45
2	11.46	15.60
3	15.61	19.54
4	19.55	23.40[a]

[a]This is Station 17—the point at which the creek exits the boundary of Y-12 and represents the farthest upstream point at which samples can be collected without additional access requirements. Station 17 also represents the boundary between upper and lower EFPC.

As described in Section 3.0, the Hg concentrations in the bulk streambed sediments (n = 19) averaged 16.1 mg/kg with a minimum and maximum of 9.1 and 27.3 mg/kg, respectively (Figure 2-2a) (Brooks et al. 2017). When compared with Hg concentrations in the much more variable stream bank soils, Hg concentrations in the streambed sediment samples are consistent with each other. The ratio between Hg in stream bank soils and stream sediments decreased from 16 to 0.3 in the upper 9 km of EFPC. The concentrations of Hg in stream bank soils and streambed sediments are similar to each other in downstream Reaches 2 and 1.

MeHg in the HRD soil samples was approximately five times greater ($p << 0.05$) than MeHg concentrations from the longitudinal survey (Figure 2-2b). The influence of higher MeHg concentrations in the HRD areas is apparent in Reaches 4 and 3 compared with Reaches 2 and 1. The concentration of MeHg in bulk stream sediments ranged from 0.55 to 10 ng/g with a mean of 2.11 ng/g and a median of 1.10 μg/kg (Figure 2-2b), as described in Section 3.0 (Brooks et al. 2017). Similar to the Hg results, soil MeHg concentrations in Reaches 4 and 3 are much higher than those in the streambed sediments, whereas streambed and soil MeHg concentrations are similar in Reaches 2 and 1.

In summary, the HRD clearly has an important influence on overall creek bank soil Hg and MeHg concentrations in the upper reaches of EFPC. Therefore, the study has accomplished a major goal of identifying locations containing the highest Hg and MeHg concentrations for potential future remedial activities. The next phase of this work involves understanding factors influencing the mobility of Hg from the creek bank soils and the HRD (e.g., dissolution and erosion).

2.2.2 Release of Mercury from Historical Release Deposit and Creek Bank Soils in Batch Experiments

The release of Hg from the HRD and the creek bank soils in lab-scale experiments can indicate the potential for mobility of Hg into EFPC waters from eroding bank soils. Over the past three years, researchers have conducted batch experiments involving four creek bank and seven HRD soils and four different reactant solutions. Initially, researchers observed high variability resulting from the use of bulk soils, whereas later experiments successfully reduced variability by separating the different size fractions into the following fractions: <0.053, 0.053–0.125, 0.125–1.00, 1.00–2.36, and >2.36 mm. All experiments were performed at an optimized ratio of 1 g soil to 30 mL solution and an optimized reaction time of 6 h.

As described in the FY 2015 and FY 2016 reports (Peterson et al. 2016; Peterson et al. 2017), the bank soils released 0.003% to 0.015% of the original Hg concentrations, whereas the HRD soils released 0.003% to 0.025% (Figure 2-3).

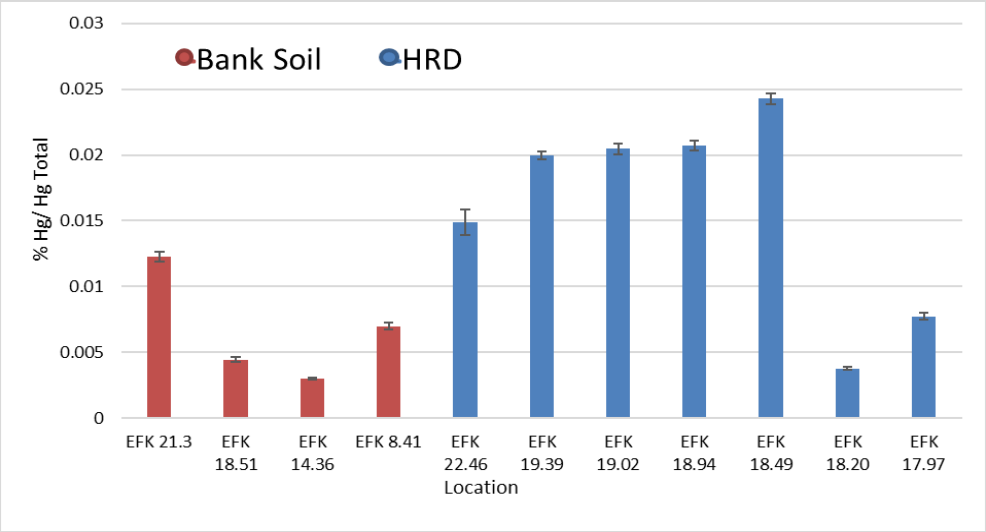

Figure 2-3. The extent of Hg release from creek bank and HRD soils, as a function of initial concentration of Hg in the soils. (Note: EFK = East Fork Poplar Creek kilometer.)

Batch experiments in FY 2017 focused more on determining release mechanisms (e.g., desorption or dissolution) or a combination of the two processes. Specifically, the kinetics of Hg release, and the effect of solid:solution ratio, were investigated, using all 11 soils from Figure 2-3 (only selected results are shown in the figure).

In the kinetic experiments, the HRD released much higher concentrations of Hg compared with the bank soils, which is expected. The release of Hg was rapid, sometimes reaching a maximum concentration in the first hour (Figure 2-4). In general, changes as a function of time were minimal for both HRD and creek bank soils. Mercury concentrations tended to remain flat or to have either small increases or decreases over periods as long as 500 h. The observed variability between the sample points is most likely due to small differences in Hg concentrations between the samples, although specific Hg measurements were not taken on each sample. Solutions from each reacted soil sample were analyzed for Hg, pH, anions, cations, DOC, and specific absorbance at 254 nm (specific ultraviolet-absorbance, or SUVA) (not shown in the figure). In FY 2018, the results will be tested with a geochemical model to predict solution-phase Hg speciation.

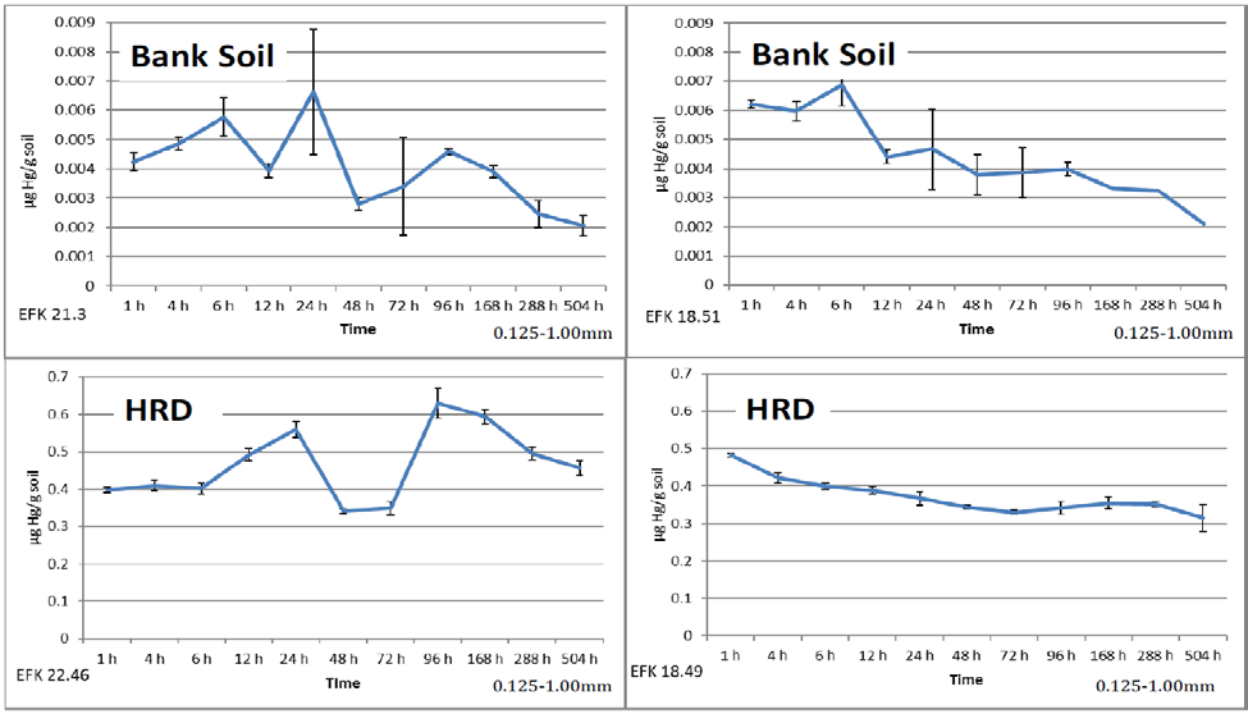

Figure 2-4. The rate of Hg release from the 0.125 to 1.00 mm size fraction of creek bank and HRD soils.

Additional experiments also involved varying the solid:solution ratio (Figure 2-5). It was observed that higher concentrations of Hg were released with lower soil:solution ratios. These findings are consistent with a mechanism of dissolution and are less consistent with a mechanism of desorption.

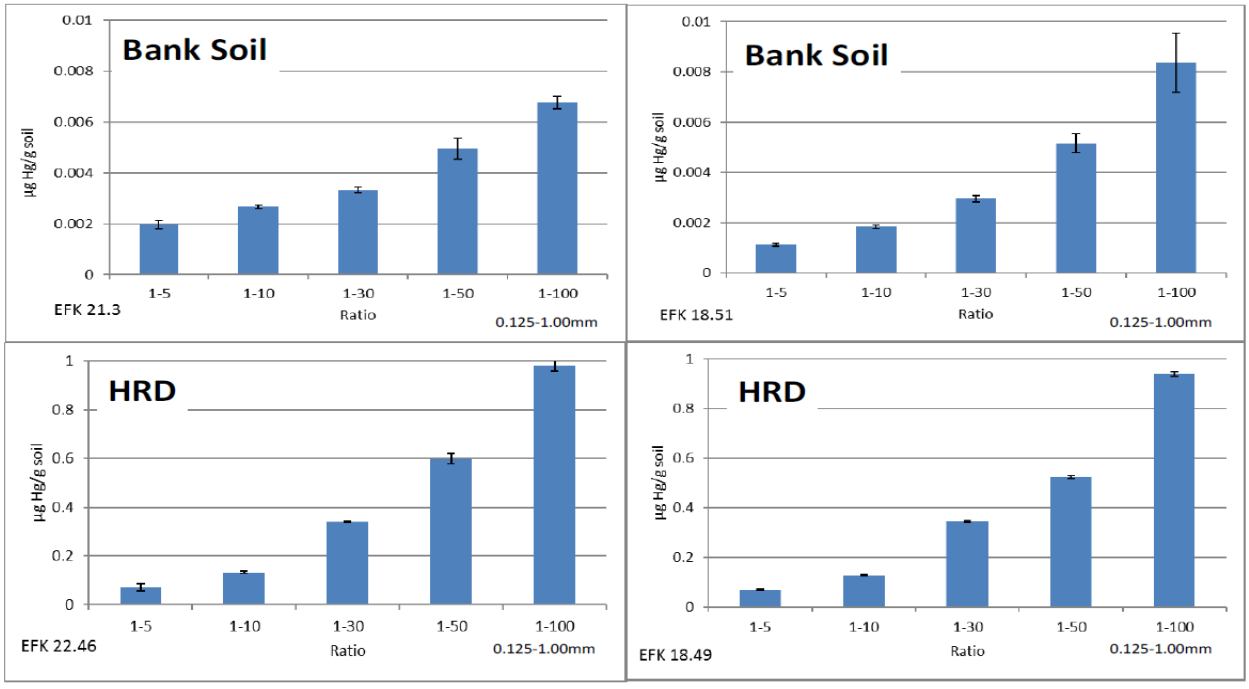

Figure 2-5. The extent of Hg release from the 0.125 to 1.00 mm size fraction of creek bank and HRD soils as a function of varying amounts of soil material.

In summary, a complete dataset of how much Hg is released from creek bank and HRD soils under a range of geochemical conditions has been collected. Next steps will include predicting the aqueous speciation of Hg and synthesizing the results. Although the fraction of total Hg released from creek bank and HRD soils is low under all test conditions, the lowest concentrations are still two to three orders of magnitude higher than the typical base-flow conditions (~30 ng/L) in EFPC stream water. These results indicate the importance of designing strategies to reduce the release of inorganic Hg from creek bank and HRD legacy sources. To date, researchers have not conducted measurements to examine the mobility of MeHg from the soils but will do so in FY 2018 and FY 2019.

2.2.3 Mobility of Mercury from Historical Release Deposit Soils in Column Experiments

Sections 2.2.1 and 2.2.2 detailed the importance of the HRD in terms of its total loading of contaminants to the system and potential for release; therefore, recent experiments are focusing exclusively on the HRD soils. A number of column experiments were performed to understand factors affecting the extent and rate of Hg release. The HRD is composed of many aggregates >2 mm that are black on the outside and red on the inside. The differences in coloration could imply that geochemical conditions (e.g., O_2 content, redox status, or mineralogy) were distinct between the inside and the outside of the aggregates. Therefore, the chemistry of Hg might be different on the inside versus on the outside of the aggregates. Additionally, the physical characteristics of the aggregates could limit the rate of Hg release, so several studies were performed to understand the hydraulic properties of the soils. These studies were in collaboration with the ORNL AFRI project and involved student researchers from the Minority Serving Institutions Partnership Program (MSIPP). HRD soils that were intact were compared with those that were sieved to 2 mm to examine whether or not the physical characteristics of the aggregates would affect the rate of Hg release from the soils.

Soils were collected from an HRD layer in one of the vadose zone pits at the former Bruner's Market (EFK 8.7; see Section 2.4). Soil columns were constructed of 3.6 cm in diameter and 8 cm in length. Two columns of each were repacked with either aggregated (intact) soils or soils crushed to pass a 2 mm sieve. The columns were saturated with simulated EFPC water without Hg (Table 2-2) and leached at a flow velocity of 1.5 cm/h, resulting in a residence time of 5.3 h.

Table 2-2. Artificial EFPC water

Compound	*mM*
KNO_3	0.0482
NaNO3	0.0676
Na_2SO_4	0.3525
NaCl	0.4182
$Mg(NO3)_2{*}6H_2O$	0.4957
$Ca(NO3)_2{*}4H_2O$	1.0355

For all columns, the extent of Hg release was low, even though the soils in the columns contained initial concentrations of 178 ± 21 mg Hg/kg soils (Figure 2-6). The initial release of Hg was delayed somewhat, but once Hg was detected the concentrations were relatively steady. The two replicate columns of the sieved soils are very similar, and the replicate sieved columns are similar. More Hg was released from the sieved soils (average of 181 ± 22 pg/mL) than from the unsieved soils (136 ± 19 pg/mL), which means that sieving, which disrupts soil aggregate structure, caused greater amounts of Hg release. A mass balance calculation of the area under the curves also found statistically significant differences between the sieved soils and the intact soils, confirming that the intact soils released only 62% of the Hg that was released from the sieved soils.

There were important differences between column and batch experiments. The HRD soils in the batch experiments (Section 2.1.2) released between 1,000 and 12,000 pg/mL of Hg. However, the initial concentration of Hg in the soils in the batch experiments was about an order of magnitude higher than Hg concentration in the column soils, so the results are not strictly comparable. However, it does seem that the column experiments released lower concentrations of Hg in comparison to the batch experiments. This might be because the batch experiments used 1 g (dry weight) of soil, whereas the intact columns used 92 g (dry weight) of soil, and the sieved soils used ~80 g (dry weight). In the columns, there is a much greater potential for readsorption of released Hg because of the large amount of sorptive capacity provided by the much greater amount of soil. Further tests are necessary to understand the mechanisms.

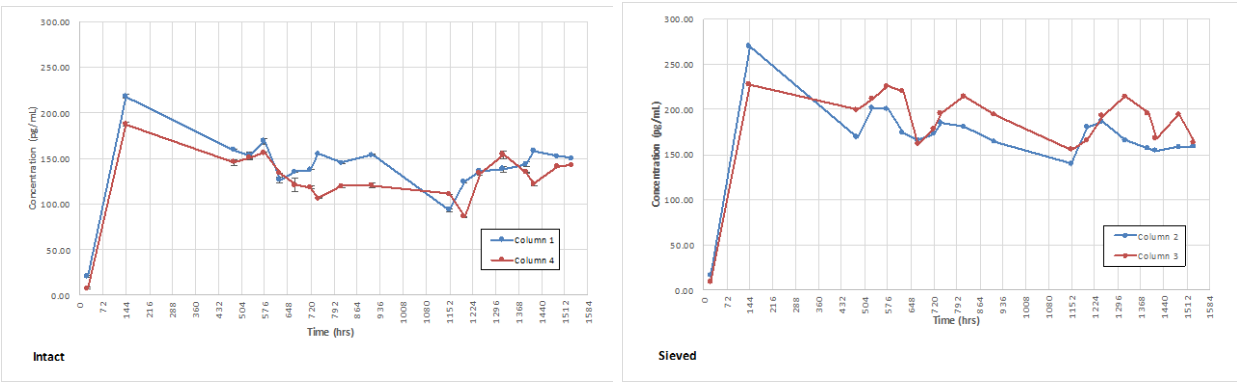

Figure 2-6. Leaching curves of Hg from (a) intact HRD soil columns and (b) sieved HRD soil columns. Note: in addition to contributions from the Mercury Technology Development project, these experiments were supported by the Applied Field Research Initiative Program and the Minority Serving Institutions Partnership Program.

Because of the observation of aggregates and the difference in Hg release between batch and columns, it was important to understand whether physical hydrological processes (i.e., diffusion) caused Hg to be released differently from the aggregated (intact) soils versus the sieved (disaggregated) soils. The assumption with this test is that the sieved soils will achieve a steady-state condition more quickly than the aggregated soil column because the physical structure of the soil will allow for instantaneous diffusion of Hg. In comparison, the intact soils might exhibit a slower approach to equilibrium because diffusion can limit the rate of transport into and out of the aggregates. Researchers applied several tests—analysis of dispersion in breakthrough curves of nonreactive tracers, multiple nonreactive tracers with different diffusion coefficients, and flow interruption (Mayes et al. 2003; Mayes et al. 2009; Reedy et al. 1996). Greater dispersion was indeed apparent in the intact soils, as evidenced by the slower approach to C/C0 = 1 (where C = effluent concentration and C0 = influent concentration) shown in Figure 2-7a versus Figure 2-7b. The difference can be quantified using the advective-dispersive equation, which is in progress. Dispersion was likely due to the greater degree of diffusion into the aggregates in the intact soils when compared with the sieved soils, causing the observed asymmetry in the shape of the breakthrough curves.

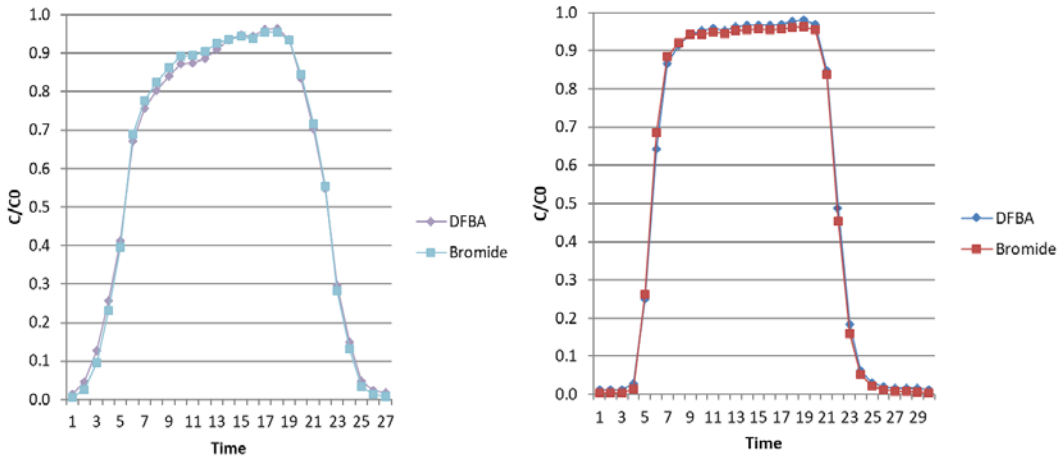

Figure 2-7. Breakthrough curves from soil columns involving the displacement of nonreactive tracers difluorobenzoic acid and bromide in (a) intact HRD soils and (b) 2 mm sieved HRD soils as a function of time (hours). Tracer concentrations are presented as relative concentrations (C/C0), where C = effluent concentration and C0 = influent concentration. Replicate columns of each were performed with similar results. Note: in addition to contributions from the Mercury Technology Development project, these experiments were supported by the Applied Field Research Initiative Program and the Minority Serving Institutions Partnership Program.

There was some separation of the two nonreactive tracers bromide and 2,6 difluorobenzoic acid (DFBA), and the separation was somewhat greater in the intact soils (Figure 2-7a versus Figure 2-7b). Bromide diffuses about 2.5 times faster than does 2,6 DFBA (Bowman and Gibbens 1992), so it breaks through in higher concentrations than does 2,6 DFBA (Mayes et al. 2003). The larger separation of tracers in the intact materials, most obvious near the peak of the breakthrough curves, suggests that diffusion was more important in the aggregated versus the sieved soils.

However, there was no response to a 6-h duration flow interruption, performed at about 0.95 C/C0. This finding clearly suggests that diffusion was not very important. Although the degree of dispersion and the separation of the multiple nonreactive tracers suggests that diffusion was more important in the intact soils than in the sieved soils, the magnitude of these effects was minor compared with observations in more structured soils (Reedy et al. 1996; Mayes et al. 2003, 2009). Overall, these findings are consistent with the lack of response to flow interruption. Consequently, these results suggest that diffusion into and out of the aggregates was unlikely to significantly affect the rate of release of Hg from the soils, at least at the flow velocities and residence times used in these columns. Consequently, diffusional limitations in intact HRD aggregates can be ignored in future column work. In other words, researchers can assume that the physical properties of the soils do not affect the rate of Hg release. This also means that the low Hg leaching concentrations are not a result of physical hydrology but rather chemical or geochemical processes.

Additional preliminary column tests are ongoing. First, the sensitivity of the soils to column area is being tested. It is clear from the much larger amount of Hg released in the batch experiments compared with the column studies that the soils in the columns are highly reactive to released Hg. The batch experiments used 1 g of soil, and the columns used 80–90 g of soil; so there is a much greater potential for readsorption of released Hg in the columns. Therefore, the same soils were used to test the release of Hg from a much smaller column width (with similar length). Results were comparable, suggesting that Hg concentrations were not particularly sensitive to soil column area. Secondly, fresh HRD soils were collected from one of the higher areas of contamination (1,160 ± 55 mg Hg/kg soil) in the Bruner's Market (EFK 8.7) area. Using an identical column setup and intact HRD soils, the release of Hg from

fresh soils will be tested and compared with the 178 ± 21 mg Hg/kg soils used in the study just described. All future column studies will use the fresh soils with 1,160 ± 55 mg Hg/kg and 57 ± 4 ng MeHg/g soil.

Planning activities for the next round of column experiments are complete, and these experiments are expected to require six months to a year for completion. The goal of the experiments is twofold: (1) determine the rate and extent of Hg and MeHg release over time and (2) quantify how much of the Hg and MeHg are sorbed onto sorbent materials. Thus, these columns will be a direct test of the efficacy of sorbent materials to take up Hg and MeHg. There are two potential sizes for the HRD soil columns under consideration, 3.6 cm diameter × 11.4 cm length and 8.9 cm diameter × 34 cm length; the final decision will depend on the results of the ongoing tests just mentioned. The columns will flow from bottom to top, and at the effluent side of the columns a valve will be employed to periodically allow for sampling of constituents released from the soils. From there, the remaining column effluent will be routed into a column packed of sorbent materials, from which effluent solutions will be collected continuously as a function of time. The effluents from both columns will be analyzed for pH, Hg, MeHg, DOC, specific absorbance at 254 nm (specific ultraviolet absorbance [SUVA]), and anions and cations as a function of time and volume eluted. The project has ordered a number of pumps, column setups, and fraction collectors to support experiments involving two control columns, three sorbents, and two replicates each (eight total columns). More details on the sorbent columns are available in Section 2.3.

2.2.4 Form of Mercury in Historical Release Deposit Soils

The form of Hg in the creek bank soils and in the HRD might be an important factor in understanding Hg leachability. Two different techniques were applied to increase understanding of Hg chemistry in the soils—sequential extractions and scanning electron microscopy (SEM). A set of sequential extractions on seven HRD samples and on four creek bank soil samples was completed following the methods of Bloom et al. (2003). Briefly, extractant solutions F1 through F5 are increasingly strong and therefore release increasingly resistant Hg complexes. The F1 fraction involves deoxygenated deionized water, the F2 fraction involves 0.01 M hydrogen chloride (HCl) and 0.1 M acetic acid, the F3 fraction uses 1 M KOH, the F4 fraction uses 12 M HNO_3, and the F5 fraction involves a full aqua regia digest. There were important differences between the HRD and bank soils, in that the HRD might have higher proportions of the more "available" fractions of Hg. For the HRD soils, 89.3 ± 5.8% of Hg is in the most resistant F5 fraction, with <6% in the F4 and F3 fractions together, 4.8 ± 4.3% in the F2 fraction, and almost none in the F1 fraction (Figure 2-8). For the bank soils, 84.0 ± 8.7% of Hg is in the most resistant F5 fraction, with 13.5 ± 6.1% in the F4 fraction, 2.5 ± 4.6% in the F3 fraction, and almost none in the F2 or F1 fractions. In summary, the HRD contains proportionally more Hg in the most resistant F5 fraction but also contains substantial Hg in the intermediate F4 and F3 fractions, as well as in the relatively labile F2 fraction. The creek bank soils contained proportionally less Hg in the most resistant F5 fraction compared with the HRD; they contained substantially more Hg in the F4 fraction and almost no Hg in the F3, F2, and F1 fractions, with the notable exception of the sample from EFK 21.3.

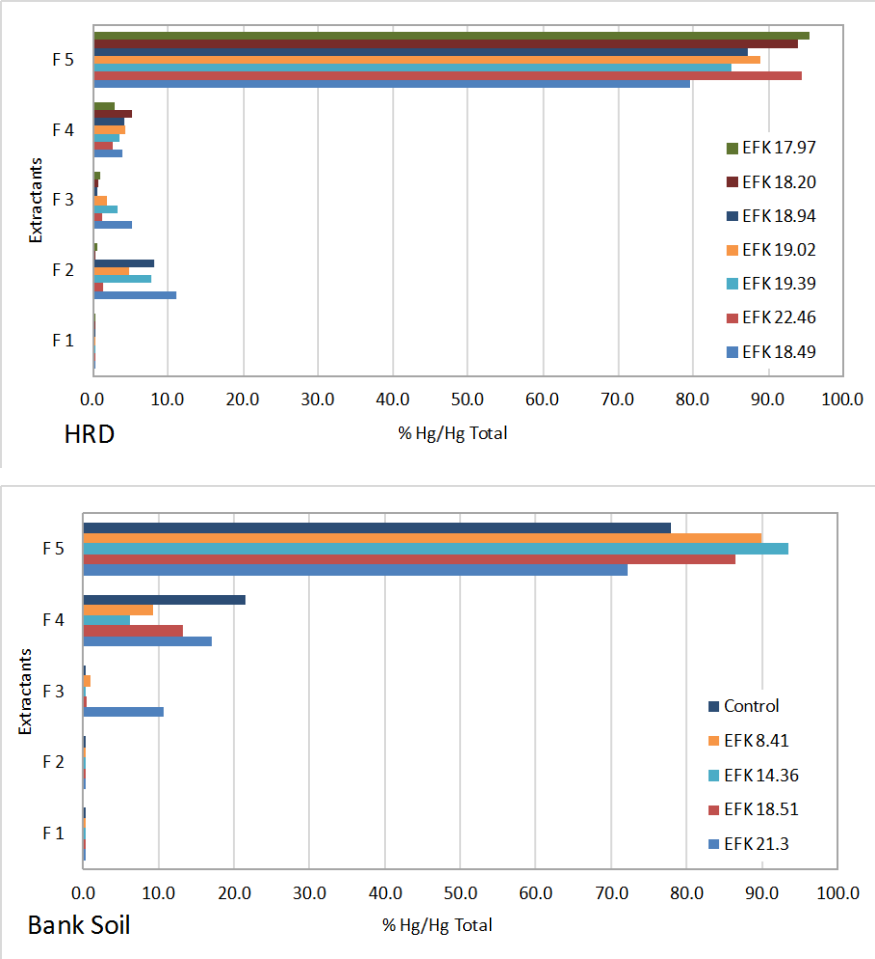

Figure 2-8. Sequential extractions of Hg in fractions F1–F5 obtained from the (a) HRD soils and (b) creek bank soils. Notes: in addition to contributions from the Mercury Technology Development project, these experiments were supported by the Applied Field Research Initiative Program and the Minority Serving Institutions Partnership Program. EFK = East Fork Poplar Creek kilometer.

Through a partnership with the AFRI program, the chemistry of Hg in the HRD soils was determined. Thin sections were prepared with HRD soils and were analyzed by SEM and energy dispersive x-ray (EDX). The Hg was found in discrete aggregates, as identified by the bright spots on the SEM image (Figure 2-9). The chemistry of the high-intensity regions was conclusively identified with EDX as a function of space on the SEM images. The Hg "M" line and the sulfur "K" line both show enrichments associated with the location of the bright spots, whereas the other elements do not show a consistent association (Figure 2-9). Consequently, the form of Hg in the HRD can conclusively be identified as Hg sulfide (HgS), which is consistent with previous results (Barnett et al. 1997). The size distribution of the HgS enriched particles ranged from 0.15 to 4.2 µm.

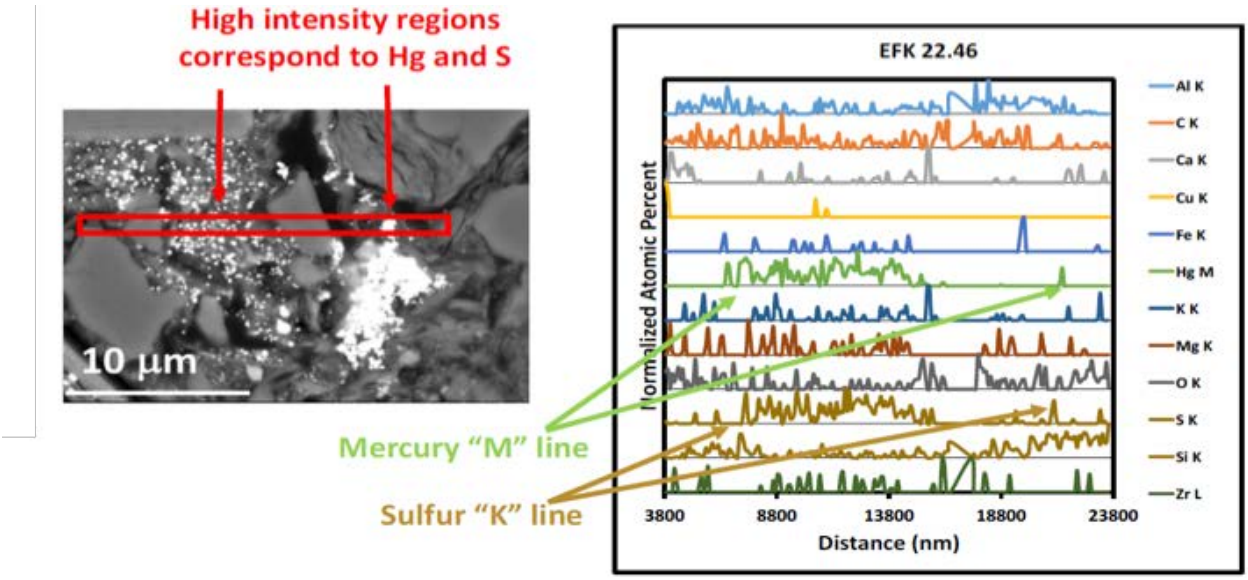

Figure 2-9. SEM and EDX analyses of historical release deposit soil samples. Note: these analyses were contributed by the ORNL Applied Field Research Initiative Program using soils collected under the Hg Technology Development project. EFK = East Fork Poplar Creek kilometer.

2.3 SORBENT EVALUATION

2.3.1 Introduction

Sorbents are evaluated as a potential low-impact, low-cost approach for limiting the release of Hg species from soils and sediments in EFPC. The goal is to identify sorbents amenable for incorporation into sediments, soils, or physical barriers such as bank stabilization structures with minimal impact on the ecosystem. The application of sorbents aims to capture Hg and MeHg within a high-affinity sorbent matrix with the intent to limit migration, Hg methylation, and bioaccumulation. The primary mode of action is strong binding of a contaminant species to the sorbent material, resulting in a reduction in the pore water concentration. The effectiveness of sorbent treatments is generally defined by the partitioning of Hg species between sediments and solution phase (Gomez-Eyles et al. 2013). The lower the native sediment:water partition coefficients for Hg and MeHg of the system, the more effective a potential sorbent treatment is (Gilmour et al. 2013). NOM, sulfidic species, and suspended solids exert significant influence on the speciation of Hg and MeHg. Thus, the presence of NOM, suspended particles, and sulfidic species might have a significant impact on the effectiveness of sorbent treatments.

New experiments involving columns packed with sorbents were designed to evaluate sorbents under controlled conditions. The studies described here focus on evaluating the effectiveness of sorbent materials for the removal of Hg species from solution in a laboratory setting over intermediate to long periods. These column experiments will allow the research team to address key parameters such as removal efficiency as a function of flow rate and residence time, water chemistry (HRD effluent vs. EFPC water), and Hg speciation (Hg-NOM, MeHg, Hg associated with suspended particles, etc.). Various hydrological tests have been performed in the columns to assess hydraulic conditions for a subset of sorbent materials. Furthermore, initial experiments have been conducted to determine Hg sorption from EFPC water under controlled flow conditions. As outlined in Section 2.1, future work will focus on the removal efficiency for effluents from high-level HRD soils by coupling HRD soil columns to sorbent columns to test the extent and rate of removal by the sorbents.

COP is a novel sorbent material recently developed at Flinders University, Australia. This new material is made entirely from industrial by-products in a simple, low-cost process. Researchers evaluated samples of the material in controlled batch sorption experiments using Hg(II) and the standardized Hg(II)-NOM complex described in the FY 2015 and FY 2016 reports (Peterson et al. 2016; Peterson et al. 2017). Data comparing Hg(II)-nitrate and Hg(II)-NOM have shown that complexation with NOM drastically affects removal efficiency and sorption capacity of the material. The results were incorporated into a joint manuscript on the synthesis and characterization of COP. The study covers a broad range of potential applications for the sorbent. Based on the data collected, the most promising applications are capture of Hg^0 from the gas phase and the organomercurial fungicide 2-methoxyethylmercury chloride. At environmentally relevant concentrations, up to ~80% reduction of Hg-NOM was achieved in solution, although the sorption isotherms indicate that the sorption capacity for these species is limited. The manuscript was accepted for publication in *Chemistry—A European Journal* (Worthington et al. 2017).

In the coming year, research will be centered on column studies to assess strategies for removal of Hg and MeHg using sorbents. The experiments will incorporate data from the characterization efforts and will be designed with long-term effectiveness and scale-up in mind. The aim is to inform future engineering solutions to limit release and migration of Hg in EFPC.

2.3.2 Column Studies

Studies evaluating engineered sorbents under controlled hydrologic conditions will provide key data to support the informed design of effective remediation technologies. The aims are to determine the efficacy of sorbent technologies under realistic conditions and to define key parameters, including the ratio of sorbent to contaminated sediments, characteristics of the sorbents such as particle size and chemistry, importance of environmental controls such as pore water flow and geochemistry, and variety of responses possible in floodplain, creek bank, and HRD soils. Eventually, this work will transition to long-term experiments under conditions relevant for deployment in the field. A solid set of validation experiments to identify potential benefits and challenges is essential before pilot-scale testing in the field can commence.

The initial set of column experiments described in this section is designed to understand hydraulic properties and physical characteristics of engineered sorbent materials, which have a significant impact on removal efficiency and deployment strategies. All column experiments described here were conducted under saturated conditions and controlled flow. The aims of these initial experiments were to test the experimental setup, determine hydrology and transport parameters from breakthrough curves using nonreactive tracers, and evaluate sorption of Hg species from EFPC water. In addition to contributions from the Mercury Technology Development project, these studies involved student researchers from MSIPP.

2.3.2.1 Experimental design

Acrylic columns with a length of 9 cm and an inner diameter of 2 cm were packed with sorbent or clean quartz sand, a reference material. The top and bottom of the columns were packed with glass wool to prevent leaking. The total volume of the columns before packing was 28.3 cm^3. Prior to wetting, the columns were flushed with pure CO_2 for several minutes to displace air and prevent the formation of residual air pockets. Controlled flow through the columns was achieved using a Deltec 3000 Large Volume Infusion Pump with proprietary disposable pump tubing cassettes. The flow direction was against gravity, from the bottom to the top of the column. The column effluent was collected using a Retriever II fraction collector with 13 × 100 mm test tubes (Figure 2-10). The influent solutions consisted of artificial creek water (ACW) for tracer experiments or unfiltered EFPC water collected in the field.

The columns were packed with biochar sorbent manufactured by Biochar Now, LLC (Loveland, Colorado) and HCl-cleaned quartz sand (IOTA high purity quartz sand, particle size of ~0.175 µm) as a nonreactive reference material with limited sorption capacity (Figure 2-11).

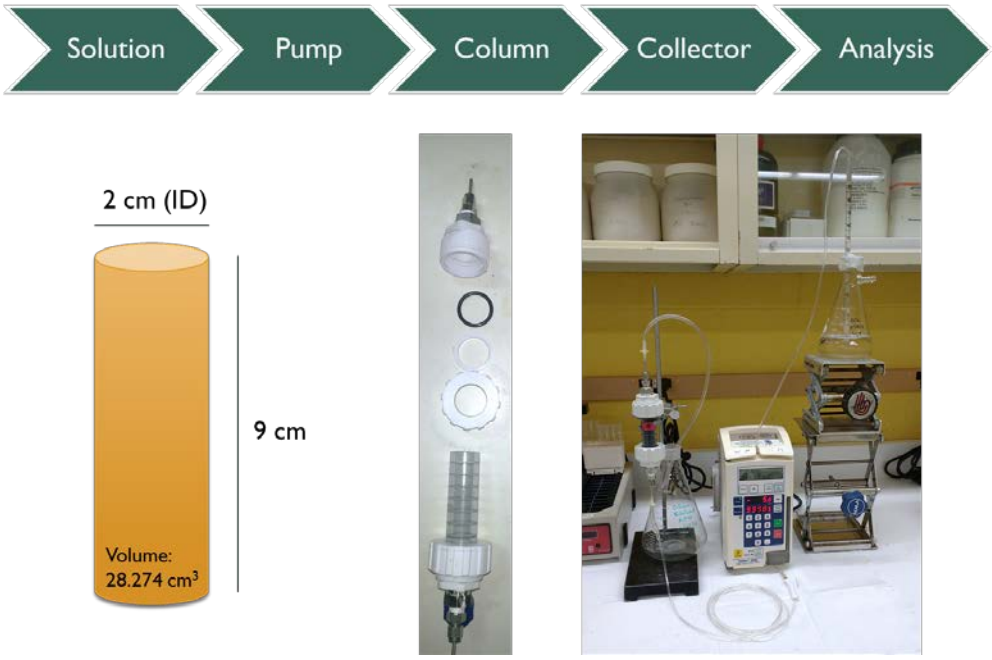

Figure 2-10. Column assembly, geometry, and experimental setup. Note: In addition to contributions from the Mercury Technology Development project, these experiments were supported by MSIPP.

Figure 2-11. Assembled columns packed with biochar and quartz sand after wetting. Note: In addition to contributions from the Mercury Technology Development project, these experiments were supported by MSIPP.

The pore volume fraction of the packed and saturated columns was determined as follows:

$$\theta = \frac{V_{total} - V_{sorbent}}{V_{total}}, \quad (2.1)$$

where θ is the pore volume expressed as a fraction of the V_{total}, which is the total column volume, and $V_{sorbent}$ is the volume occupied by the sorbent. $V_{sorbent}$ was determined by subtracting the weight of the column assembly packed with dry sorbent from the weight of the column assembly packed with wetted sorbent multiplied by the volumetric mass density of the solution. The pore volume fractions were 0.505 and 0.462 for biochar and quartz sand, respectively.

2.3.2.2 Tracer experiments

Two nonreactive tracers, 2,6-DFBA and calcium bromide ($CaBr_2$), were used to determine breakthrough curves. Tracers were prepared as 1,000 ppm stock solutions. For DFBA, an aliquot of the stock solution was added to ACW to obtain a final tracer concentration of 30 ppm. The concentration of the DFBA tracer was measured by ultraviolet-visible absorption spectroscopy (UV-Vis) at a wavelength of 260 nm (Figure 2-12). For $CaBr_2$, an aliquot of the stock solution was added to ACW to obtain a final tracer concentration of 10 ppm. $CaBr_2$ is not detectable by UV-Vis absorbance; therefore, a colorimetric bromide assay was used. The columns were equilibrated overnight with ACW before the tracer experiments, and the flow rate was set to 15 mL/h for all experiments. The fraction collectors were set to collect 2 mL of column effluent per tube.

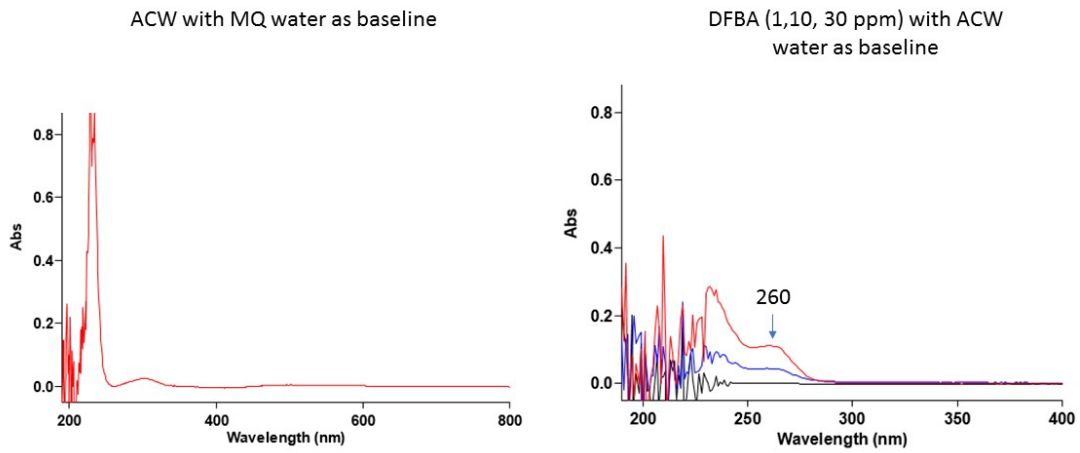

Figure 2-12. UV-Vis spectra of ACW and 2,6-DFBA. Note: In addition to contributions from the Mercury Technology Development project, these experiments were supported by MSIPP.

A colorimetric assay was adapted to determine bromide concentrations (Lepore and Barak 2009). Briefly, a 2.45 mM stock solution of N-chloro-*p*-toluenesulfonamide (Chloramine T) and a 1.63 mM stock solution of phenolsulfonphthalein (Phenol red) were prepared in ultrapure water. A buffer was prepared using 0.5 M sodium acetate, 0.5 M glacial acetic acid, and 12.32 mM ammonium acetate and was then adjusted to pH 4.6. The buffer and Phenol red stock solutions were mixed in a 1:1 volume ratio before use. In a 1.5 mL microcentrifuge tube, 870 µL of a bromide standard, or sample, was combined with 65 µL of the Phenol red–buffer mixture before initiating the reaction by the addition of 65 µL Chloramine T stock solution. The reaction was complete after 30 minutes, and the reaction mixture was transferred to a disposable plastic semi micro cuvette. The absorbance at a wavelength of 590 nm was recorded. The

reaction with bromide results in a visible color change from yellow to light blue. A calibration curve within a bromide concentration range from 1 to 10 ppm was prepared (Figure 2-13). Furthermore, it was verified that ACW components do not interfere with the colorimetric bromide assay.

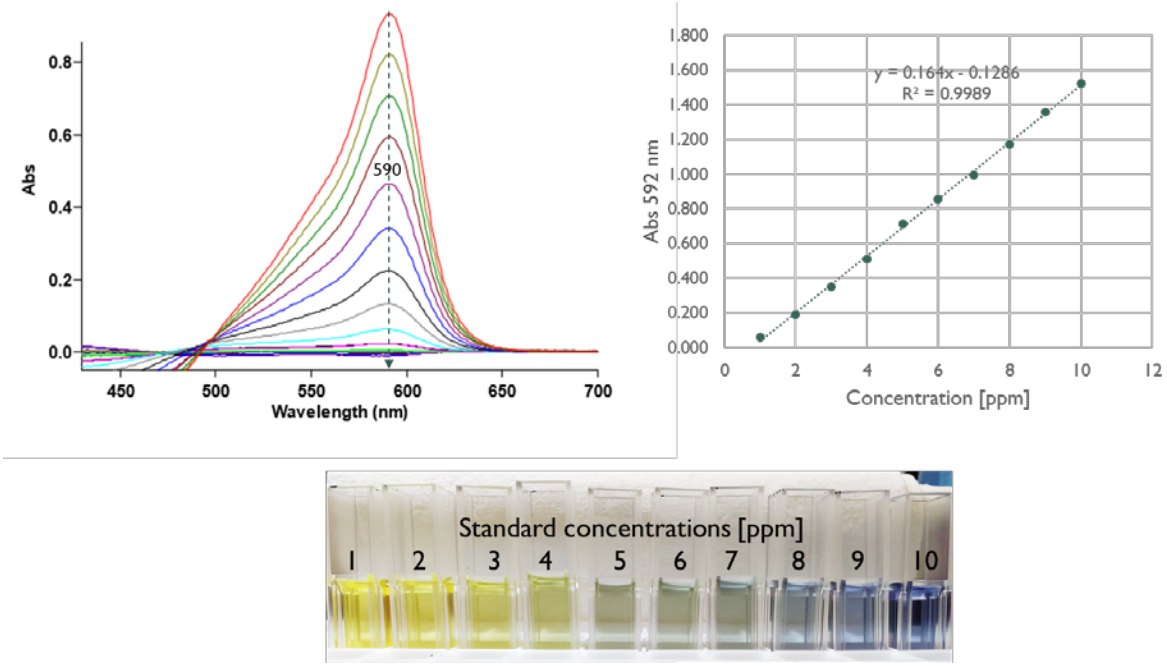

Figure 2-13. Bromide assay: UV-Vis absorption and calibration curve for bromide concentrations from 1 to 10 ppm. *Note:* In addition to contributions from the Mercury Technology Development project, these experiments were supported by MSIPP.

The breakthrough curves obtained from separate experiments with two nonreactive tracers reveal the hydraulic characteristics of the sorbent columns under saturated conditions. The breakthrough curves for quartz sand (Figures 2-14A and 2-15A) exhibit ideal behavior with little dispersion with both tracers. The results for the biochar column indicate that the tracer DFBA might be retained by the biochar because it was not possible to reach breakthrough (Figure 2-14B), whereas breakthrough was observed for the bromide tracer (Figure 2-15B). The shape of the breakthrough curve obtained for biochar using the bromide tracer indicates some degree of dispersion.

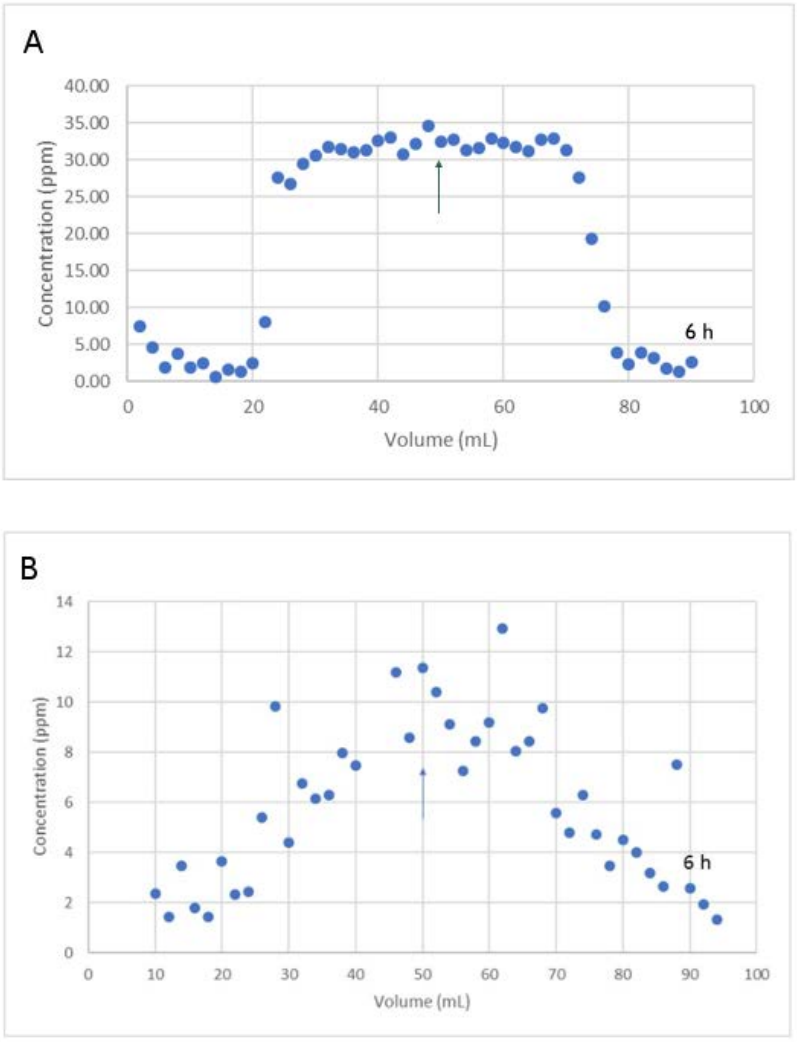

Figure 2-14. Breakthrough curves obtained with the tracer 2,6-DFBA. The flow rate was 15 mL/h, and DFBA concentration in the influent was 30 ppm. The arrow indicates the switch from tracer to no tracer in the influent. Panels show data for columns packed with (A) quartz sand and (B) biochar. Note: In addition to contributions from the Mercury Technology Development project, these experiments were supported by MSIPP.

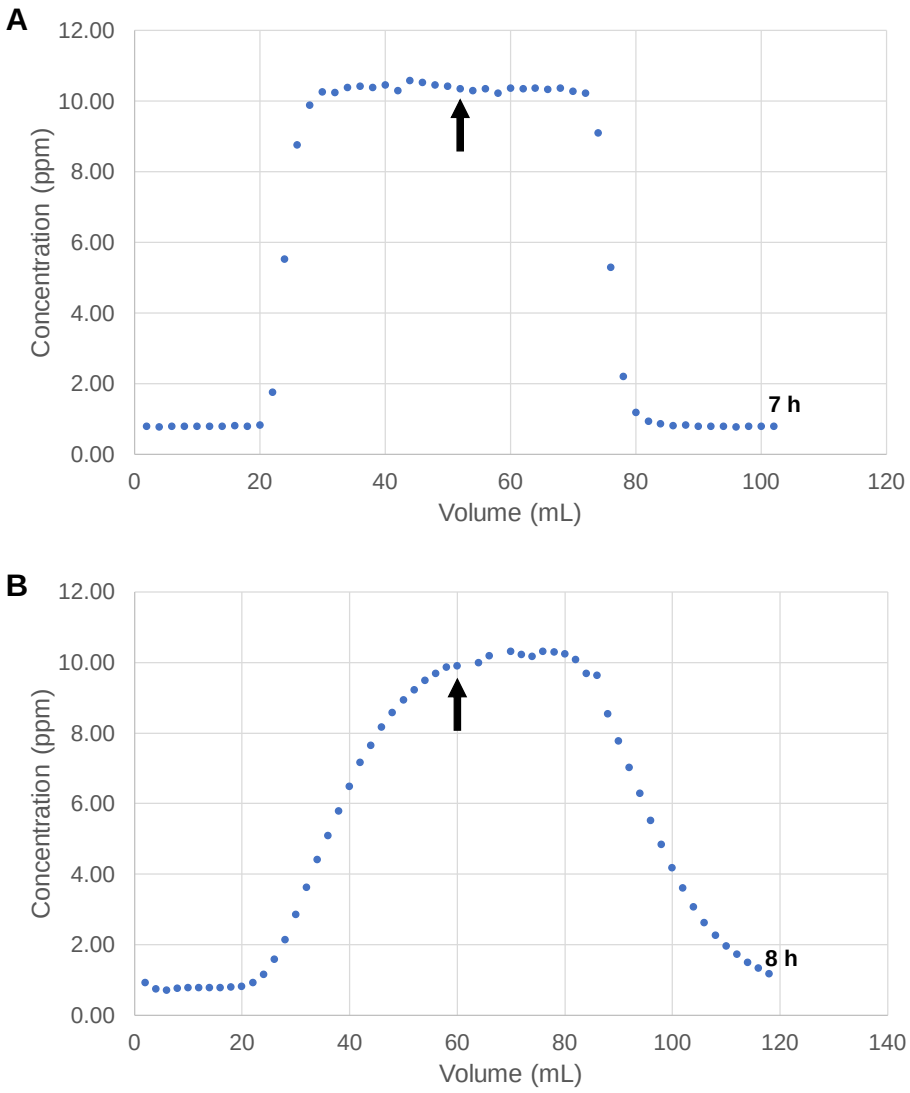

Figure 2-15. Breakthrough curves obtained with $CaBr_2$ as a tracer. The flow rate was 15 mL/h, and bromide concentration in the influent was 10 ppm. The arrow indicates the switch from tracer to no tracer in the influent. Panels show data for columns packed with (A) quartz sand and (B) biochar. Note: In addition to contributions from the Mercury Technology Development project, these experiments were supported by MSIPP.

2.3.2.3 Column experiments with East Fork Poplar Creek water

Water samples were collected in EFPC at EFK 18.49 (Figure 2-16). The collection containers were rinsed three times with creek water, and 8 L was collected. The columns (quartz sand and biochar) were equilibrated overnight with ACW. The flow rate was set to 15 mL/h, and the fraction collectors were set to collect 7 mL of effluent per tube. To determine total Hg concentrations, 100 µL bromine chloride (BrCl) (20 g/L) was added to 5 mL of each effluent fraction and reacted overnight to break down NOM, which can interfere with the analysis. An aliquot of the solution was added to an excess of 20% (weight/volume) stannous chloride and purged with ultrahigh purity N_2. The emerging Hg^0 was quantified in a cold vapor atomic absorption spectroscopy Zeeman effect Hg analyzer (Lumex RA-915+, Ohio Lumex Company, Inc., Twinsburg, Ohio). The concentration of Hg in the sample was determined based on a series of calibration standards.

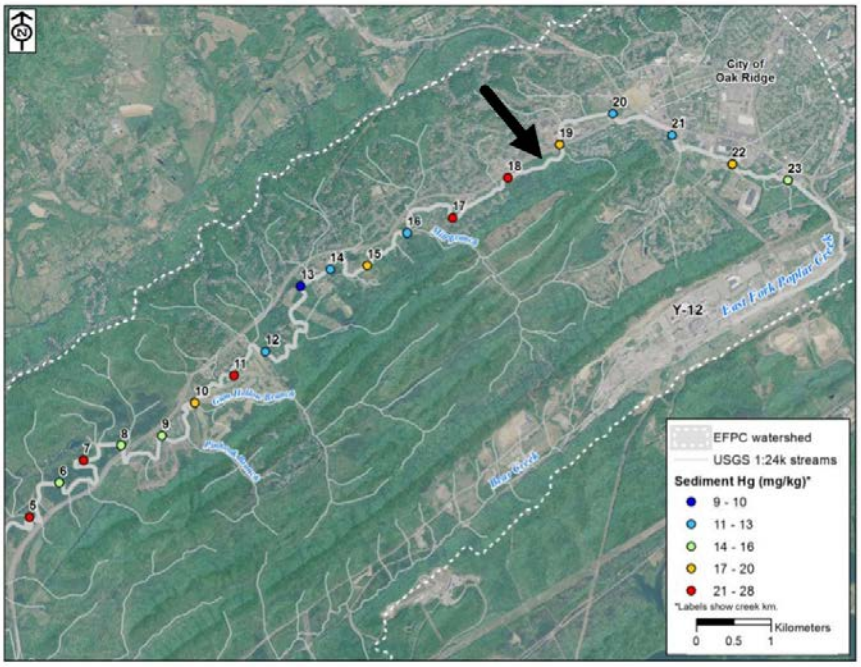

Figure 2-16. EFPC water sampling location (EFK 18.49) for column experiments. Note: In addition to contributions from the Mercury Technology Development project, these experiments were supported by MSIPP.

The total Hg concentration in the collected EFPC water was 32 ng/L. The recorded effluent concentration show that Hg levels were effectively reduced by both biochar and quartz sand, resulting in effluent concentrations of approximately 1.6 ng/L and 2.4 ng/L, respectively (Figure 2-17). These results could indicate that filtering of Hg bound to suspended particulates might contribute to the removal of Hg from EFPC water. However, additional experiments are needed to evaluate the sorption capacity of quartz sand and potential sorption to other components of the column assembly. Nevertheless, given the relatively low concentration of Hg in EFPC water, it was surprising to find that a small percentage of Hg elutes through the biochar column. The removal efficiency of the biochar column under the experimental conditions is approximately 95%.

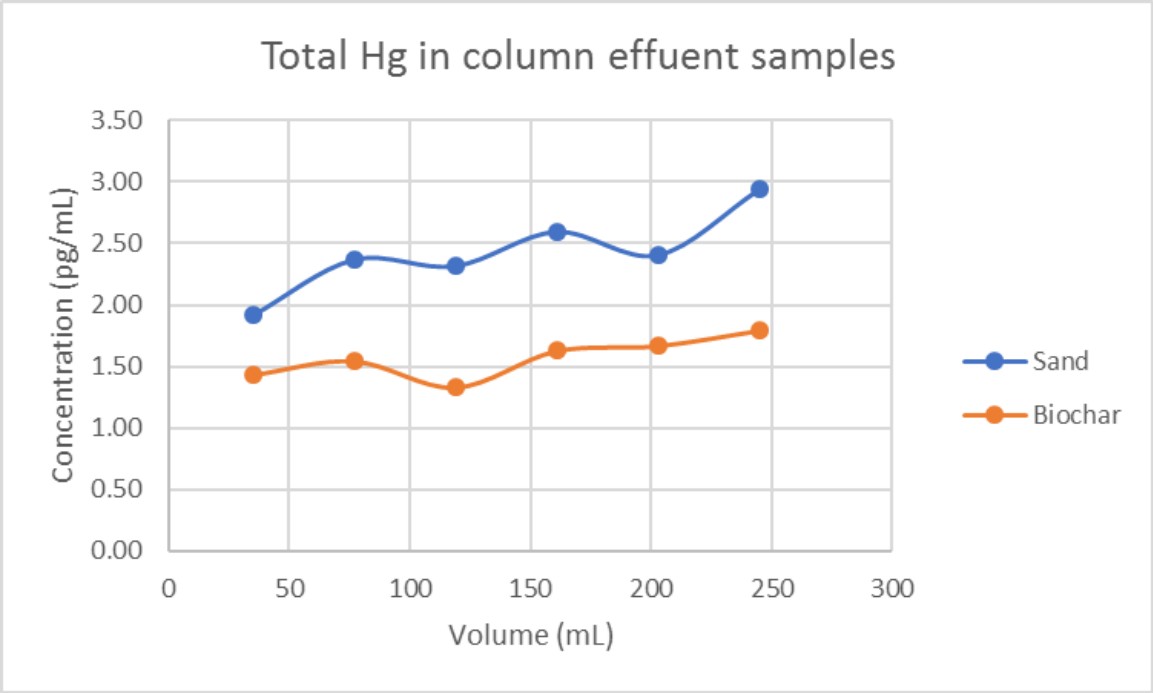

Figure 2-17. Total Hg concentrations in quartz sand and biochar column effluents as a function of collected effluent volume. The Hg concentration in the influent was 32 ng/L. Note: In addition to contributions from the Mercury Technology Development project, these experiments were supported by MSIPP.

2.3.3 Evaluation of Canola Oil Polysulfide

The synthesis of polysulfides by inverse vulcanization established a new class of materials with high sulfur content. The inverse vulcanization of the renewable plant oil limonene and its use for the sorption and detection of mercuric chloride ($HgCl_2$) in aqueous solution was reported recently (Crockett et al. 2016). The synthesis process involves melting of elemental sulfur and then heating it above its floor temperature of 159°C followed by trapping of the generated thiyl radicals with a polyene resulting in a crosslinked polysulfide in quantitative yields and without the need for a solvent (Chung et al. 2013). Thus, it is possible to prepare polysulfides from feedstocks that are highly abundant, very inexpensive, and easy to handle. Here, researchers characterize Hg sorption to COP, which is the inverse vulcanization product of sulfur and food-grade canola oil. Because sulfur is an abundant by-product of petroleum refining and used cooking oils are a by-product of the food industry, there is the intriguing prospect of making a low-cost Hg-binding polymer in which every atom in the product is derived from industrial waste.

2.3.3.1 Sorption isotherms

The complexation and speciation of Hg and MeHg with NOM is known to affect its mobility, as well as chemical and biological transformation in aquatic environments (Aiken, Hsu-Kim, and Ryan 2011; Haitzer, Aiken, and Ryan 2002; Pham 2014).

For the polysulfide polymer to capture this Hg, a ligand exchange would need to occur. To determine the potential for ligand exchange, sorption isotherms for $Hg(NO_3)_2$ and a Hg-NOM complex were determined at environmentally relevant Hg concentrations. Suwannee River aquatic natural organic matter (SR-NOM), reference material 2R101N (International Humic Substance Society), and a 1 ppm $Hg(NO_3)_2$ standard (Brooks Rand Instruments, Seattle, Washington) were used to prepare Hg-NOM complexes containing

40 µg/L Hg and 2,400 µg/L total carbon (C_{NOM}) equivalent to a molar Hg:C_{NOM} ratio of 1.8×10^{-5}. SR-NOM was dissolved in 10 mM sodium phosphate buffer (pH 7.8) and filtered through a 0.2 µm syringe filter to remove residual particulates. $Hg(NO_3)_2$ was added, and the pH was readjusted to 7.8 and allowed to age at 4°C for at least five days. The Hg-NOM stock solution was diluted with 10 mM sodium phosphate buffer to obtain working solutions with Hg concentrations from 0.2 to 7.7 µg/L. A dilution series of the 1 ppm $Hg(NO_3)_2$ standard in 10 mM sodium phosphate buffer was prepared as an NOM-free control.

Sorption isotherms were determined in triplicate batch experiments by adding 30 mL Hg-NOM complex at Hg concentrations of 0.2, 0.4, 0.7, 1.5, 3.6, and 7.7 µg/L or $Hg(NO_3)_2$ in phosphate buffer at concentrations of 0.2, 0.5, 0.8, 1.6, 4.0, and 16 µg/L to 40 mL amber borosilicate glass vials. The vials contained approximately 100 mg of COP, porous COP, or reduced porous COP after equilibration for 48 h on a rotary shaker. The suspensions were filtered through a 0.2 µm polyethersulfone (Supor) syringe filter for total Hg and sulfate analyses by ion chromatography. To determine Hg equilibrium concentrations, 5 mL of the filtered samples were oxidized by the addition of 150 µL BrCl (20 g/L). An aliquot of this solution was added to an excess of 20% (weight/volume) stannous chloride and purged with ultrahigh purity N_2. The amount of emerging Hg^0 was determined by a cold vapor atomic absorption spectroscopy Zeeman effect Hg analyzer (Lumex RA-915+, Ohio Lumex Company, Inc., Twinsburg, Ohio). The concentration of sorbed Hg was determined by the difference between the known initial amount of Hg added and the equilibrium aqueous Hg concentrations, which also included Hg sorbed to the wall of the amber glass vials. Within the tested concentration ranges, a linear correlation was obtained for the sorption to all COP variants when Hg was added as $Hg(NO_3)_2$. The sorption isotherms with Hg added as Hg-NOM show a nonlinear characteristic, which was approximated by the Langmuir isotherm model. The Langmuir adsorption isotherm assumes monolayer adsorption onto a surface containing a finite number of uniform adsorption sites. The surface reaches a saturation point, where maximum sorption of adsorbate on a monolayer is reached. The relationship between adsorbed and solution concentrations for the Langmuir isotherm is as follows:

$$Y = \frac{Y_{\max} \cdot K_L \cdot C_{eq}}{1 + K_L \cdot C_{eq}}, \tag{2.2}$$

where Y is the concentration of the adsorbate on the sorbent, Y_{max} is the sorption capacity, C_{eq} is the solution concentration at equilibrium, and K_L is the Langmuir adsorption equilibrium constant. The isotherm fits for all COP variants are shown in Figure 2-18. The results show that all tested COP samples removed >90% of Hg when added as $Hg(NO_3)_2$. The strong complexation of Hg with functional groups on NOM competes with the sorption of Hg to any sorbent, thus presenting a unique challenge for the removal of Hg from contaminated ecosystems. Under the conditions of the isotherm experiments, a dilution series was prepared from a concentrated Hg-NOM stock solution. Thus, the concentration of Hg is coupled with the concentration of NOM. In a freshwater creek ecosystem, the level of NOM can span a wide range of concentrations, whereas the level of Hg typically corresponds to the low end of the experimental range, even in contaminated systems (Southworth et al. 2013). Efficient removal of Hg from solutions containing strong Hg-NOM complexes is achievable because it is determined by the sorbent to solution ratio and the concentration of Hg-NOM. A measure of how efficiently the sorbent can remove the contaminant at a specific concentration can be obtained as follows:

$$R[\%] = \frac{C_0 - C_{eq}}{C_0} \cdot 100 \ , \tag{2.3}$$

where R is the removal efficiency, C_0 is the initial Hg concentration, and C_{eq} is the Hg concentration after equilibration with the sorbent. Surface modification of COP had a significant impact on Hg removal. At

the lowest initial Hg-NOM concentrations (0.2 µg/L Hg) and a sorbent-to-solution ratio of 1/300, *R* was 36% for unmodified COP, 79% for porous COP, and 81% for reduced porous COP. The results show that the surface modification of COP, particularly the increased surface area in porous COP, results in a highly effective sorbent that can sorb Hg in the presence of competing ligands such as NOM.

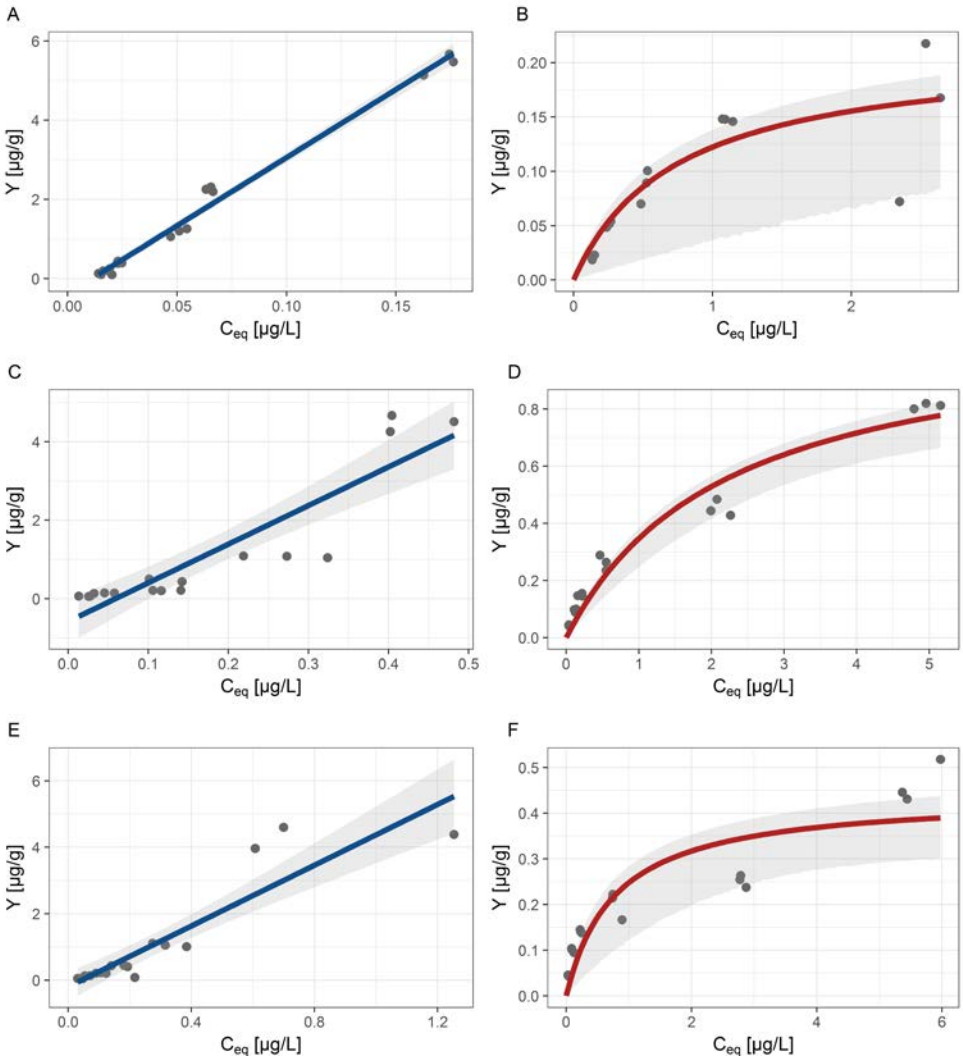

Figure 2-18. Equilibrium sorption data (dots) and fits to isotherm models for the sorption of Hg at low Hg concentrations. The 95% confidence bands are shown in gray. (A) Unmodified COP with Hg added as $Hg(NO_3)_2$ and linear fit (blue), residual standard error of the fit: 0.21 µg/g. (B) Unmodified COP with Hg added as Hg-NOM complex and model fit to the Langmuir isotherm model (red). Langmuir fit parameters: K_L = 1.35 L/µg, Y_{max} = 0.21 µg/g, residual standard error of the fit: 0.032 µg/g. (C) Porous COP with Hg added as $Hg(NO_3)_2$ and linear fit (blue), residual standard error of the fit: 0.71 µg/g. (D) Porous COP with Hg added as Hg-NOM complex and model fit to the Langmuir isotherm model (red). Langmuir fit parameters: K_L = 0.46 L/µg, Y_{max} = 1.11 µg/g, residual standard error of the fit: 0.061 µg/g. (E) Reduced porous COP with Hg added as $Hg(NO_3)_2$ and linear fit (blue), residual standard error of the fit: 0.65 µg/g. (F) Reduced porous COP with Hg added as Hg-NOM complex and model fit to the Langmuir isotherm model (red). Langmuir fit parameters: K_L = 1.29 L/µg, Y_{max} = 0.44 µg/g, residual standard error of the fit: 0.065 µg/g.

Over the concentration range from 0.2 to 16 µg/L used for the sorption experiments, the sorption of $Hg(NO_3)_2$ was found to follow a linear isotherm, confirming that in the absence of NOM all forms of the polysulfide removed >90% of the Hg in solution and that the sorbent did not approach saturation or Hg binding capacity (Figure 2-18). By comparison, when Hg is associated with NOM (i.e., Hg-NOM), functional groups on NOM compete with the polysulfide for Hg binding. Nevertheless, the removal efficiency at low Hg-NOM concentrations for the porous and the reduced porous polysulfide reached 79% and 81%, respectively. As Hg-NOM concentrations increased, the removal efficiency decreased as indicated by a fit of the equilibrium data to the Langmuir sorption isotherm. The sorption capacity for the porous polysulfide reached a value of 1.11 µg-Hg/g-sorbent under the experimental conditions (Figure 2-18). The results clearly show that the porous polysulfide material is effective on Hg-NOM complexes, particularly at concentrations typically encountered in Hg-contaminated freshwater systems. Partial reduction of the polymer surface to install thiols had only a small impact on removal efficiency in the presence of Hg-NOM and resulted in a lower sorption capacity compared with the porous polysulfide.

2.3.3.2 Sulfate release studies

Additionally, researchers investigated whether sulfate was released from the polymer. High sulfate concentrations in low oxygen subsurface environments can enhance Hg methylation by promoting sulfate-reducing bacteria, which are considered the primary methylators in marine and estuarine environments (Gilmour, Henry, and Mitchell 1992; Fitzgerald, Lamborg, and Hammerschmidt 2007). Researchers determined sulfate concentrations in solutions obtained from batch sorption studies (Figure 2-19). Briefly, solutions of 30 mL Hg-NOM complex dissolved in 10 mM sodium phosphate buffer (pH 7.8) at various concentrations were added to amber glass vials containing approximately 100 mg of COP and equilibrated for 48 h on a rotary shaker. The solid-to-solution ratio was constant for all samples. Sulfate concentrations were determined by ion chromatography with a Dionex ICS 2100 AS9HC9 (Dionex Instruments Corporation, Sunnyvale, California) from filtered sample solutions using 9 mM K_2CO_3 as the eluent. The amount of sulfate released was normalized to the mass of the polysulfide for each sample. The amount of sulfate released correlated with the concentration of Hg-NOM initially added to the sample (Figure 2-19). In the absence of NOM, sulfate concentrations were typically <100 µg per g of sorbent. For samples containing NOM, the sulfate concentration was proportional to the NOM concentration. The results indicate that canola oil polysulfate does not significantly elevate sulfate naturally present in the NOM used in the experiments. Therefore, the deployment of the polysulfide sorbent is not expected to enhance Hg methylation by stimulating sulfate-reducing bacteria in the system.

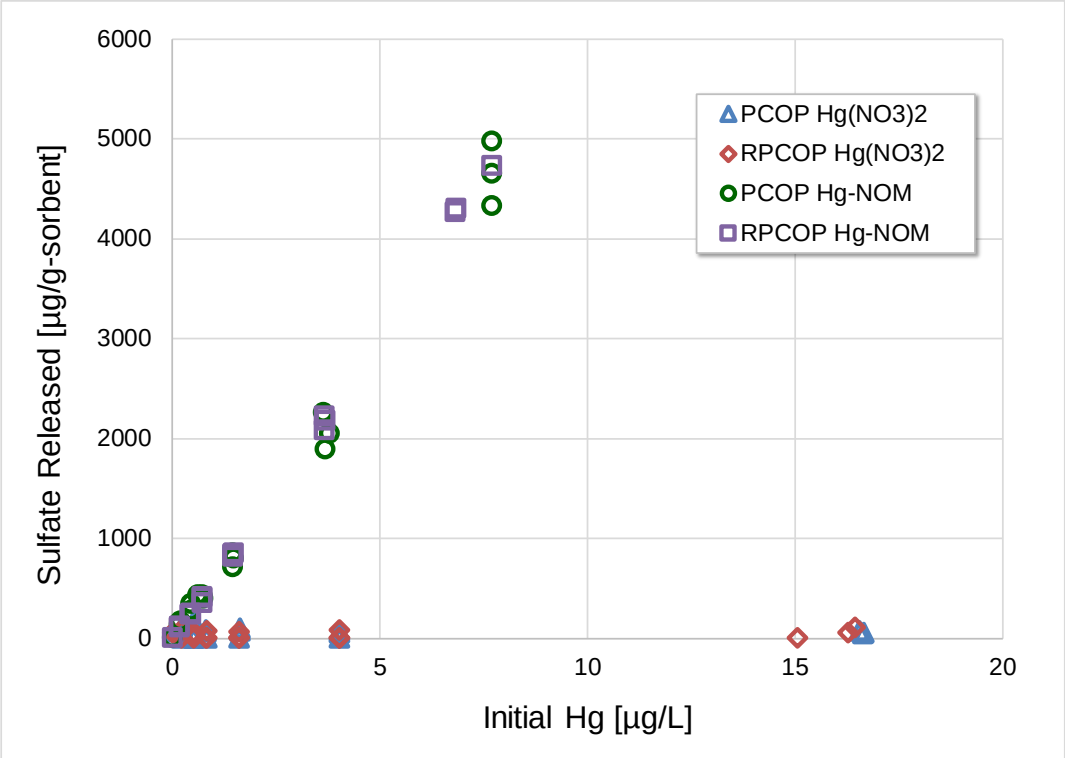

Figure 2-19. Sulfate concentrations normalized to mass of sorbent in 48 h batch equilibrium experiments for porous canola oil polysulfide (PCOP) and reduced porous canola oil polysulfide (RPCOP).

Acknowledgement: Samples of COP for Hg sorption and sulfate release studies were provided by Justin Chalker, Flinders University, Bedford Park, South Australia, Australia.

2.4 GROUNDWATER

Groundwater can contribute to Hg leaching caused by infiltration through contaminated floodplain soils and subsequent discharge by groundwater into LEFPC, and recent recommendations for EFPC call for it to be studied (Looney et al. 2008; US Department of Energy 2014). Further, MeHg production can be significant in the interface between groundwater and surface water, that is, the hyporheic zone (Stoor et al. 2006; Kolka et al. 2011). Previous Hg transport modeling by ORNL researchers suggests a very small potential of Hg or MeHg groundwater contribution to EFPC, but it was deemed that additional on-site data were needed at high Hg locations where HRD was present and that a better understanding of mechanisms was also needed. Because of the earlier recommendations for study (Looney et al. 2008; US Department of Energy 2014), and because of the potential importance of groundwater in generating MeHg (Stoor et al. 2006; Kolka et al. 2011), a groundwater investigation was planned in FY 2015 and implemented in FY 2016–2017. Possible mechanisms of interest for this investigation involved (1) the potential for Hg release due to desorption (see Section 2.2) and (2) the potential for in situ MeHg production in groundwater. Researchers monitored the concentrations of Hg and MeHg in groundwater near LEFPC seeking to understand the relation to surface water Hg and MeHg concentrations. Researchers also wanted to know how Hg and MeHg concentrations, as well as other indicators of groundwater chemistry, change over time and with seasonal variations in water table elevation.

Briefly, the FY 2017 investigations found many results similar to those from FY 2016. Mercury concentrations in groundwater near EFPC are often significant, with total Hg concentrations ranging from

1 to 70 ng L^{-1} and variable over time and location. Of the three observation sites (Figure 2-20), the concentration of Hg was the highest in the vicinity of the HRD layer near EFK 17.8, where the groundwater wells directly penetrate the HRD, which was similar to FY 2016 findings. In this location in particular, groundwater Hg concentrations are usually greater than stream water concentrations. In the other two sites, stream water Hg concentrations typically exceed groundwater concentrations. In addition, limited vadose zone observations at EFK 18.7 continued to identify persistent high moisture contents within the HRD itself and lower moisture contents in the overlying and underlying soils. This suggests that the moisture within the HRD could promote leaching into underlying groundwater and/or the in situ production of MeHg.

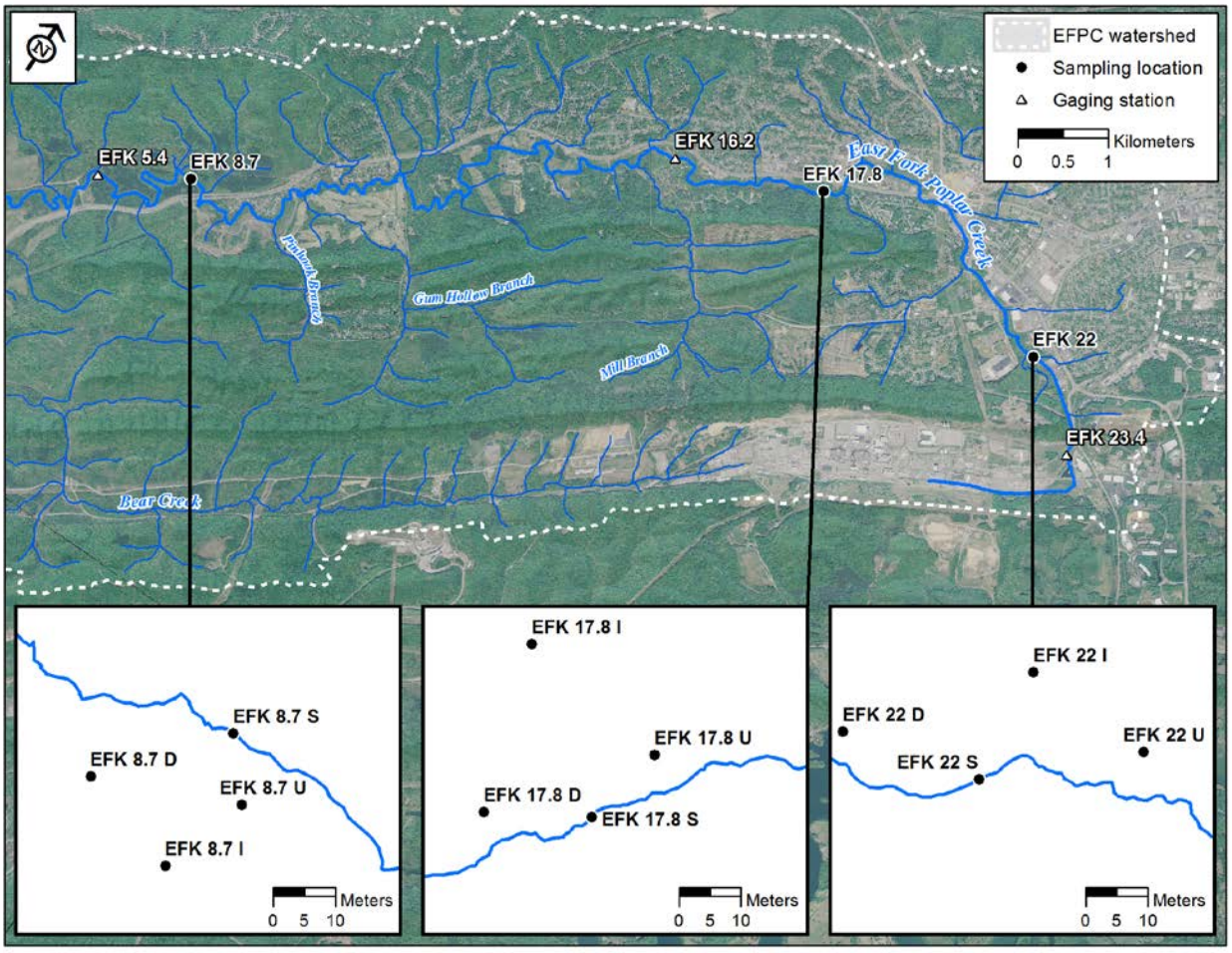

Figure 2-20. Mercury Technology Development project groundwater sampling locations at the National Oceanic and Atmospheric Administration (EFK 22), Bruner (17.8), and Horizon (EFK 8.7) along EFPC.
(Notes: U = upstream; D = downstream; S = stream; I = inland).

In FY 2017, MeHg concentrations were observed that ranged from 0.1 to 10 ng L^{-1}, which was lower than observed in FY 2016 (up to 28 ng L^{-1}). As before, most EFPC values are much higher than expected in uncontaminated sites; for example, less than 0.6 ng L^{-1} near the Great Lakes (Stoor et al. 2006). Importantly and again in FY 2017, concentrations of MeHg in EFPC were *always* greater than concentrations in surface water, which could suggest production of MeHg in groundwater. A predominance of reducing conditions in groundwater was identified, including significant concentrations of sulfide, dissolved iron, and reduced iron in many wells. Methylmercury production is associated with reducing conditions because the microbes responsible are typically sulfate reducers and methanogens and

these microbes are less active under oxic conditions. It is apparent that surface water and groundwater concentrations of all surveyed ions were quite different from each other, suggesting that conditions in groundwater differ from conditions in the stream. The FY 2016 and FY 2017 conclusions suggest that groundwater monitoring provides new and important insights into potential sources of Hg and MeHg. However, the overall similarity of the results from FY 2016 and FY 2017 calls for reductions in groundwater monitoring in FY 2018.

2.4.1 Groundwater Well Installation and Sensor Instrumentation

Installation of the groundwater wells was presented in the FY 2015 report (Peterson et al. 2016). Briefly, there were three sites—the National Oceanic and Atmospheric Administration site at EFK 22, the former Bruner's Market site at EFK 17.8, and the Horizon site at EFK 8.7. Three groundwater wells were installed at each site. Two wells were installed in relatively upstream (U) and downstream (D) positions near the creek bank, respectively, and one well was installed somewhat inland (I), to make a triangle shape in the map view (Figure 2-20). Wells at EFK 22 ranged from 5 ft, 5 in. to 7 ft, 6 in. below ground surface (BGS); wells at EFK 17.8 ranged from 10 ft, 5 in. to 10 ft, 10 in. BGS; and wells at EFK 8.7 ranged from 7 ft, 2 in. to 10 ft, 4.5 in. BGS. There is one stilling well at each site in the stream (S) and attached to the creek bank. In Situ Aqua Troll 200 sensors were installed in FY 2017 to gather continuous data on pressure head (water table elevation), temperature, and conductivity for all groundwater and stream water wells.

As mentioned in Peterson et al. (2016), continuous cores from each location were collected and are currently in storage at -80°C at ORNL. A complete investigation of the cores, including microbiological characterization, is necessary. Because microbiology is out of scope for this project, other funding sources for this activity might be sought in FY 2018.

2.4.2 Results of Groundwater Monitoring

Continuous automated monitoring of the pressure head levels (water table elevation) of the U, D, and I groundwater wells coupled with the instream S well will facilitate construction of the potentiometric surface of the water table in the vicinity of the creek (e.g., Figure 2-21). The direction of stream flow is shown with blue arrows. Flow can be inferred to be in the direction of decreasing groundwater elevations and perpendicular to the gray flow lines. In Figure 2-21, groundwater elevations are averaged over every month. The coverage of data is far improved over FY 2016, and unlike in FY 2016, no flow reversals are observed; that is, flow is consistently toward the creek from the wells. However, analysis of individual precipitation events has not yet been completed, so shorter-term flow reversals could still occur. Note that data are available but are not yet updated for March to September.

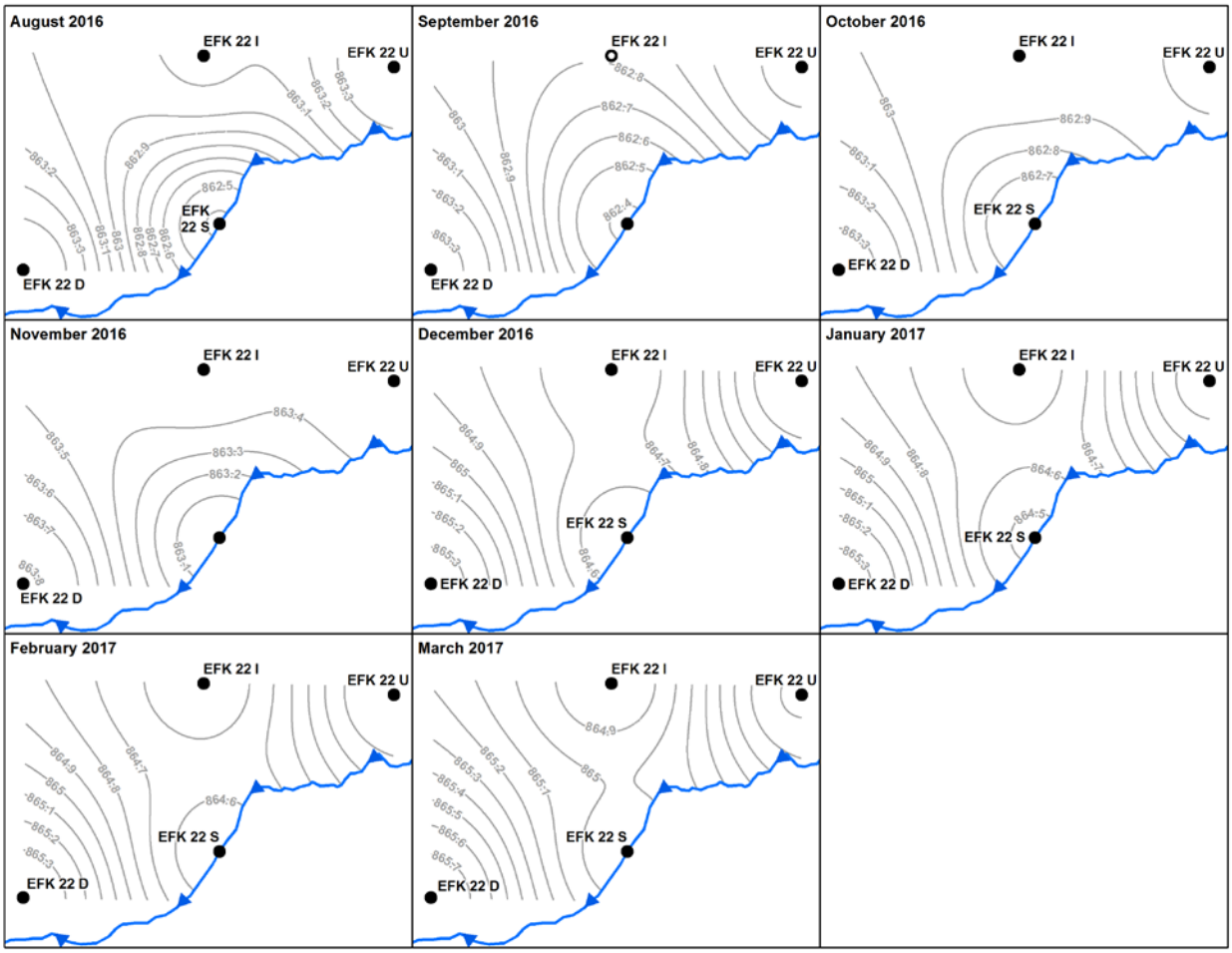

(A)

Figure 2-21. Example potentiometric surfaces (i.e., elevations of equal head) at (A) EFK 22, (B) EFK 17.8, and (C) EFK 8.7. The inland (I), upstream (U), and downstream (D) wells, as well as the instream (S) stilling well, are depicted in real space on the inset figures. The stream is noted by the blue lines, and flow direction is noted by the arrows. The potentiometric surface (water table elevation) is depicted with subparallel gray flow lines with groundwater elevations noted in feet. Flow direction can be inferred to be perpendicular to the flow lines.

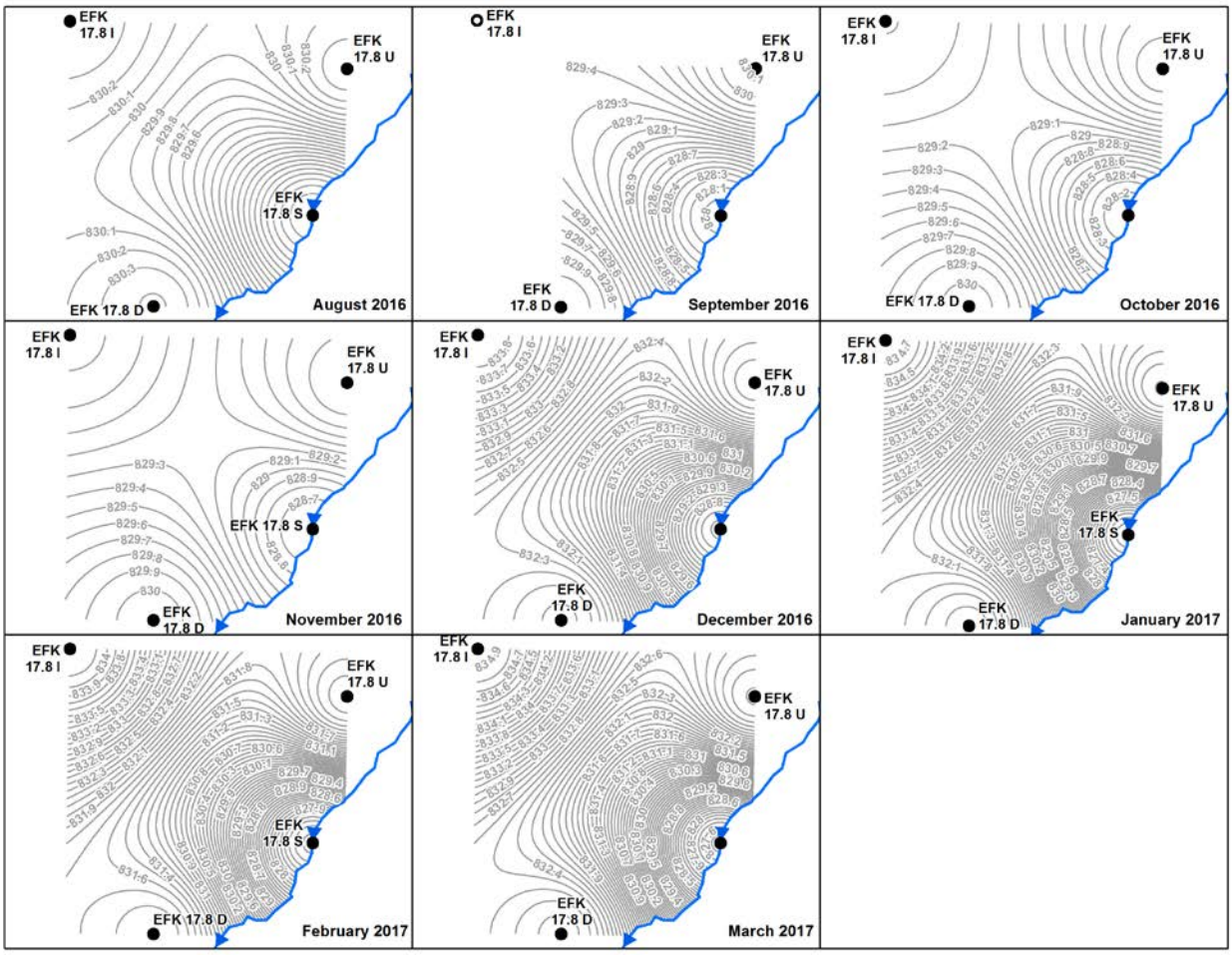

(B)

Figure 2-21. (continued)

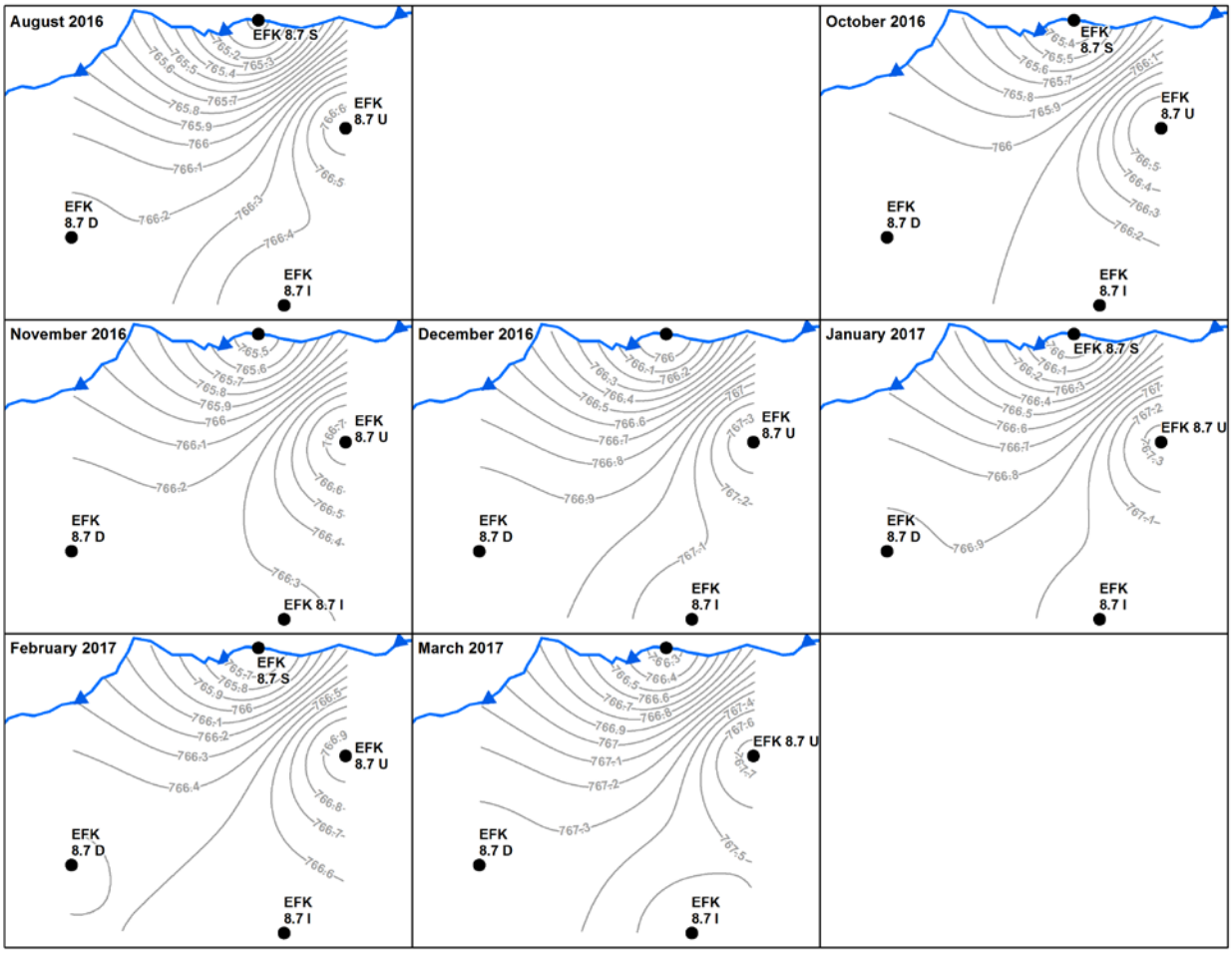

(C)

Figure 2-21. (continued)

An understanding of how water table elevation changes as a function of time—for example, during seasonal changes, storm events, drought events—is possible because automated data are collected every 15 min. This is a powerful way to understand relationships between groundwater and surface water and the extent to which groundwater contributes to the stream and vice versa. In particular, examining the data as a function of time during different seasons, and during specific events, will also be interesting. With years of data now available, analyses provide consistent information suitable for a conceptual and quantitative interpretation. The temperature and conductivity readings (not shown) might also help elucidate the signature of the groundwater versus the surface water and connect to the potentiometric surface interpretations.

Manual sampling is performed to determine Hg and MeHg concentrations, DOC, dissolved oxygen (DO), pH, ferrous (Fe^{2+}) and total iron (FeT), sulfate (SO_4^{2-}) and sulfide (S^{2-}), anions, and cations. since December 2015, 11 groundwater samplings have occurred on a bimonthly schedule. Instream Hg concentrations decrease with downstream distance, and MeHg concentrations increase downstream (Figure 2-22), which is consistent with findings from Task 2 of this project. Figure 2-22a shows the average Hg concentrations for all 11 sampling events. The color scheme represents DOC concentrations, where yellow concentrations are low and green concentrations are high. High DOC is not consistently associated with high Hg, which is a different interpretation than was suggested by the FY 2016 data. Overall, both stream and groundwater average Hg concentrations were higher in FY 2017 than in FY 2016. Seasonal variability is significant in groundwater Hg concentrations, causing around twofold variations over the course of a year.

Figure 2-22b shows average MeHg concentrations for all 11 sampling events, with the color scheme representing dissolved sulfide concentrations, where yellow concentrations are low and green concentrations are high. Qualitatively, most MeHg concentrations in groundwater wells are associated with high sulfide, which could be related to the fact that methylation and sulfate reduction occur under similar geochemical conditions (i.e., reducing conditions) and involve a similar suite of the microbial community. High sulfide is not observed in stream water because sulfide is associated with anoxic conditions. Overall, average groundwater MeHg concentrations were lower in FY 2017 than in FY 2016, whereas average stream water MeHg concentrations appear unchanged. Seasonal variability is more significant than that observed for Hg, causing up to fourfold variations in MeHg concentrations over the course of a year. Concentrations of iron and sulfur redox indicators were also highly variable.

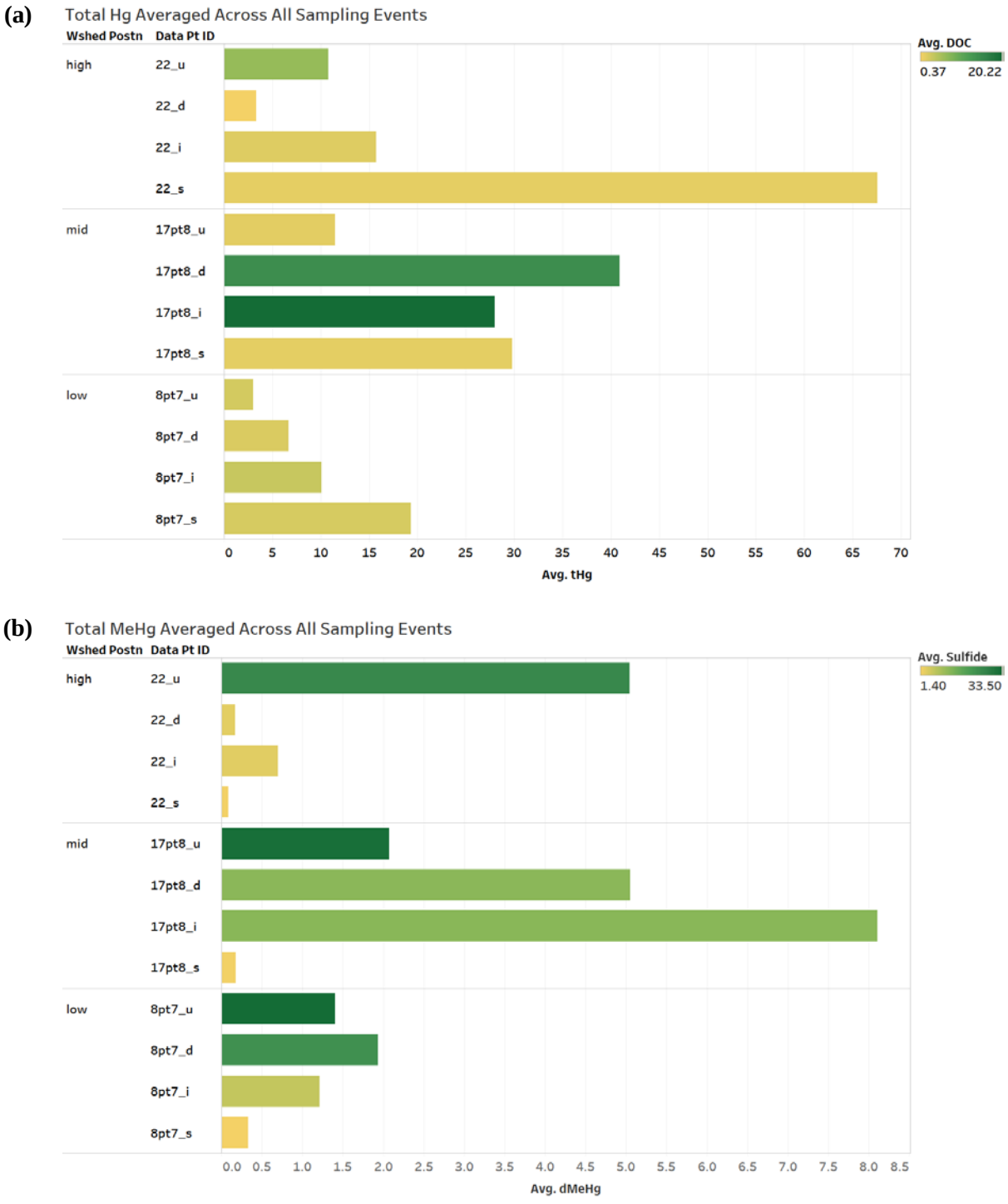

Figure 2-22. Groundwater and stream water analyses at EFK 22, 17.8, and 8.7, at upstream (U), downstream (D), and inland groundwater wells (I), and in stream water (S) for all sampling events since December 2015. (top) Total Hg (ng L^{-1}) as a function of DOC concentrations, and (bottom) dissolved MeHg (ng L^{-1}) as a function of sulfide (S^{2-}) concentrations.

2.4.3 Vadose Zone Monitoring

Researchers were particularly interested in understanding the moisture dynamics of the HRD layer because if it remains wetter than the overlying and underlying soils it could promote leaching of Hg or become a localized zone for MeHg generation. The HRD is known to be texturally distinct, with lower bulk density, higher water content, and coarser particle sizes in comparison to the overlying and underlying soils (Section 2.2). Normally, these properties would promote drainage. However, the overlying and underlying soils have high clay contents and are restrictive to infiltration (Dickson et al. 2015; Peterson et al. 2016). Therefore, researchers hypothesized the tighter surrounding bank soils could cause perching of moisture in the HRD layer. In FY 2016, the creek bank was instrumented with four moisture and temperature sensors (Table 2-3). Researchers identified clear and persistent high moisture contents in the HRD, especially at 70 cm but also at 50 cm (Figure 2-23), where the scale on the y-axis refers to relative moisture content (i.e., 1.0 means the layer in the vicinity of the sensor is saturated). These conditions persisted from the beginning of taking measurements in April to June 2016 (Dickson et al. 2015; Peterson et al. 2016), after which moisture content dropped. Later, events in August and September each caused saturation in the lower HRD layer, followed by rapid desaturation. By late December 2016, the lower part of the HRD layer was saturated again.

Table 2-3. Depths (in centimeters below ground surface) of moisture and oxygen sensors in the floodplain near EFK 18.7. Boldface type indicates sensors within the HRDs

Pit 1 (96 ft from creek bank)		Pit 2 (56.5 ft from creek bank)		Creek bank
Moisture	**Oxygen**	**Moisture**	**Oxygen**	**Moisture**
18	18	24	29	20
30.5	**35**	**49**	**53**	**50**
38.5		**53**		**70**
56	55	72	80	115

In FY 2017, two additional outlays of vadose zone sensors were installed near EFK 18.7. Two pits were hand dug in the floodplain at 56.5 and 96 feet from EFPC, respectively. The sensors were emplaced between the downstream and inland groundwater wells. In both locations, the HRD was visibly observed after the excavation (Figure 2-24). Moisture sensors were installed at four locations in each pit, and Apogee oxygen sensors were installed in three locations in each pit (Table 2-3), with the middle sensors placed within the HRD. The oxygen sensors are designed to identify low oxygen content in the subsurface, which would be consistent with conditions for MeHg production. Example results are shown for only a short period (Figure 2-25) because the installation experienced many difficulties in FY 2017, including floods, data logger failure, problems with coding, and vandalism. However, the persistent high moisture content of the lower HRD is apparent. The oxygen results are as expected; high O_2 is observed near the surface, which declines as a function of depth, so there is no indication of low O_2 content in the HRD. The site has been fully operational for several months late in FY 2017, but the data have not been curated yet.

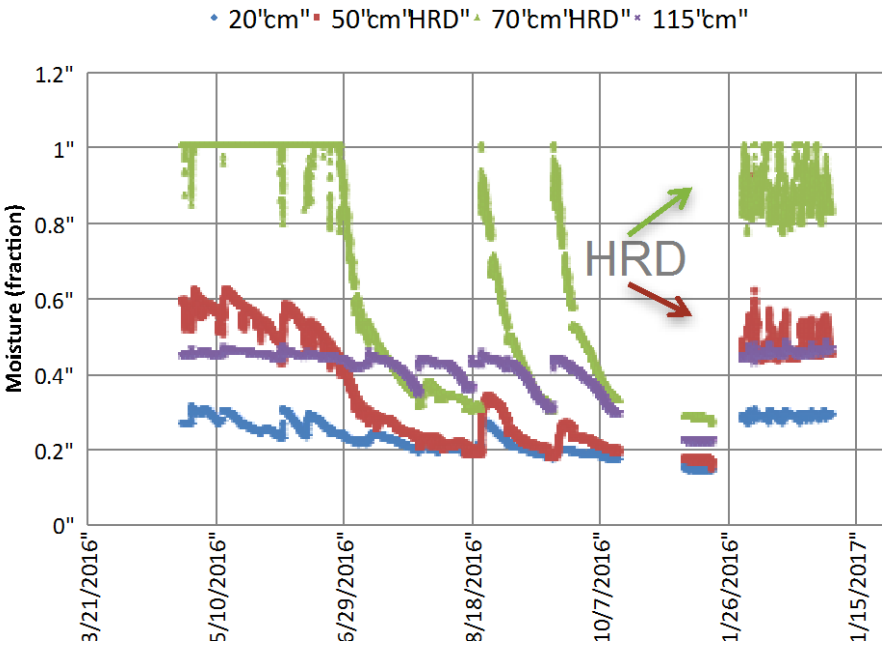

Figure 2-23. Soil moisture in the creek bank at EFK 17.8. Sensors are emplaced overlying the HRD at 20 cm BGS, two inside the HRD at 50 and 70 cm BGS and one below the HRD at 115 cm BGS.

2.5 TASK 1 FUTURE DIRECTIONS

Research to-date has isolated the highest priority materials in the EFPC stream banks, the HRD layer, and its outcrop locations. Additional work connecting erosion with Hg/MeHg concentrations remains of interest for FY 2018 but needs to involve an integrated multitask perspective. To better evaluate the results from earlier batch release experiments, in FY 2018 additional analyses of cations in the reacted solutions and geochemical reaction modeling will be conducted. FY 2018 will focus on evaluation and interpretation of the various Task 1 studies to date—in conjunction with other Task results—to provide a comprehensive watershed-scale conceptual model of Hg processes and the targeted potential sources and pathways for remediation and technology development. To proceed with identifying and testing development applications, a comprehensive and integrated conceptual model is needed that involves data and input from all three tasks.

The field-scale groundwater effort will decrease dramatically in FY 2018. The primary focus of future groundwater studies will be at the Bruner Site where Hg concentrations in soil are greatest. A major direction in Task 1 will involve a continued effort to evaluate sorbent materials under field-relevant conditions. Future studies will focus on column experiments with a select set of sorbent materials and effluents from HRD soil columns. Researchers will evaluate sorbent performance over intermediate to long timescales and characterize the speciation of sorbed Hg and its desorption potential. Furthermore, the effect of temporary nonsaturating conditions on the hydraulic properties and removal efficiency of sorbent material will need to be determined. The success of a potential deployment of engineered sorbents will depend on the ability of the sorbent to effectively limit migration of Hg and MeHg associated with NOM, suspended particles, and other mobile species. Studies using contaminated HRD soil columns with downstream engineered sorbent columns will provide key information to validate the efficacy of engineered sorbents. Current results show that only a small amount of Hg is released from soil columns and that the concentrations are much lower than those in batch experiments. Current results also show that

Figure 2-24. Soil moisture and oxygen sensor installation at EFK 17.8. Photos by Carlos Jones, ORNL.

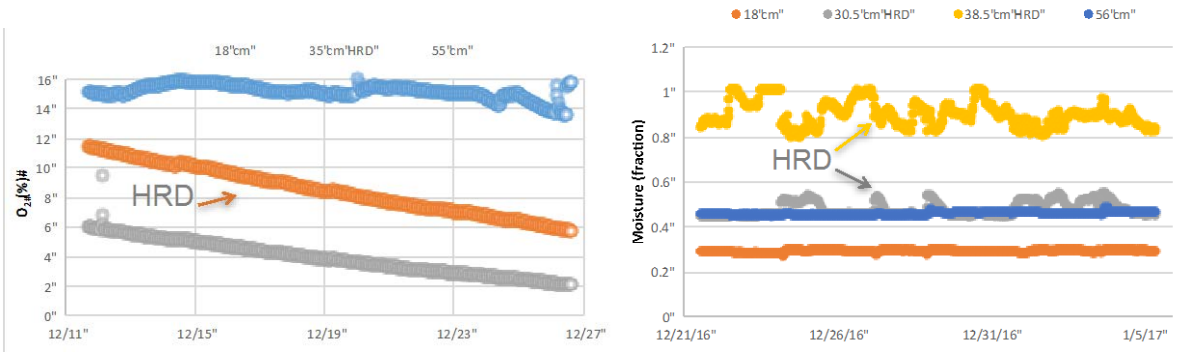

Figure 2-25. Oxygen content and soil moisture in the vadose zone near EFK 17.8. Sensors are emplaced overlying the historical release deposit (HRD) within the HRD, and below it.

the sorbents effectively take up Hg but that the reaction in column experiments is incomplete; that is, Hg elutes the columns. Therefore, more column studies will be essential to validate the utility and mechanisms of the sorbents. Further, only minimal work has considered the release of MeHg and its adsorption to the sorbents; therefore, monitoring MeHg will be an important part of these experiments. Eventually, this work will transition to the Aquatic Ecology Laboratory (AEL). The AEL will enable many more experiments at larger and more field-relevant scales and will minimize the production of wastes in the laboratory environment. A solid set of long-term, larger-scale validation experiments is truly essential before pilot-scale testing in the field can commence.

The coupled soil column and sorbent work might be placed within TRLs 2–3, where technological solutions are beginning to be applied to problems with sufficient scientific underpinning. Sorbent technologies are expected to limit mobilization of Hg species from contaminated soils and thereby effectively reduce bioaccumulation of MeHg in LEFPC. Bank stabilization might be combined with in situ amendments informed by the studies in Section 2.3, allowing deployment of sorbents in key locations identified in Section 2.2 with minimum perturbation to the existing environment and the ecosystem. Ideally, bank stabilization approaches designed to avoid large-scale, expensive, and destructive soil removal will be identified. It is likely that sorbents will need to be applied in concert with other bank rehabilitation methods such as vegetation removal, bank angle reductions, bank stabilization through physical armoring, and vegetative replantings to stabilize creek banks. Monitoring baseline conditions and manipulation responses is essential to determining the outcomes of pilot-scale tests and identifying the most promising technologies for full-scale implementation. In combination with comprehensive field characterization efforts, these studies will establish a solid scientific basis for testing and future implementation of remediation activities to reduce Hg fluxes and Hg concentrations in fish.

3. TASK 2: SURFACE WATER AND SEDIMENT MANIPULATION

3.1 SURFACE WATER

3.1.1 Approach to Water Chemistry Investigations

Water chemistry can affect the speciation, transformation, and transport of Hg and MeHg, but there remain significant knowledge gaps, particularly in freshwater stream systems. These knowledge gaps limit the ability to make informed remediation decisions for EFPC. In FY 2015, as part of earlier TD project efforts, the current understanding of factors and variables controlling Hg transformations and potential remediation alternatives was summarized (Peterson et al. 2015a), and several key questions were developed to guide research efforts, including the following:

- What changes in Hg and MeHg flux occur along the length of EFPC? Can these changes help prioritize shorter reaches of the creek for targeted action(s) addressing specific issues?

EFPC is operationally divided into two sections: upper EFPC (UEFPC, the ~ 2 km portion of the creek within the Y-12 facility boundaries) and LEFPC (the ~23 km of stream downstream of the Y-12 facility). The water chemistry between these two portions of the stream is very different, and Hg and MeHg behavior is thus very different. Control and mitigation strategies need to account for these differences in Hg behavior and speciation as the water chemistry changes throughout the creek. Although the bulk of this project deals with TD to develop strategies for mitigating Hg contamination in LEFPC, there are reasons to consider treating UEFPC within the broader strategy. Mercury in surface water in UEFPC is accessible, is under DOE control, and is primarily dissolved Hg(II)—a highly mobile, reactive, and bioavailable form of Hg. This combination of access and chemistry provides an opportunity to manipulate the water chemistry to reduce the flux of Hg and the accumulation of MeHg in fish throughout the entire LEFPC stream system.

In FY 2017, through a combination of laboratory and field studies, researchers (1) examined the role of chemicals present in UEFPC water due to ongoing plant operations on the flux and forms of Hg present and Hg methylation processes, (2) estimated Hg flux at several locations along EFPC, (3) performed additional characterization of streambed sediments along the length of EFPC, and (4) conducted laboratory experiments to determine whether sorbents decreased MeHg production. These efforts are ongoing and will provide a solid knowledge base upon which the effects of in-stream manipulations can be evaluated. Results presented in this section are given in terms of both concentration and flux. Whereas biological receptors are likely responsive to concentration, flux is more important from a site management perspective. Flux estimates (1) help support site characterization and conceptual model development; (2) help prioritize locations within a site for remedial action; (3) are used in exposure and risk assessment; (4) inform remediation selection and design; and (5) are used in performance, compliance, and long-term monitoring.

3.1.2 Role of Upper East Fork Poplar Creek Y-12 Water Chemistry and Flux on Lower East Fork Poplar Creek

Historical spills of liquid Hg beads ($Hg[0]_l$) in buildings, soils, and storm drains in the West End Mercury Area (WEMA) and east plant area are the sources of dissolved Hg (HgD) in UEFPC surface water and the Hg that is attached to creek sediment. Mercury-contaminated sediments and $Hg(0)_l$ found in the Y-12 storm drains and UEFPC are exposed to some anthropogenic chemicals on a continual basis, whereas other chemicals are discharged only episodically (Peterson et al. 2015a). Chlorine (in potable water), dechlorination chemicals (ammonium bisulfite), and steam plant corrosion inhibitors (primarily amines) are released on a continuous basis via permitted discharges at Y-12. Treatment chemicals from cooling

tower blowdown water are used and discharged only on an intermittent basis, primarily in hotter weather. Many of these low-level continuous- and intermittent-use chemical discharges are known to or have the potential to affect the form and increase the flux of Hg to LEFPC.

The role of these chemicals present in the UEFPC water due to ongoing plant operations on the flux and forms of Hg present and Hg methylation processes is being evaluated in a phased approach using a combination of laboratory- and field-scale experiments. The results of these experiments are being used to help determine the degree to which certain changes in Y-12 chemical usage and discharges could reduce the flux of Hg to LEFPC. In past fiscal years the focus has been on conducting laboratory experiments and site characterization activities to determine the chlorine, chlorination byproducts (e.g., trihalomethanes and chloramine), and dechlorination chemicals that are present and what their impacts are on Hg forms and mobility. In FY 2017, the focus has transitioned to designing and conducting field tests to assess the viability and potential effectiveness of alternative treatment/chemical addition methods for reducing Hg fluxes to LEFPC.

Previously conducted laboratory experiments have shown that chlorine- and sulfite-based dechlorination compounds have the potential to mobilize Hg from beads of $Hg(0)_l$ and Hg-contaminated sediments and that dechlorination with ascorbic acid can reduce this mobilization potential. Residual chlorine is aggressive in its oxidation and solubilization of Hg and, therefore, the Hg in water exiting Outfall (OF) 200 and other OFs contains reactive dissolved Hg(II). Although storm drain discharges are dechlorinated before being released to UEFPC, test results show that eliminating or reducing chlorine concentrations in the storm drain system could significantly reduce the amount of soluble Hg(II) produced from chlorinated water coming in contact with the beads of $Hg(0)_l$ and contaminated sediments found in the storm drains. Reduction of chlorine concentrations in the storm drain system could be accomplished by dechlorinating the process water before or just downstream of discharge points to the storm drains. Reducing the discharge of excess dechlorination compounds (e.g., ammonium bisulfite and sulfite) and/or switching to an alternative dechlorination compound like ascorbic acid could also help reduce the concentration and flux of Hg in surface water. It is also believed that removing chlorine from the storm drain system will result in less Hg being transformed to the oxidized Hg(II) state and a greater fraction of the Hg discharged in the more volatile gaseous Hg(0) form.

The purpose of FY 2017–2018 field testing is to conduct short-term experiments in Hg-contaminated storm drain systems to determine whether dechlorination in the subsurface piping using ascorbic acid (i.e., vitamin C) has the potential to reduce Hg flux from the OFs.

3.1.2.1 Locations for dechlorination field tests

ORNL plans to conduct several short-term field experiments in the storm drain systems of Y-12 and ORNL to determine whether dechlorination in the subsurface piping using ascorbic acid has the potential to reduce Hg flux. Locations at Y-12 being considered for testing include the piping systems leading to OFs 34, 150, 160, 163, and 169. Because site access is easier at ORNL, a preliminary test was conducted in FY 2017 at the ORNL OF211 location to refine the testing methodology. Short-term field tests will focus on continuously adding ascorbic acid in the storm drain piping for one or more OFs for a short period (~4 h) during base flow conditions with the Hg and chlorine concentrations monitored at the OFs. Low concentrations of ascorbic acid would be metered into the pipe through upstream manholes to remove chlorine to the extent possible before encountering Hg contamination within the pipe. Approximately 2.5 parts of ascorbic acid are required for neutralizing 1 part chlorine. It is anticipated that chlorine concentrations in the storm drains will be a maximum of 2.0 ppm; therefore, an equivalent of 10 ppm ascorbic acid would be added to the drains, assuming a treatment safety factor of 2.

Detailed work plans have been prepared for both the Y-12 and ORNL field-test locations. A field test was conducted at OF211 on August 24, 2017, and a Y-12 field test is planned for early FY 2018.

3.1.2.2 ORNL outfall 211 dechlorination test methodology

An initial short-term field test was conducted at OF211 and the associated subsurface drainage system that discharges to White Oak Creek. The test involved adding ascorbic acid through manhole MH211-3 for a short period (~4 h) during base flow conditions with Hg and chlorine concentrations monitored at OF211 (Figure 3-1). Shortly before the test was to be conducted, flow conditions at OF211 changed dramatically when a valve was repaired and discharges dropped from ~60 gpm to ~12 gpm. ORNL proceeded with the field test anyway to refine the testing methodology for use at Y-12 and because Hg and chlorine were still present despite the lower flows at OF211.

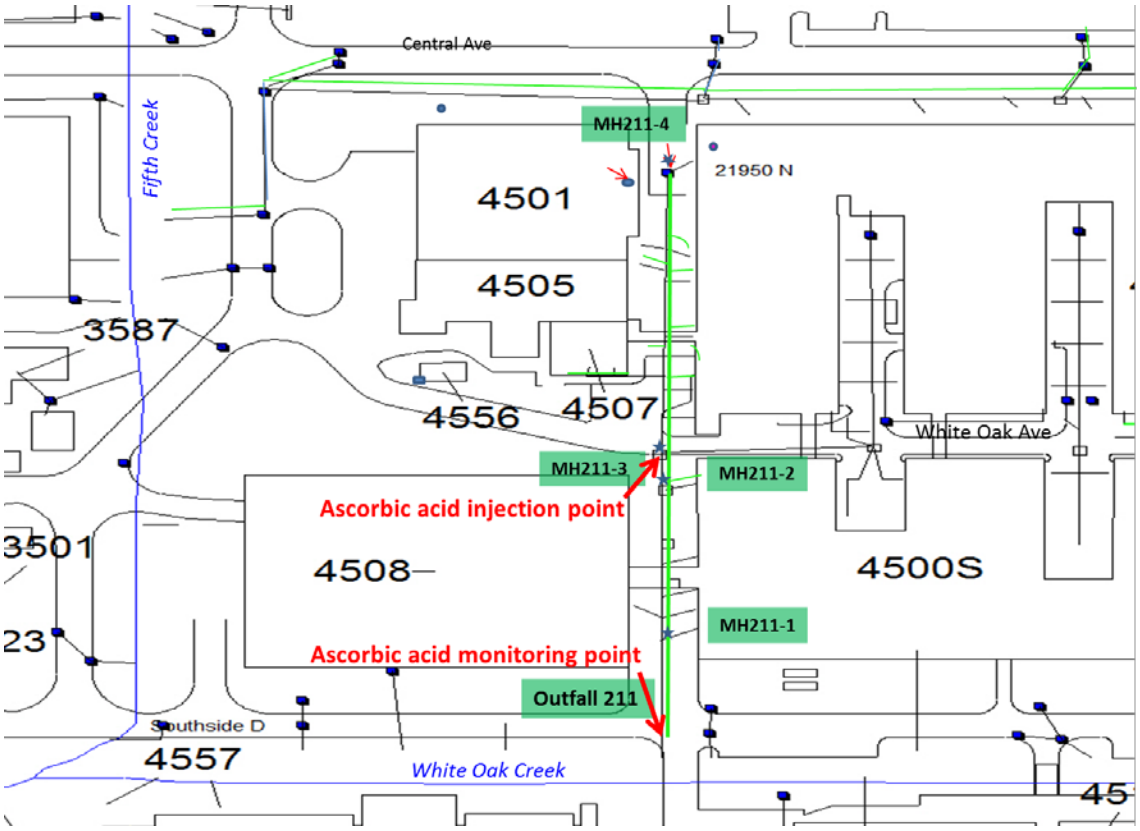

Figure 3-1. Location of ORNL dechlorination field test.

Ascorbic acid was added in the form of soluble Vita-D-Chlor commercially available dechlorination tablets into the drainpipe through manhole MH211-3. The tablets were deployed in mesh flow-through bags (Figure 3-2) lowered into the manhole on a string and placed in the flowing water on the bottom of the drainpipe. During the test, researchers determined that the fast release version of the tablets lasted approximately 2.5 h and that the slow release tablets lasted much longer (~24 h). However, the slow release tablets did not release sufficient ascorbic acid to achieve dechlorination at the flows (~12 gpm) and chlorine concentrations (~1.4 mg/L) encountered during the test.

Figure 3-2. Deployment of ascorbic acid tablets in mesh bags into Manhole MH211-3.

The Hg-filtered (dissolved) and unfiltered (total) samples were preserved with BrCl in the field and run on the Lumex (Zeeman effect atomic absorption spectroscopy) following stannous chloride ($SnCl_2$) reduction. Dissolved gaseous Hg was determined by sparging (bubbling) a water sample in the field with nitrogen to remove all Hg(0), preserving the sparged sample with BrCl, and analyzing the sample in the laboratory using the Lumex system. The amount of Hg(0) can be estimated by subtracting the concentration of Hg in the sparged sample from the concentration of Hg in the unfiltered total Hg sample. An estimate of the Hg(0) concentration was also obtained by running a sample (with no headspace) on the Lumex soon after it was collected with no BrCl or SnCl treatment. The two methods of determining Hg(0) were found to provide similar results, and both are adequate for determining the magnitude of the shift from the Hg(II) form to the Hg(0) form because of the addition of ascorbic acid.

Total and free chlorine were analyzed with a Hach chlorine test kit. Some spot measurements of total chlorine were also made using AccuVac vials to confirm complete dechlorination during the test. Field measurements (i.e., pH, DO, Eh, electrical conductivity, and temperature) were made with a calibrated In-Situ Troll 9500 system. ORNL compliance staff installed a combination temperature/pressure probe beneath the lip of the OF211 concrete culvert. The pressure probe readings provided relative changes in water level at the OF211 outlet.

3.1.2.3 Results of ORNL outfall 211 dechlorination test

Figure 3-3 shows when OF211 and MH211-3 samples were collected in relation to ascorbic acid tablet additions and OF211 temperature and water level fluctuations. Table 3-1 provides a summary of how field parameters (pH, DO, and conductivity), OF211 water temperature and level (flow), chlorine concentrations, and Hg concentrations (unfiltered [HgT], filtered [dissolved], and gaseous Hg[0]) responded during the ascorbic acid dechlorination test. A summary of significant findings and conclusions from the test includes the following:

- The fast release ascorbic acid tablets effectively removed all chlorine from the OF211 storm drain system for time increments of 2 to 2.5 h. The addition of three slow release tablets alone was not effective in removing the chlorine.

- DO and pH were not impacted significantly by the ascorbic acid additions.

- Most of the Hg discharging at OF211 appears to be coming from above MH211-3. Therefore, a reduction in HgT flux at OF211 would not be expected from the ascorbic acid addition at MH211-3 during the test.

- Mercury concentrations at OF211 were higher during the ascorbic acid additions, but it is not clear that there was a cause-and-effect association with the ascorbic acid. The trends in OF211 temperatures, water levels, and conductivity appear to indicate that there is an association between changing storm drain flow and discharge conditions and the variable Hg concentrations observed at OF211.

- Mercury was primarily in the dissolved form at OF211 and MH211-3 before and during ascorbic acid addition.

- The ascorbic acid addition created a significant shift from the Hg(II) to the gaseous Hg(0) form (as much as 86%).

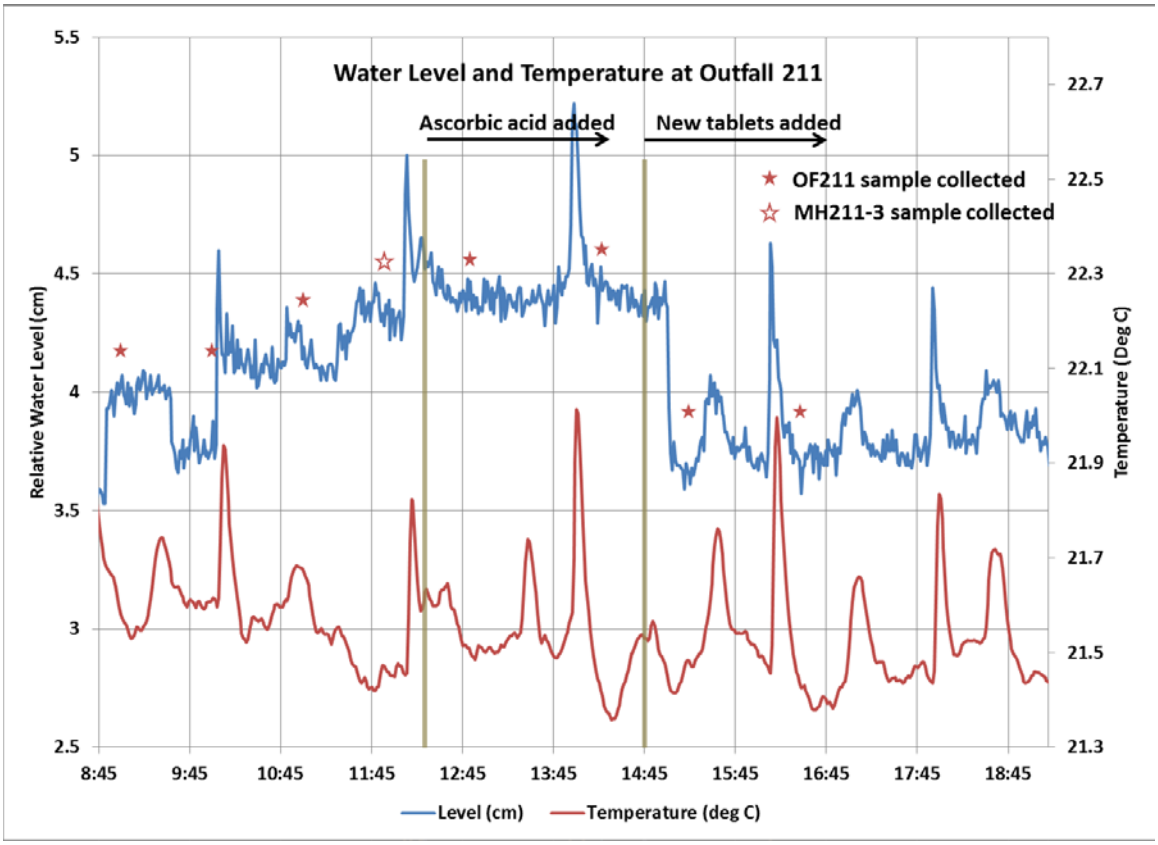

Figure 3-3. Sampling times and ascorbic acid tablet additions compared with temperature and water level fluctuations at OF211.

Table 3-1. Summary of ORNL OF211 ascorbic acid dechlorination test results

Parameter/ observation	OF211 before dechlorination	OF211 after dechlorination	MH211-3 conditions	Comments
Chlorine	Total and free chlorine are similar, ~1.4 mg/L	Total and free = <0.1 mg/L	• Total = ~0.8 mg/L; trace levels present in the past • Free = <0.1–trace	Ascorbic acid tablets effective at removing chlorine; not a good reading at MH211-3
Flow/ temperature	• ~12 gpm initially • ~22°C • Changes in level and temperature coincide	• ~12 gpm, but flow decreases at later times • ~22°C • Changes in level and temperature coincide	• ~5 gpm • ~29°C	Suggests changing variable conditions during test that might correspond to Hg discharges
Specific electrical conductivity	Lower conductivity in general (~250 µS/cm)	• Higher conductivity especially in the beginning (~370 µS/cm) • Might be associated with higher Hg concentration	Somewhat lower (225 µS/cm) conductivity than OF211	Seems to be some association of conductivity with changing flow conditions and Hg concentrations
DO	~8.3 mg/L	~7.8 mg/L	~6.6 mg/L	DO reduced somewhat by the ascorbic acid?
pH	~7.8	~7.7	~7.9	pH not reduced significantly by the ascorbic acid
Unfiltered/ filtered Hg	• HgT ~0.27-0.4 µg/L • Mostly dissolved	• HgT varies between 0.37–0.81 µg/L • Mostly dissolved	• HgT is very high ~3.4 µg/L • Mostly dissolved	Most Hg is coming from above MH211-3; source of HgT fluctuation is unclear
Dissolved gaseous Hg(0)	• Low (1.4–6.9%) • Primarily Hg(II)	• High (55–86%) • Mostly Hg(0)	• Low (0.9–3.2%) • Primarily Hg(II)	Ascorbic acid addition created a significant shift from Hg(II) to Hg(0)

The results of the dechlorination test suggests that ascorbic acid additions combined with gaseous Hg(0) sparging (and/or vacuum extraction) and carbon capture has potential for use as a remedial action to reduce Hg fluxes in storm drain effluent. Laboratory tests are recommended to ensure additives such as binding agents or slow release compounds in the ascorbic acid tablets do not impact Hg mobility.

3.1.2.4 Assessment of chlorine and dechlorination chemical impacts on $Hg(0)_l$ transformations and mobilization from Upper East Fork Poplar Creek

Chemical additions in the Y-12 east plant area (e.g., chlorine, ammonium bisulfite, and cooling tower water) are being investigated because they are thought to have an impact on the Hg dynamics and flux to LEFPC and are not going to be captured by the water treatment facility being constructed at OF200. Testing of the impact of chlorine and dechlorination chemicals on $Hg(0)_l$ beads conducted in FY 2015 (Peterson et al. 2016) clearly show that chlorine and certain dechlorination chemicals enhance the transformation of $Hg(0)_l$ to the more soluble and mobile Hg(II) form, but this testing focused on conditions found in the WEMA. In FY 2016, ORNL conducted additional $Hg(0)_l$ bead tests on water samples collected from east plant area OFs.

Results of $Hg(0)_l$ bead tests conducted on OF034 and OF109 (see Figure 3-1 for locations) are shown in Figures 3-4 and 3-5.

The methodology used to conduct the $Hg(0)_l$ experiments on OF034 and OF109 water was similar to experiments conducted in FY 2015 (Peterson et al. 2016). Small beads of acid-washed $Hg(0)_l$ (50 µL) were removed from a stock container using a gastight syringe and placed in a 40 mL glass vial. All tests were conducted in duplicate. The vial cap was fitted with an outlet port consisting of a Teflon tube (1.6 mm internal diameter) secured approximately 10 mm from the base of the vial. Aqueous samples (1 mL) were withdrawn from the vial with a plastic syringe following a 0.5 mL flush of the sample line. A subsample was analyzed immediately for dissolved $Hg(0)_d$, and the remaining aliquot was preserved with bromine monochloride for total Hg analysis. The concentrations of dissolved $Hg(0)_d$ and total Hg were measured multiple times between 10 and 300 min using a modification of EPA method 1631E (Miller et al. 2013). Oxidized Hg, the combination of Hg(I) and Hg(II), was determined by the difference between HgT and $Hg(0)_d$. However, Hg(II) is used to denote all oxidized species of Hg because Hg(II) is the most likely species present.

For the OF034 testing, samples were collected at the OF034 discharge point before treatment (i.e., with residual chlorine) and after treatment with the ammonium bisulfite drip system to remove the residual chlorine. The $Hg(0)_l$ experiments were conducted on (1) the OF034 water sample containing residual chlorine, (2) the OF034 sample treated at the point of discharge with ammonium bisulfite, and (3) the OF034 water sample with residual chlorine treated with ascorbic acid to remove the chlorine instead of ammonium bisulfite. The OF034 tests show that there is about 2.5 times less HgT generated if the sample is dechlorinated with ascorbic acid instead of the current practice of using ammonium bisulfite (see Figure 3-4). As might be expected, the chlorinated sample from OF034 produces the most HgT in solution, ~10 times more than the sample dechlorinated with ascorbic acid (see Figure 3-4).

For the OF109 testing, samples of OF109 water from the point of discharge were collected and tested before and after treatment with ascorbic acid in the laboratory to remove any trace amounts of chlorine. This testing was conducted to determine whether even these trace amounts of chlorine detected in OF109 could affect the $Hg(0)_l$ transformation to Hg(II). The results shown in Figure 3-5 indicate that for OF109, there is about three times less HgT generated if the sample is dechlorinated using ascorbic acid compared with the total HgT that is generated if the water currently discharging directly to UEFPC at OF109 containing trace chlorine is exposed to the beads of $Hg(0)_l$.

These results are significant because they suggest that the presence of chlorine and bisulfite compounds in UEFPC could significantly increase the concentration and flux of HgT in the creek if $Hg(0)_l$ is present. The use of an alternative dechlorination chemical such as ascorbic acid might reduce the Hg concentration and flux.

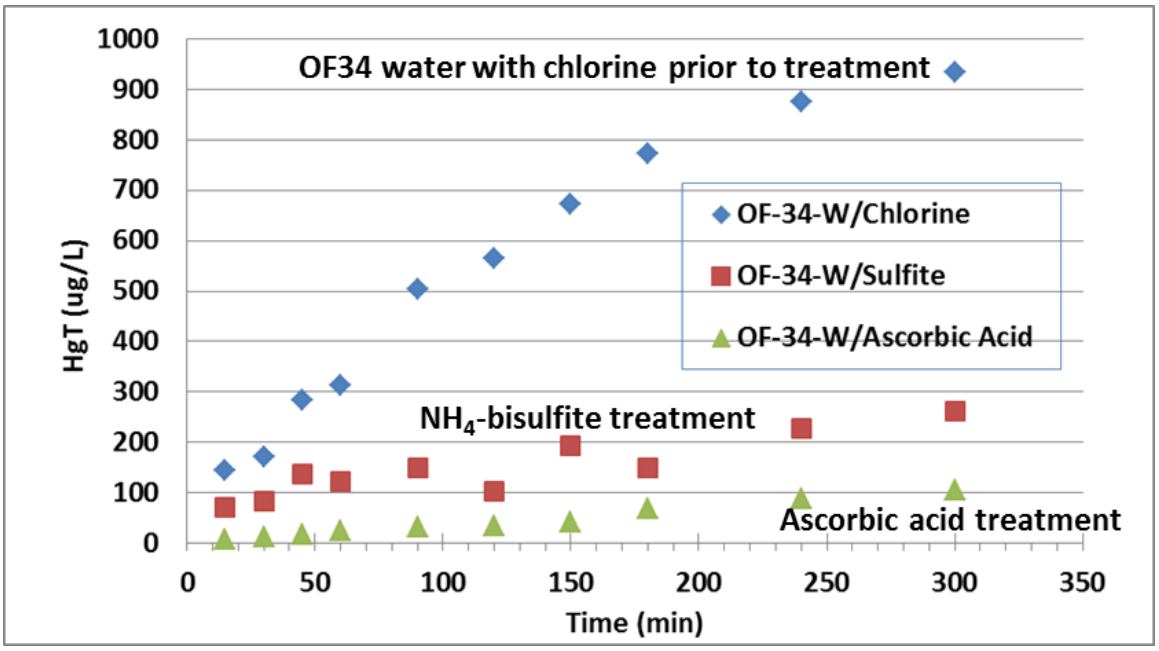

Figure 3-4. OF34 Hg(0)$_I$ bead testing shows that the current practice of treating chlorine in OF034 with ammonium bisulfite might enhance the leaching and mobilization of HgT compared with the alternate use of an ascorbic acid dechlorination treatment.

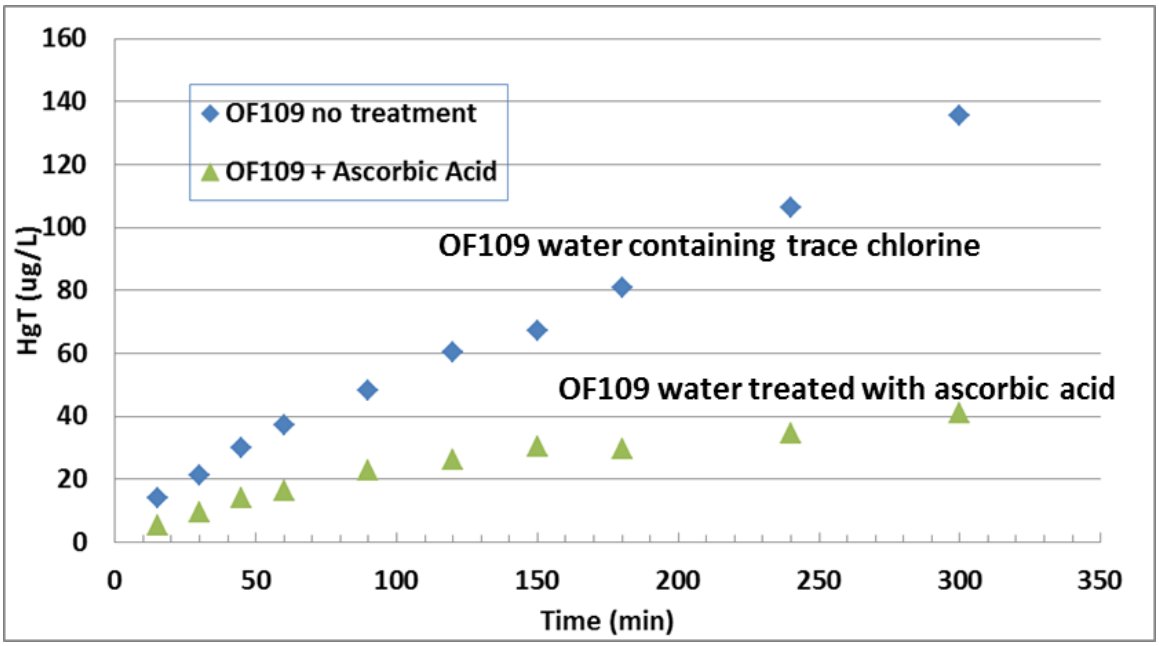

Figure 3-5. OF109 Hg(0)$_I$ bead testing shows OF109 water with trace chlorine results in more leaching and mobilization of HgT than OF109 water treated with ascorbic acid.

3.1.2.5 Assessment of chlorine and dechlorination chemical impacts on mercury transformations and mobilization of Upper East Fork Poplar Creek contaminated sediment

The Hg found on contaminated sediments in UEFPC is likely to be in Hg(II) form complexed to the sediments. Therefore chlorination (oxidizing) and dechlorination (reducing) chemicals will interact and react differently with the Hg on the sediment than previously observed in experiments using $Hg(0)_l$ beads. The general experimental design for the sediment testing was similar to the methods described previously for the $Hg(0)_l$ bead tests, with the primary difference being that 0.5 or 1 gram of sediment collected from near OF109 was placed in the test container instead of a $Hg(0)_l$ bead. Two different sediment size fractions tested include (1) a fine sediment fraction having a 125–250 micron particle size and (2) a medium fraction having a 250 micron to 1 mm particle size. The concentration of Hg on the fine fraction was 100.1 mg/kg, and the concentration on the medium fraction was 64.4 mg/kg. The tests assessing dechlorination compounds were conducted initially using tap water, but the chlorine in the water was causing quantification and data interpretation problems, so chlorine-free deionized (DI) water and/or an artificial (synthetic) creek water that has similar pH (~8.0) and major ion composition to LEFPC were used instead. To reduce the number of analyses required, time series testing was initially conducted to determine how much the concentrations changed over time and to determine whether a single 6 h incubation and sampling time would be representative of equilibrium concentrations (see Figures 3-6 and 3-7).

Figure 3-6 shows that the concentration of Hg in solution per gram of sediment does not change much over a 24 h incubation period when the medium fraction sediment is exposed to tap water containing ~2.6 mg/L chlorine. This experiment (and other tests not presented) resulted in a concentration of approximately 1.0 µg of Hg in solution/g of sediment that remained fairly steady throughout the 24 h incubation period. Figure 3-7 shows that the concentration of Hg (~0.045 µg Hg in solution/g of sediment) does not change very much from 3 to 24 h when the medium fraction sediment is exposed to tap water (~2.6 mg/L chlorine) that has been dechlorinated with ammonium bisulfite. The resulting sulfite concentration in solution was ~1.9 mg/L for this test. At the concentrations tested, exposure of the medium fraction sediment to ammonium bisulfite did result in an increase in the Hg in solution; however, it was much less than what resulted from exposure of the sediment to residual chlorine. From these initial tests, it was determined that for comparison purposes between experiments, a 6 h incubation period is adequate and representative of equilibrium conditions.

Because some relatively high concentrations of sulfite were measured near OF200 (~7.0 mg/L in OF135 and ~5.1 in the creek), testing was conducted with DI water and ACW to assess the impact of ammonium bisulfite concentration on the leaching of Hg from UEFPC sediments. Figure 3-8 shows that for both types of water and for both the fine and coarse sediment fractions the HgT in solution increases in a fairly linear fashion as the sulfite concentration (i.e., ammonium bisulfite) increases. The exception is the batch test, where fine (125–250 micron) sediment that was incubated in ACW resulted in unexplained higher HgT in solution and greater scatter in the concentration detected relative to the other test scenarios. It was not conclusive what combination of sediment type (fine versus medium) and water solutions (DI versus ACW) resulted in more Hg being leached. However, it is clear that the addition of ammonium bisulfite to the solutions (sulfite up to 10 mg/L) could increase the HgT in solution from <0.01 µg Hg in solution/g of sediment to as much as 0.14 µg Hg in solution/g of sediment.

Figure 3-9 shows that for a similar set of sediment incubation experiments conducted using ascorbic acid the amount of HgT in solution was generally less than what resulted from the ammonium bisulfite incubations and was not sensitive to the concentration of ascorbic acid in solution. For the ascorbic acid experiments, the HgT concentration in solution per gram of sediment was actually greater for the medium sediment fraction than for the fine fraction, even though the fine fraction had a higher concentration of Hg. This suggests that the Hg is probably bound to the fine fraction differently and more tightly than it is bound to the medium fraction. Sequential extractions conducted on these two sediment samples also showed that more Hg was extracted using the F1, F2, and F3 extraction solutions for the medium fraction (3.8 mg/kg) than for the fine

fraction (~0.5 mg/kg). This could be because the organic carbon that the Hg might be bound to was higher in the fine fraction (5.2 mg/kg) than it was in the medium fraction (3.1 mg/kg). The DI water resulted in greater HgT in solution than the ACW, probably because the pH of the DI water is lower compared with the ACW water.

These sediment testing results are significant because they suggest that the presence of chlorine and bisulfite compounds in UEFPC could increase the concentration and flux of HgT in the creek due to mobilization of Hg from the Hg-contaminated sediments and bank material. The testing also shows that the use of an alternative dechlorination chemical such as ascorbic acid might reduce the Hg concentration and flux in UEFPC. However, it is important to note these are controlled laboratory studies and that storm drain water chemistry, and stream sediment chemistry, at Y-12 can be complex and highly variable. As was evidenced by the preliminary study using ascorbic acid at ORNL storm drains in late FY 2017, further field evaluation and study is needed before changes are made to dechlorination methods at Y-12.

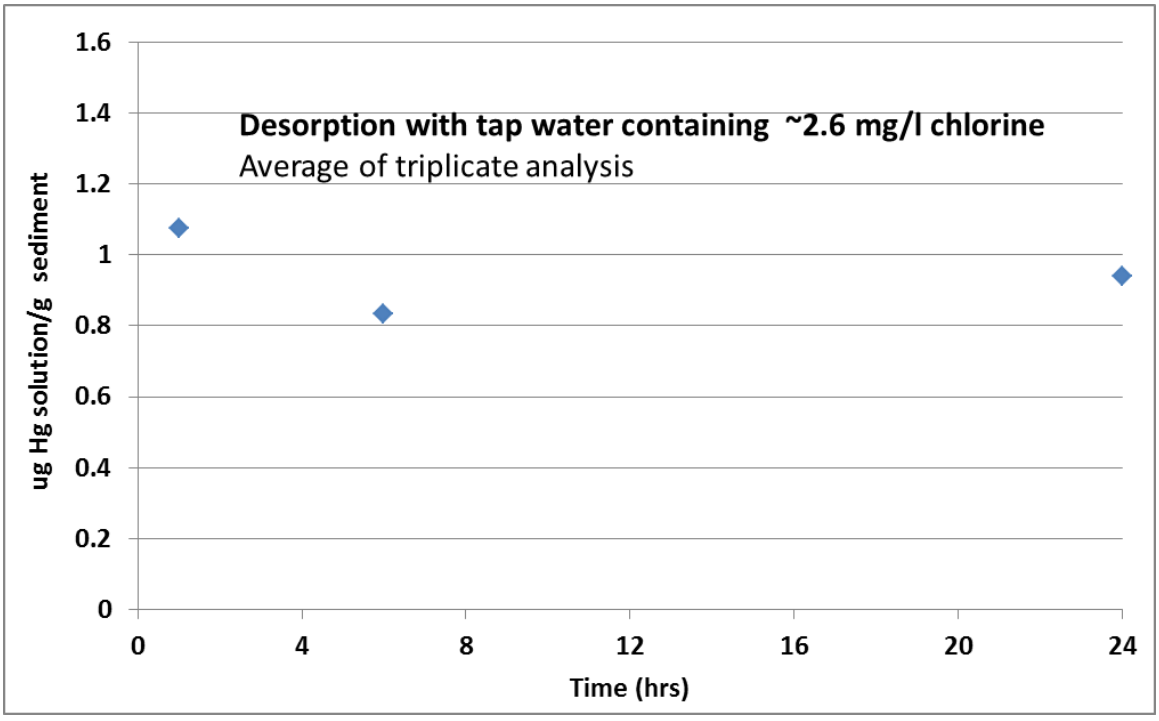

Figure 3-6. Impact of residual chlorine in tap water on leaching of HgT from UEFPC sediments over time (sediment: HgT = 64.4 mg/kg; medium size fraction = 250 µm–1 mm).

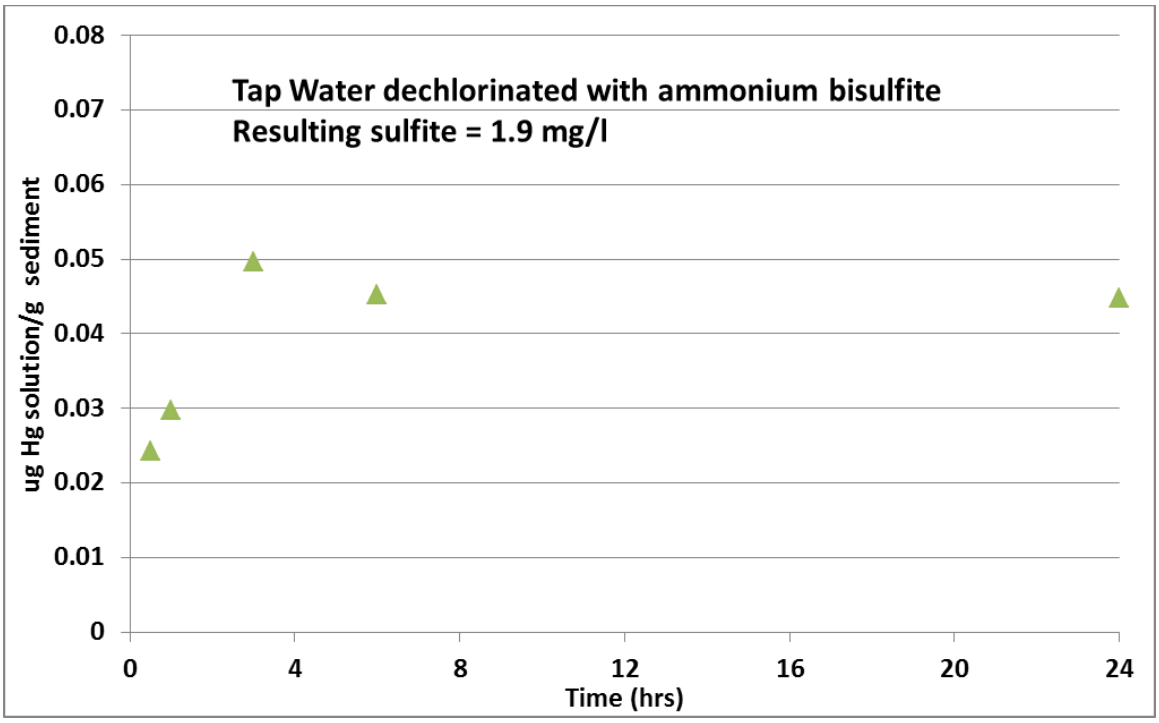

Figure 3-7. Impact of ammonium bisulfite on leaching of HgT from UEFPC sediments over time (sediment: HgT = 64.4 mg/kg; medium size fraction = 250 µm–1 mm).

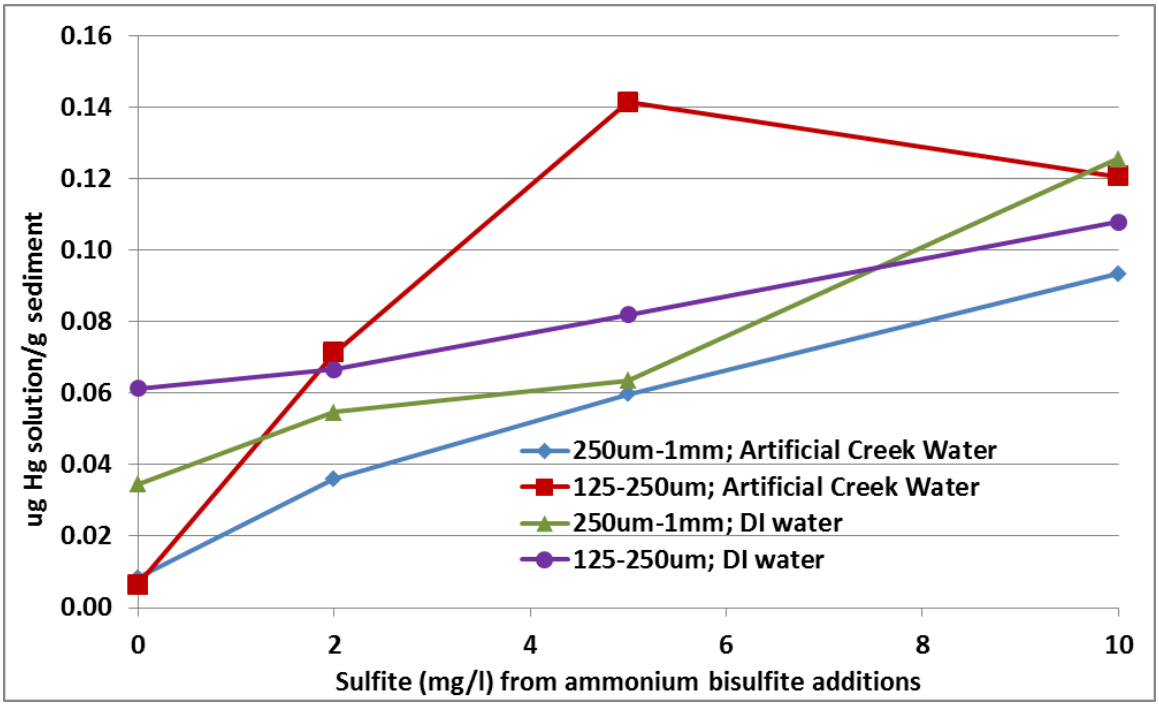

Figure 3-8. Impact of ammonium bisulfite concentration on leaching of HgT from UEFPC sediments with DI water and ACW (sediment: medium size fraction = 250 µm–1 mm; HgT = 64.4 mg/kg; fine

fraction = 125–250 µm; HgT = 100.1 mg/kg).

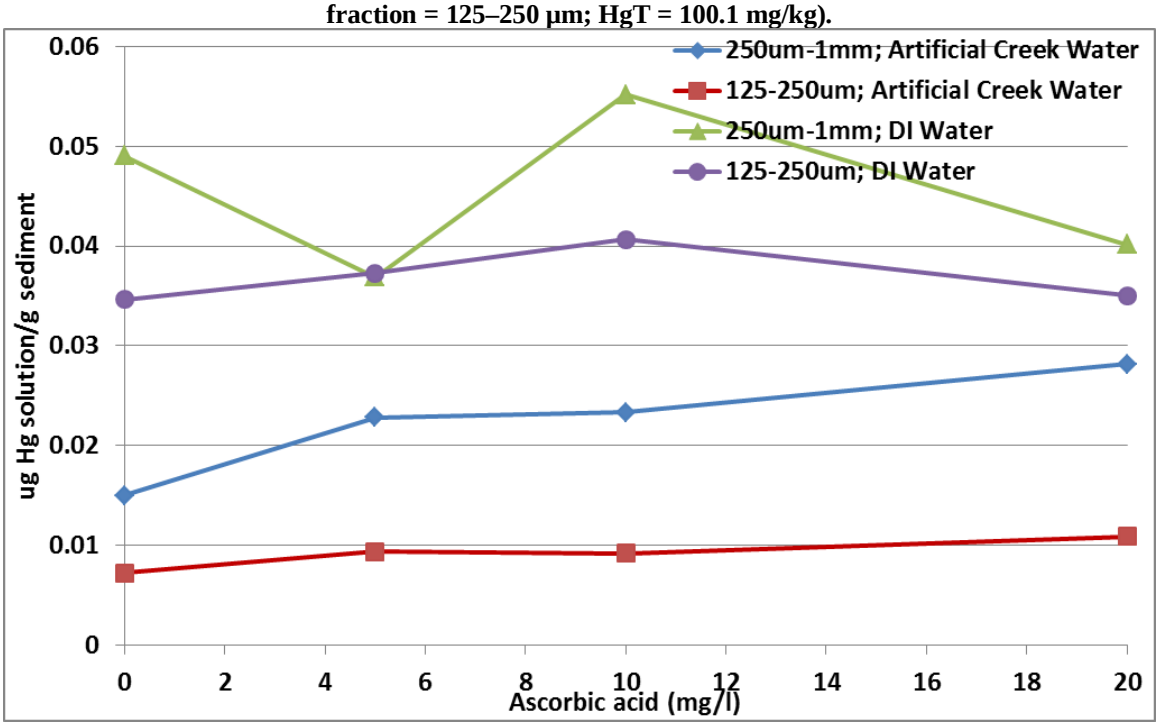

Figure 3-9. Impact of ascorbic acid concentration on leaching of HgT from UEFPC sediments with DI water and ACW (sediment: medium size fraction = 250 µm–1 mm; HgT = 64.4 mg/kg; fine fraction = 125–250 µm; HgT = 100.1 mg/kg).

3.1.3 East Fork Poplar Creek Flow Regime

EFPC is a mixed-use watershed that is highly developed upstream with a large percentage of impervious surface area. Watershed land cover characteristics gradually change downstream, transitioning to more forested and some open field areas. The surrounding land cover has direct implications for the flow regime in EFPC and possible consequences for creek bank stability and habitat suitability.

A high percentage of impervious surface area results in high runoff ratios—the runoff from a 1 acre parking lot is 16 times greater than the runoff for 1 acre of undeveloped land. During stormflow events, water levels rise and fall faster and reach higher peak flows than would be the case without impervious surfaces. These changes lead to channel instability and increased bank erosion. To the extent creek banks hold a significant inventory of Hg (see Task 1), alterations to stream flow resulting from land cover changes can accelerate the delivery of bank soil–derived Hg loads to EFPC.

Installation of equalization tanks in the city of Oak Ridge and future installation of similar tanks inside Y-12 associated with the Mercury Treatment Facility likely will alter flow regime characteristics of EFPC. In turn, bank erosion and sediment transport rates and processes might be altered. Decreased bank erosion associated with lower peak flows would be viewed as a positive change. Conversely, lower peak flows would decrease sediment transport characteristics and could lengthen or diminish the effectiveness of natural contaminated sediment-removal processes. The net effect of these competing processes remains to be determined.

3.1.4 Estimates of Mercury and Monomethylmercury along Flux East Fork Poplar Creek

Both particulate and HgD concentrations in water decrease with distance downstream, whereas creek discharge increases downstream. One question to ask of this pattern is whether the decrease in concentration

is due to actual removal of Hg from the water or, alternatively, whether it is due to dilution by cleaner water entering the creek. One approach to resolving this question is to make measurements of concentration and stream discharge to calculate mass flux:

$$J = CQ\ , \tag{3.1}$$

where J = mass flux (mass per time), C = concentration (mass per volume), and Q = discharge (volume per time).

Regular measurements of stream discharge and water composition are being made under base flow conditions at three locations along EFPC to support flux calculations. These measurements are made at EFK 23.4, EFK 16.2, and EFK 5.4; and by comparing the flux between consecutive stations, one can estimate whether that reach of the creek is a net source or sink of the measured constituent. Additionally, flux is monitored for the OF for the Oak Ridge Wastewater Treatment Facility (ORWTF) at EFK 13.5. All sampling locations are in the LEFPC administrative section of the creek. For purposes of the discussion that follows, the reach from EFK 23.4 to EFK 16.2 is referred to as the upper reach of LEFPC, and the reach from EFK 16.2 to EFK 5.4 is referred to as the lower reach of LEFPC. The upper reach spans the HRD layer described previously in Task 1.

3.1.4.1 Total and dissolved Hg(II) flux

On average, discharge from the ORWTF constitutes less than 1% and 3.2% of HgT and HgD flux, respectively, as measured at EFK 5.4. These amounts ranged as high as 6% and 18% for HgT and HgD, respectively. Nevertheless, the ORWTF is not considered a significant source of Hg flux to EFPC.

Total Hg flux increases in both the upper and lower reaches of EFPC (Figure 3-10a). The additional HgT flux is added most consistently in the upper reach of EFPC. Over the first half of the record, the lower reach made comparable or greater HgT additions to the upper reach. Since approximately April 2016, the lower reach has been neither a source nor a sink with respect to total Hg flux. During that same period, there appears to be a gradual increase in flux in the upper reach.

Dissolved Hg flux (Figure 3-10b) generally increased from EFK 23.4 to EFK 5.4 during the first half of the record. Since June 2016, that pattern is less apparent. The upper reach alternately appeared to be a sink or a source of HgD. Additionally, at both EFK 23.4 and EFK 16.2, there is a statistically significant increase in HgD flux during the period of record (slope of the best fit line to data: EFK 23.4, 7.7E-4 g d^{-1} d^{-1}, $p = 0.021$; EFK 16.2, 7.5E-4 $p = 0.003$ g d^{-1} d^{-1}).

Mercury stable isotope studies, conducted under the Hg Science Focus Area project, suggest that hyporheic water might be a likely source of the added Hg. This finding supports investigations that target creek sediments to control Hg flux in EFPC.

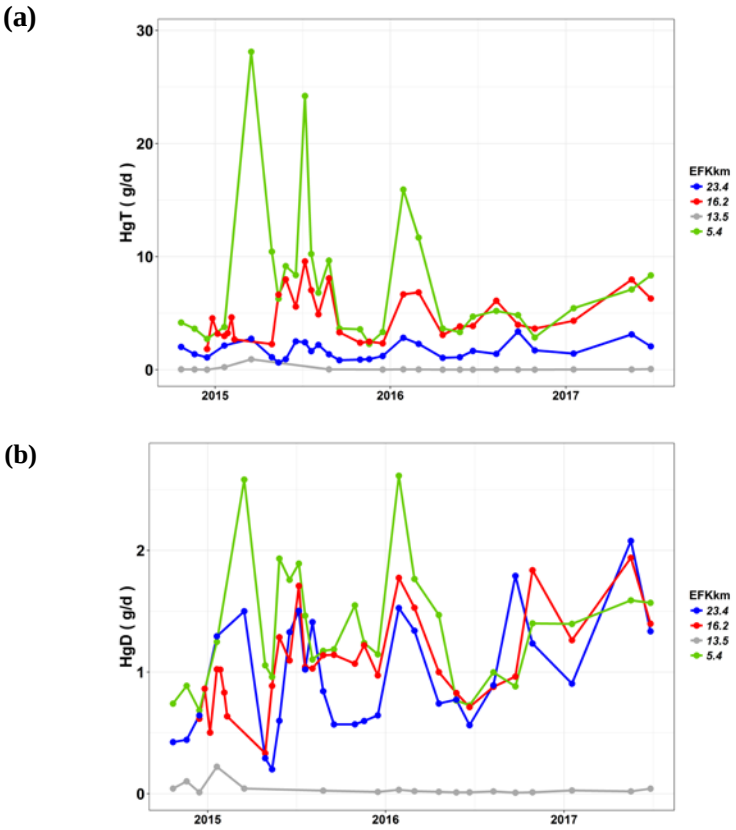

Figure 3-10. (a) HgT and (b) HgD base flow flux at four locations along EFPC. EFK 13.5 is the outfall from the ORWTF.

3.1.4.2 Total and dissolved monomethylmercury flux

Both the upper and lower reaches of EFPC are sources of total and dissolved MeHg (MeHgT and MeHgD, respectively; Figure 3-11). Methylmercury loading from the ORWTF is comparable with that at EFK 23.4. This OF constitutes on average less than 5% of the MeHgT and MeHgD flux as measured at EFK 5.4, although it has contributed up to 15% of that flux.

Total MeHg and MeHgD flux for the upper reach is relatively constant throughout the year. In contrast, MeHg flux in the lower reach shows strong seasonality with higher flux in the spring through autumn and lower flux in late autumn through winter. The different effect of season on MeHg flux patterns for the two reaches might be related to different land cover and land use for their surrounding watersheds. The upper reach is heavily developed with a large percentage of impervious surface, whereas the watershed around the lower reach is largely forested with some open fields and much less impervious surface.

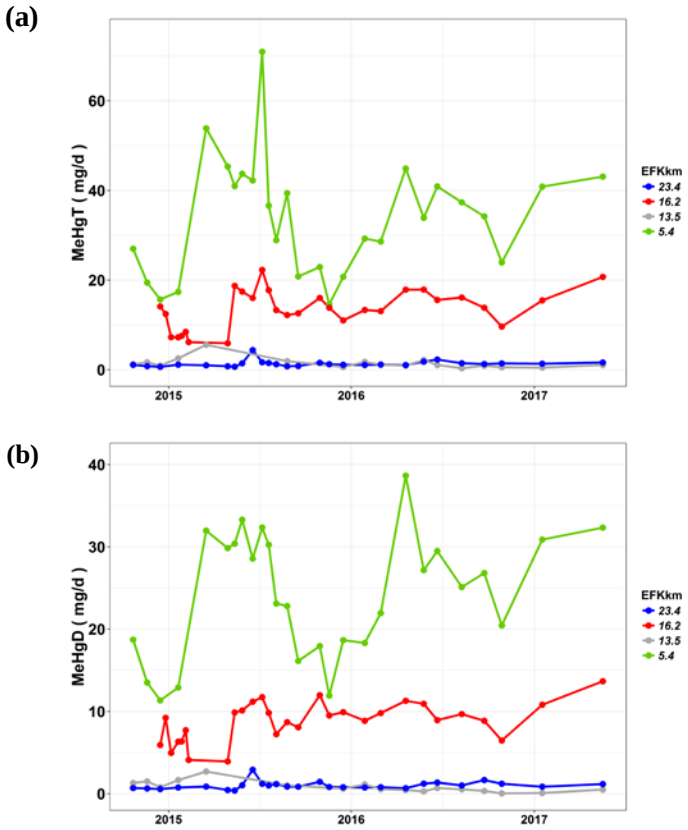

Figure 3-11. (a) MeHgT and (b) MeHgD flux at four locations along EFPC. EFK 13.5 is the OF from the ORWTF.

3.1.4.3 Indications from flux measurements

The results presented here are base flow flux estimates for four locations along lower EFPC. Previous work has shown that annual Hg and MeHg flux budgets are dominated by high flow events (Riscassi, Miller, and Brooks 2016). Nevertheless, the base flow measurements provide important insights that would not be apparent from sampling low-frequency, high-discharge storm events. As discussed previously, flux measurements contribute to conceptual model development and help prioritize locations for remedial action.

Total Hg flux consistently increases in the upper study reach (EFK 23.4 to EFK 16.2), whereas in the lower study reach (EFK 16.2 to EFK 5.4) there has been no increase in flux over the last 18 months. This suggests that the upper study reach would be a priority location for actions to lower Hg input to the creek from locations outside of Y-12. More detailed measurements of erosion and leaching are needed, but it seems that the HRD (located entirely within the upper study reach) would be a high priority target for directed remedial actions to lower the additional Hg flux occurring outside of Y-12.

The lower study reach is the larger contributor to MeHg flux and would be a higher priority for targeted actions directed at addressing the MeHg issue. Higher spatial resolution sampling conducted under the Mercury Science Focus Area project has not identified more localized areas within this reach to further concentrate actions.

3.1.5 Effect of Flow Management Cessation in Lower East Fork Poplar Creek

Beginning in late 1996, a flow management project was initiated in which ~4.5 million gallons of water per day from Melton Hill Lake were added to UEFPC just a few meters downstream from OF200. The flow management project ceased on April 30, 2014, with the intent of decreasing Hg flux exiting Y-12 at EFK 23.4 (Station 17). Since that time, water quality along the length of EFPC has been monitored to assess what, if any, ancillary effects there might be throughout the creek corridor. A summary of current results follows with an emphasis on Hg and monomethylmercury (MMHg) behavior.

Early in this project, the value of monitoring and understanding Hg partitioning between the solid and dissolved phases was highlighted in Peterson et al. 2015a, p. 35. This behavior can be quantified via the distribution coefficient, or K_d:

$$K_d\left(\frac{V}{M}\right) = \frac{Hg_{solid}\left(\frac{Mass\ Hg}{Mass\ solid}\right)}{Hg_{dissolved}\left(\frac{Mass\ Hg}{Volume\ solution}\right)}, \tag{3.2}$$

where K_d = distribution coefficient (units of volume per mass), Hg_{solid} = Hg concentration on solid phase (mass per mass), and $Hg_{dissolved}$ = dissolved concentration of Hg (mass per volume). A higher K_d value corresponds to a higher affinity of Hg for the solid phase. In this work, dissolved Hg is operationally defined as that which passes a 0.2 µm pore size filter. Other workers, and much of the historical data for EFPC, have used a 0.45 µm pore size filter to operationally define dissolved Hg. Use of a larger pore size might lead to higher estimates of dissolved Hg concentration and consequently a lower, or underestimated, K_d value.

The K_d values presented here were derived by measuring the total and dissolved Hg concentration in water and the concentration of total suspended solids (mass per volume). Concentration on the solid phase was derived as the difference between the total and dissolved concentration divided by the total suspended solids value. The resulting K_d is an apparent value because these do not strictly conform to assumptions of a true K_d value. For example, samples were collected throughout the year, so temperature varied among samples, and the underlying equilibrium assumption is uncertain.

Throughout LEFPC, the K_d value for Hg has decreased substantially since cessation of the flow management program (Figures 3-12 and 3-13). Current K_d estimates are up to 10 times smaller than estimates based on historical data. The decline in K_d could be even greater—as mentioned previously, the use of larger pore size filters in previous studies might have resulted in underestimates of K_d. With respect to Eq. (3.2), the decline in K_d has been driven by a combination of both lower Hg concentration on the solid phase and increased dissolved Hg concentration.

In a more mechanistic sense, pH and DOC concentration have a large influence on metal solid:liquid partitioning in general and for Hg in particular. Neither the pH of the creek nor the DOC concentration has shown directional changes that would be consistent with the observed changes in Hg K_d. In addition to measuring DOC concentration, the UV light absorbance of water samples has been measured. This measurement, referred to as the SUVA at 245 nm (SUVA-254), is a proxy measure of organic matter composition in the water sample. This characteristic has been shown to be positively correlated with organic matter molecular weight, percent aromaticity, and hydrophobicity. More importantly in this case, the SUVA-254 value has been positively correlated with dissolved Hg and dissolution of HgS minerals and has been strongly correlated with Hg methylation rate constants. Since flow management was turned off, the SUVA-254 of water has increased throughout much of LEFPC. Thus, changes in Hg K_d might be due, in part, to changes in the composition, rather than the concentration, of organic matter in EFPC.

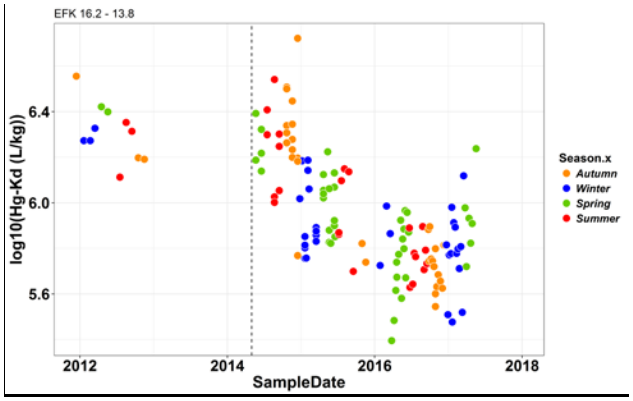

Figure 3-12. Changes in Hg solid:water partitioning coefficient after flow management stopped. Data shown are for the section of EFPC between EFK 16.2 and EFK 13.8, which is upstream of the ORWTF. In this section, the decreasing K_d is driven by increases in dissolved Hg concentration. The vertical dashed line indicates the end of flow management.

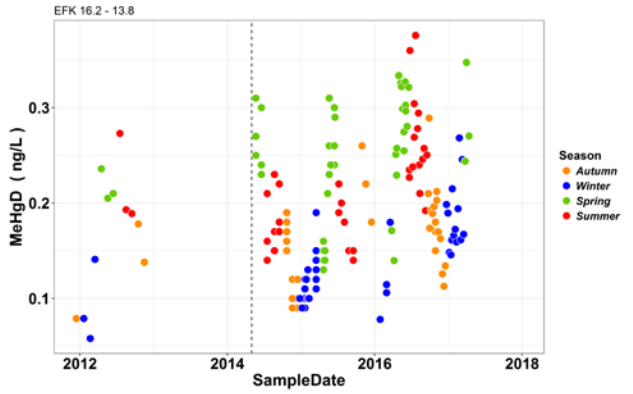

Figure 3-13. Dissolved MMHg concentration after flow management stopped. Data shown are for the section of EFPC between EFK 16.2 and EFK 13.8, which is upstream of the ORWTF. The vertical dashed line indicates the end of flow management.

In addition to monitoring Hg concentration and partitioning behavior, water sample analyses included total and dissolved MMHg. Throughout monitoring, LEFPC dissolved MMHg concentrations have increased during mid- to late spring and early summer. In some cases, measured MMHg concentrations are the highest on record. A recent analysis of predictors of Hg concentration in fish concluded that high MMHg water concentrations in the preceding year, particularly if they occur during months of the growing season, were most strongly related to Hg concentration in fish. If this general conclusion holds in EFPC, it might signal possible future increases in Hg concentration in fish.

The solid:water partitioning coefficient for MMHg has remained unchanged. Referring to Eq. (3.2), given that dissolved MMHg values have increased, for K_d to remain unchanged, the solid phase concentration must show a proportional increase. Therefore, increasing dissolved MMHg coupled with a constant K_d implies there is more total MMHg in the system.

3.2 SEDIMENT INVESTIGATIONS

Details of an investigation of EFPC sediments were included in last year's annual report and a report submitted to the sponsor (Brooks et al. 2017). The total Hg content of 0.5–1.5 g of sediment samples was less than 100 mg/kg. Over the past year, in collaboration with scientists from James Madison University, researchers have examined select sediment grains in the 1–2 mm range. Early results show that individual grains can have concentrations up to at least 800 mg/kg and likely much higher than that. These concentrations are comparable with those for bank soils in the HRD. Some of these grains are being examined by SEM and EDX analysis.

3.3 EFFECT OF SORBENTS ON MONOMETHYLMERCURY PRODUCTION

The successful use of a sorbent technology hinges on the assumption that Hg bound to a sorbent is no longer available for microbial methylation (i.e., not bioavailable). To test this assumption, Hg bioavailability was investigated via a series of bioassays employing a pure culture of *Desulfovibrio desulfuricans* ND132 (ND132) as a model organism for Hg methylation. The extent and rates of Hg methylation were evaluated in the presence and absence of sorbent materials loaded with inorganic Hg (Hg[II]) and Hg associated with natural organic matter (Hg-NOM), respectively. The results collected thus far suggest that in situ treatment using sorbents is equivocal with respect to their ability to decrease MeHg production but might be a viable option for reducing MeHg flux from distributed point-source locations in the EFPC watershed.

Early experiments exhibited high variability in experimental replicates, and the methods were reevaluated and updated in response. Additionally, complete recovery of MeHg from the sorbents, especially SediMite, has proven challenging, and additional updates to the extraction method are ongoing. The difficulty of removing MeHg from SediMite points to the potential effectiveness of using sorbents for MeHg removal. These findings are supported in the literature; for example, Gomez-Eyles et al. (2013) suggest that activated carbon successfully removed both Hg and MeHg, whereas biochar was more effective for MeHg removal than for Hg removal. These results highlight the need to test individual sorbents for both Hg and MeHg sorption properties. Researchers are planning to evaluate MeHg sorbent isotherms for the select sorbents.

Based on previously measured sorption isotherms, material cost, and the background levels of Hg and MeHg of the sorbents, researchers selected four sorbents for the bioassay tests: Biochar, Thiol-SAMMS, SediMite and Organoclay PM199. Bioassay experiments were run by first pre-equilibrating either inorganic Hg (Hg[II]) or Hg associated with natural organic matter (Hg-NOM) with each of the sorbent materials in a phosphate-buffered saline (pH 7.4). After the 48 h Hg-sorbent pre-equilibration period, washed cells of *Desulfovibrio desulfuricans* ND132 (ND132), a known Hg-methylating bacterial strain, were added to a final cell concentration of approximately 10^8 cells/mL. The entire experiment was completed in an aerobic chamber. The MeHgT, MeHgD (0.2 µm filter), and protein content were measured in triplicate over time (0–48 h). Methylmercury concentration after 7 and 24 h was used to compare among sorbents. Because of the variability of the ND132 cultures between experiments, all methylation data are normalized to a no-sorbent control experiment done in parallel for each experiment. An example of the temporal methylation (MeHgT and MeHgD) for a no-sorbent control experiment is shown in Figure 3-14. Here, 70% of the added Hg was methylated after 48 h, and approximately half of the MeHgT produced is associated with bacterial cells. This could have implications for filter feeders and grazers that directly ingest bacteria.

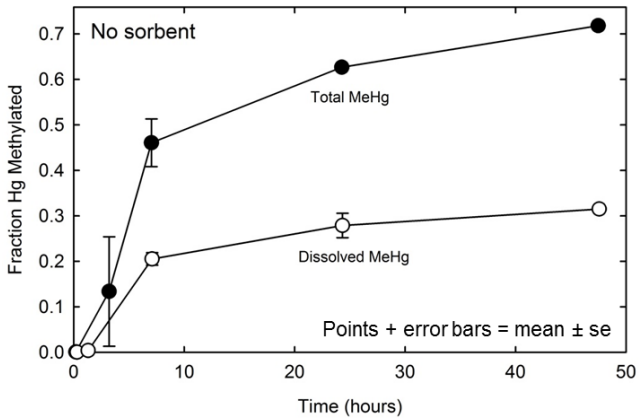

Figure 3-14. Methylation of Hg(II) by *D. desulfuricans* ND132 (without a sorbent).

Bioassay results demonstrate the importance of NOM, similar to that found in EFPC. To evaluate the effect of NOM, Hg-NOM methylation was normalized to the Hg(II) data (i.e., parallel methylation control experiment). A methylation ratio of 1 indicates there is no effect over the control experiment, a ratio <1 indicates less methylation in the Hg-NOM treatment relative to Hg only, and a value >1 shows an increase in methylation. The reference line of 1 has been added to the figures as a guide. Results show up to a 12 times relative increase in MeHg production when Hg is associated with NOM (Hg-NOM) (Figure 3-15). This might relate to findings from Task 1 of the project in which NOM decreased Hg partitioning onto sorbents. The NOM also contributes sulfate to the system, which likely stimulates bacterial activity, increasing MeHg production.

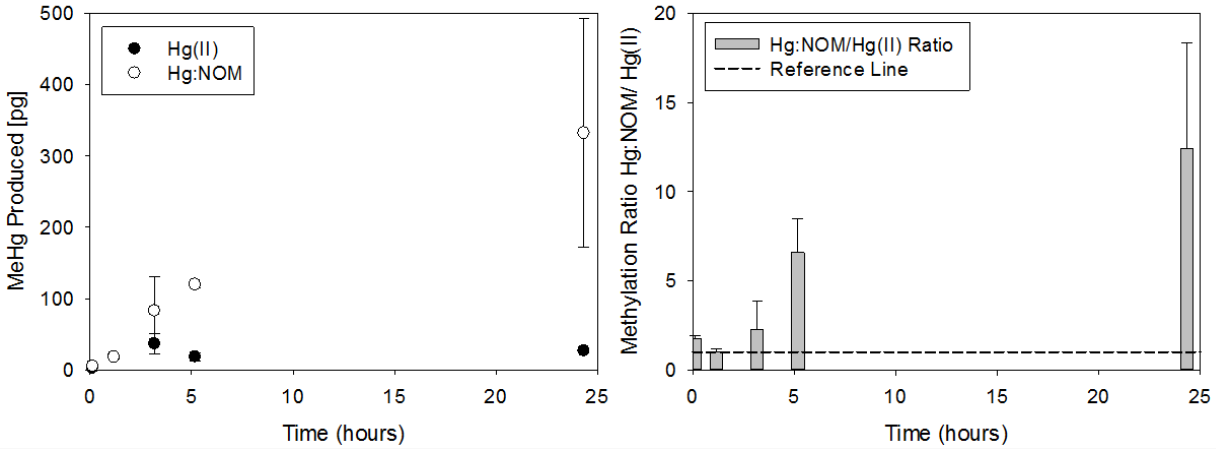

Figure 3-15. Effect of NOM on MeHg production. (Left) Total MeHg produced when Hg is added as Hg(II) and Hg-NOM. (Right) methylation ratio of Hg-NOM to Hg(II). Note: Reference line shows a ratio of 1.

Researchers have also conducted tests of MeHg production from Hg(II) sorbed onto four sorbents tested by Task 1 of the project: Thiol-SAMMS, biochar, SediMite and Organoclay PM199. Figure 3-16 provides the temporal methylation data with and without Thiol-SAMMS present as an example. Thiol-SAMMS decreased the total methylation by 23% at both 7 and 24 h. Dissolved MeHg concentrations were also lower in the Thiol-SAMMS treatment.

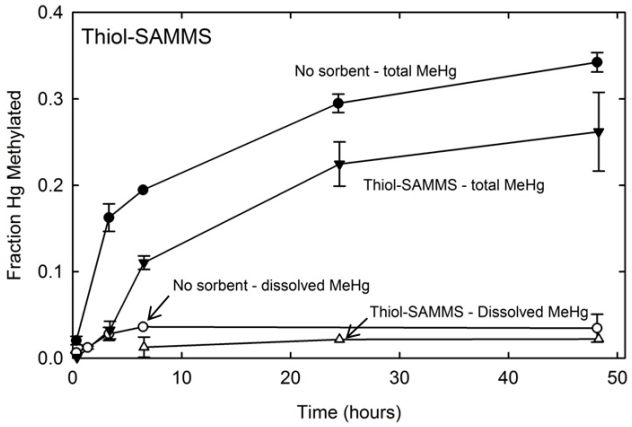

Figure 3-16. Hg(II) methylation with and without Thiol-SAMMS.

In contrast, the other sorbents increased MeHg production relative to no-sorbent controls. Organoclay PM199 increased MeHg production by 2.7 times after 7 h. Data at 24 h were not available for this sorbent. In the presence of biochar, MeHg production was 1.4 times greater than the no-sorbent control after 7 h. However, MeHg then decreased to only 82% of the control after 24 h. Figure 3-17 compares methylation ratios for the tested sorbents. Although a bioassay was completed with SediMite, because of the difficulties extracting MeHg from SediMite, no total methylation data could be obtained. The total MeHg results contradict the hypothesis that sorbents uptake inorganic Hg, making it all unavailable for methylation; however, if the sorbents can effectively bind MeHg, removal of MeHg from the pore waters might be possible. Because the regulatory target focuses on reduction of MeHg uptake by aquatic organisms, additional testing is needed to see whether MeHg bound on sorbents is available for uptake by biota (see Section 3.4, Task 2 Future Directions).

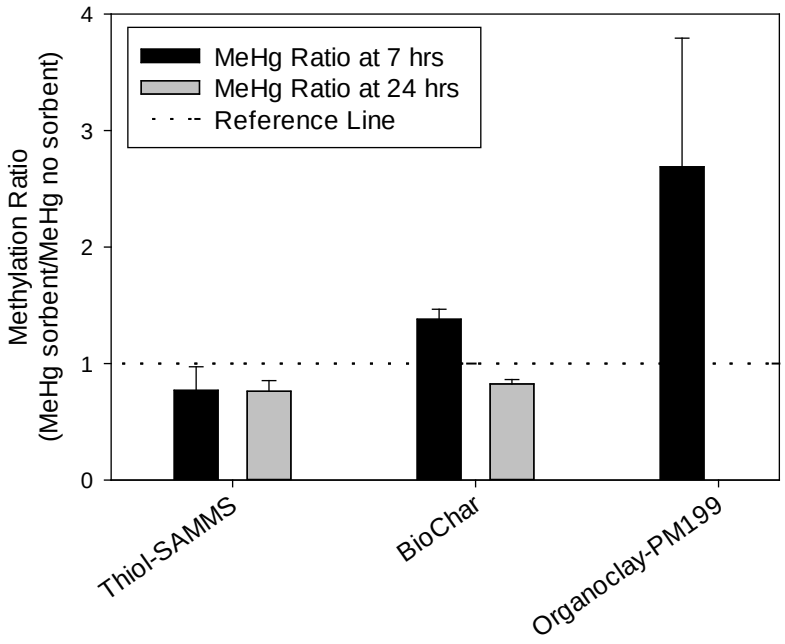

Figure 3-17. Methylation ratio for sorbents compared with no-sorbent control experiments.

Similar bioassay experiments, albeit with Hg-NOM and the four selected sorbents, have been completed, and the data are still being processed. Additionally, bioassay experiments aimed at evaluating the effect of Hg-sorbent aging on methylation are under way. These experiments will allow for extended pre-equilibration between the sorbent and Hg before the introduction of the methylator ND132. These aging experiments were set up in mid-July, and the subsequent bioassays are planned for September (i.e., allowing for two months of aging).

3.4 TASK 2 FUTURE DIRECTIONS

Within UEFPC, various alternatives (Peterson et al. 2015a) to current chemical treatment and discharge methods used in Y-12 industrial processes—in addition to controlled chemical additions and manipulations—are being considered to reduce Hg fluxes and forms that enhance migration of Hg to LEFPC. Because the impacts of some of the numerous chemicals present in UEFPC water (Table 3-1) on Hg forms and transport are still not well understood, a systematic phased approach of alternatives identification and evaluation, combined with laboratory- and field-scale experiments, is needed to test and select viable alternatives for implementation. This is particularly true for the large assortment of chemicals currently used for the treatment of cooling tower blowdown water and other intermittent industrial discharges to the storm drains.

Most of the flow in the storm drain system contains residual chlorine because of the discharge of chlorinated process water (drinking water from the City of Oak Ridge water supply system) from various uses (primarily cooling water). Residual chlorine is aggressive in its oxidation and solubilization of Hg; therefore, the Hg in water exiting OF200 and other OFs contains reactive dissolved Hg(II). Laboratory testing suggests that eliminating or reducing chlorine concentrations in the storm drain system could significantly reduce the amount of soluble Hg(II) produced as chlorinated water comes in contact with liquid $Hg(0)_l$ and dissolved $Hg(0)_d$ and could also reduce the total Hg discharged to LEFPC. Reduction of chlorine concentrations in the storm drain system could be accomplished by conducting dechlorination of process water before or just downstream of discharge points to the storm drain, especially in areas with

$Hg(0)_l$ and dissolved $Hg(0)_d$, and could also reduce the total Hg discharged to LEFPC. Future dechlorination-related investigations will focus on conducting preliminary field tests in Y-12 storm drains that examine the use of ascorbic acid as an alternative dechlorination chemical.

At a high level, the goals of the LEFPC TD project are threefold: lower the release or production of Hg and MeHg, lower the flux of Hg and MeHg from source areas and downstream along the creek, and lower the concentration of Hg in fish. Figure 3-18 is a simplified representation of the path from inorganic Hg to MeHg in fish, and the figure highlights some places where the path can be disrupted in support of the three broad goals: (1) prevent or decrease Hg methylation, (2) enhance MeHg demethylation, and (3) decrease biouptake and the consequent bioaccumulation and biomagnification steps.

Figure 3-18. Simplified representation of the path from inorganic Hg to MeHg concentrations in fish.

Work in the water and sediment chemistry task provides direct understanding of Hg flux estimates, enabled by flow and water quality data. These estimates demonstrate that diffuse legacy sources of Hg outside of Y-12 contribute additional Hg to LEFPC. Results point to the upper study reach as being a consistent source of additional Hg to EFPC. Additional data from other projects suggest that hyporheic water might be a source of some of the additional Hg. Movement of hyporheic water from the sediments to surface water might also be a source of MeHg because the fine-grained sediment deposits can harbor zones of MeHg production. Accordingly, and by working cooperatively with other projects, researchers will leverage resources to install and monitor instream piezometers at several locations to measure water composition in the sediment interstitial pore water and vertical head gradients across the hyporheic interface. These measurements will indicate the propensity for water movement and solute transport between surface water and subsurface areas that could be sources of additional Hg and active zones of Hg methylation. Understanding the potential contributions of hyporheic/subsurface water to the surface water Hg and MeHg budgets is necessary for evaluation and design of potential sediment-capping remedial strategies.

Within LEFPC, in the near term, researchers will continue to analyze collected samples. Additionally, ongoing efforts will continue to quantify water quality and creek discharge at existing locations. These results are critical to supporting evaluation of source areas and fluxes and their considerable spatiotemporal variability. Therefore, it is highly advisable to capture as much of that variability as possible. It will be difficult at best to distinguish real system response to remedial actions from natural variability without a better idea of said variability.

Noticeable changes have occurred in the flow regime of LEFPC relative to historical data from 1960 to 1988. Average and peak flows are higher today and are likely to result in an undesirable decrease in bank stability/increased bank erosion. Ongoing and planned future actions along EFPC suggest more changes are forthcoming. To document and quantify these changes, continued flow monitoring along LEFPC is warranted. Additionally, these flow measurements are integral to the flux estimates. Therefore, researchers plan to maintain flow and water-quality monitoring activities because these provide the basis against which system response to future actions will be compared.

Researchers have been working cooperatively with Task 1 to evaluate sorbents for Hg(II) removal from water (lowering Hg concentration) and will continue this collaboration to include MeHg (lowering MeHg concentration). Results show that sorbents provide marginal benefit when it comes to decreasing MeHg production (preventing Hg methylation). Nevertheless, they might prove to be very effective at sorbing Hg (lowering MeHg concentration) and preventing its entry into the food web (decreasing biouptake). Therefore, researchers are planning to complete experiments on the effect of sorbents on MeHg production and write up those results. Researchers are also planning a series of experiments to determine MeHg sorption isotherms on sorbents to better quantify the extent to which sorbents could lower MeHg concentrations in water and decrease MeHg flux.

Finally, researchers are planning a series of experiments to study the effect of sorbents on biouptake. The general concept is to have containers of EFPC sediments mixed with a sorbent and containing a representative benthic invertebrate (e.g., oligochaete worms; actual organism to be selected in consultation with Task 3). Over time, samples of water, pore water, sediment/sorbent, and invertebrate would be collected and analyzed. This would be a direct test of the sorbents' ability to lower MeHg production, lower pore water concentrations of Hg and MeHg, and disrupt biouptake of MeHg.

4. TASK 3: ECOLOGICAL MANIPULATION

4.1 BIOTA

4.1.1 Approach to Biological Characterization

In contrast to virtually all other metals, Hg (especially in its organic form, MeHg) biomagnifies, or becomes increasingly concentrated as it is transferred through aquatic food chains, leading to elevated concentrations of this toxin in fish. Because the primary exposure route for Hg in humans and other wildlife is through the consumption of contaminated fish, national guidelines for the protection of human and ecological health include a fish tissue concentration (0.3 ppm MeHg in fish fillet), which is considered to be a more consistent indicator of exposure and risk than aqueous guidelines. Because of this explicit regulatory guideline, remediation actions and research efforts have long focused on understanding and mitigating Hg bioaccumulation in EFPC fish.

The long-term Biological Monitoring and Abatement Program (BMAP) has tracked the progress of remediation efforts in EFPC since 1985. Over the past 30 years, bioaccumulation monitoring in EFPC has shown that remediation efforts have succeeded in significantly reducing aqueous HgT concentrations, but these reductions in water concentrations have not affected fish HgT concentrations (Mathews et al. 2013; Southworth et al. 2013). This disconnect is likely because (1) Hg bioaccumulation is driven largely by MeHg (not HgT) concentrations and (2) bioaccumulation of Hg occurs predominantly through food chain (not aqueous) exposure.

Like many other bioaccumulation monitoring programs at Hg-contaminated sites, BMAP has focused on comparing HgT concentrations in fish to ambient water HgT concentrations collected at strategic locations throughout the creek. Although the fish tissue guideline is a concentration of MeHg (not HgT), MeHg is not routinely measured in water or fish; MeHg analysis can be prohibitive in terms of cost and time, and previous studies have shown that >90% of the HgT in fish fillets is MeHg. Total Hg concentrations are therefore assumed to be a reasonable proxy for MeHg concentrations in fish fillet in EFPC. Further, previous studies have shown that the length of the food chain leading to fish affects Hg bioaccumulation; longer food chains offer more opportunities for Hg to biomagnify, leading to higher concentrations in fish (Cabana and Rasmussen 1994). Before this project, Hg transfer throughout the EFPC food chain had not been characterized, though food web dynamics are likely critical to understanding and explaining observed Hg bioaccumulation patterns in EFPC fish.

The objective of Task 3 is to mitigate Hg transfer to fish by manipulating the aquatic food web in EFPC. This could be achieved, for example, through the addition or removal of key species that can significantly disrupt Hg transfer, or through the manipulation of physical factors (e.g., nutrients, light) that might favor Hg transformation. There is precedent on the Oak Ridge Reservation for the proposed mitigation strategy; ecological manipulations have been implemented previously to mitigate contaminant bioaccumulation, obtaining positive results at a fraction of the cost of traditional remediation methods (e.g., Peterson et al. 2015b).

As with any other remediation technology, a thorough baseline characterization is needed before manipulation to discern the effectiveness of the action. The current understanding of Hg bioaccumulation in EFPC had previously been limited to a few target fish species; however, the BMAP fish and macroinvertebrate community data sets provide valuable information on the food web structures and, therefore, on the potential opportunities for ecological manipulations. By quantifying the Hg transfer within EFPC food webs using historical data and field surveys, the key links for Hg transfer and manipulation strategies to decrease that transfer can be identified.

In FY 2017, researchers focused on completing processing and analysis of samples collected in FY 2015 and 2016. Using these data, researchers constructed a more detailed food web to determine where ecological manipulations might be most effective in EFPC. Presented here are the results of the food web characterization studies conducted to date for this project, obtained through both the analysis of historical BMAP community structure data and targeted field sampling.

Field surveys were conducted in 2015 and 2016 to characterize Hg/ MeHg bioaccumulation and trophic transfer throughout the food chain at sites along EFPC. Water and periphyton samples were collected from five sites along EFPC—EFKs 24.5, 23.4, 18.2, 13.8, and 6.3 for Hg, MeHg, and chlorophyll analysis. In FY 2017, previously collected samples were processed and analyzed. Biota samples were dried to a constant weight in a freeze dryer and homogenized before analysis for total Hg by thermal decomposition and cold vapor atomic absorption using a direct Hg analyzer (DMA-80, Milestone). Samples were analyzed for MeHg by distillation, aqueous ethylation, purge and trap, and cold vapor atomic fluorescence spectrometry (CEBAM, Bothell, Washington). Stable isotope ratios ($\delta^{13}C$ and $\delta^{15}N$) in invertebrates and fish were measured at the University of California, Davis, by continuous flow isotope ratio mass spectrometer.

4.1.2 Results from Field Characterizations

As has been seen previously, aqueous HgT concentrations are highest upstream in EFPC and decrease with distance downstream, whereas aqueous MeHg concentrations follow the opposite pattern (Figure 4-1). Total Hg concentrations in periphyton are variable (Figure 4-2), likely because the samples includes both biological and abiotic particles (sediment entrapped within algal biomass). These data will be corrected for organic matter content by combusting samples; data are pending for organic matter content. However, patterns of MeHg accumulation in periphyton increase with distance downstream to a peak at EFK 13.8, with concentrations decreasing at EFK 6.3 (Figure 4-2). This pattern has been seen often in fish tissue concentrations throughout the creek in recent years (Figure 4-3), with the highest concentrations in fish fillets seen at EFK 13.8.

Food chain analysis for EFKs 23.4 and 13.8 presented previously show that the food chain leading to rock bass is longer at EFK 13.8 than the food chain at EFK 23.4. Figure 4-4 shows a preliminary analysis of the food web and MeHg concentrations at the other EFPC sites and at Hinds Creek. At all sites, MeHg concentrations increase with increasing del-N values; del-N values are often used as a proxy for trophic level, with a higher value corresponding to a higher trophic level. This is consistent with observations for EFK 23.4 and EFK 13.8 and with the fact that MeHg is known to biomagnify through aquatic food webs. Throughout the food web at EFK 6.3, MeHg concentrations are higher than those at EFK 24.5 (and at the Hinds Creek reference site), and the slope of the line at EFK 6.3 is greater than the slope at EFK 24.5, suggesting that the rate of MeHg bioaccumulation with increasing trophic level is greater at the downstream site. Stable isotope analyses of periphyton samples (the base of the food web) are needed to quantitatively assign trophic levels; these results are pending. With these results, researchers will be able to quantitatively compare trophic transfer efficiency among all sites.

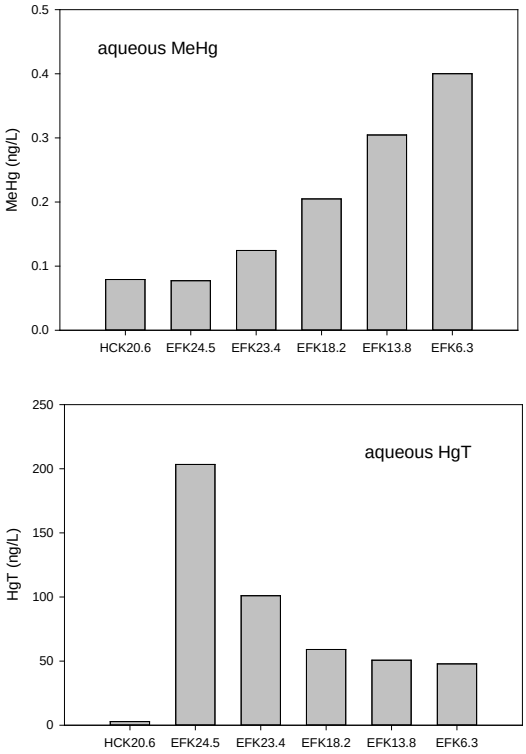

Figure 4-1. Average monthly aqueous HgT and MeHg concentrations taken as grab samples throughout EFPC at base flow.

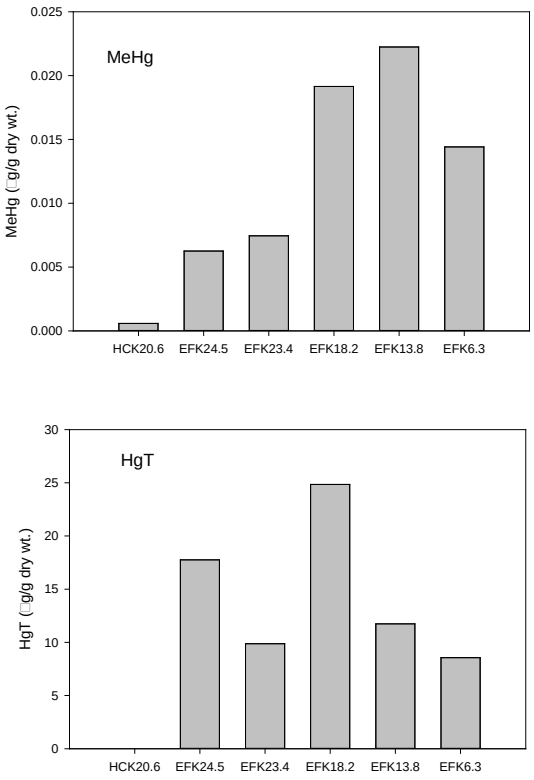

Figure 4-2. Average monthly HgT and MeHg concentrations in periphyton taken simultaneously with water samples throughout EFPC.

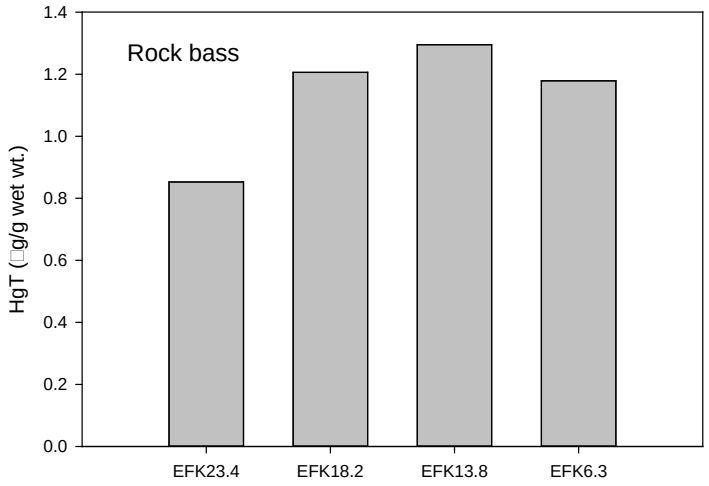

Figure 4-3. Average total Hg concentrations in rock bass collected throughout EFPC in fall 2016. Data courtesy of the Y-12 BMAP.

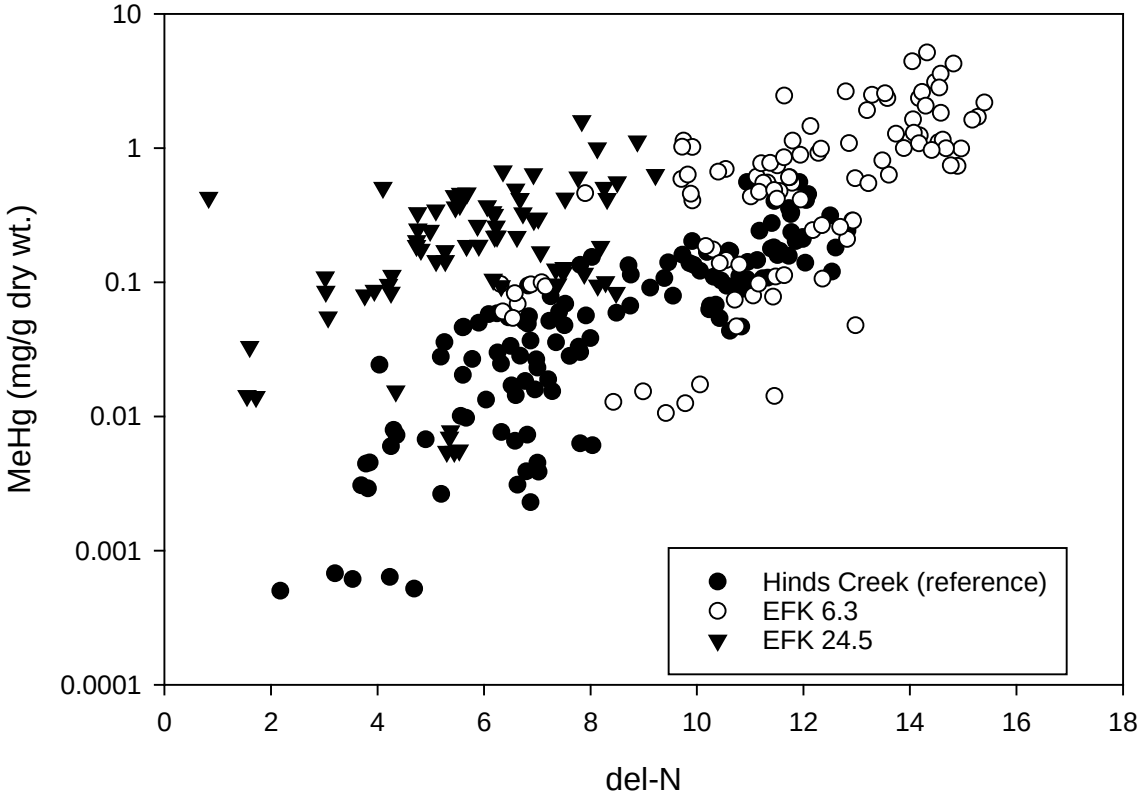

Figure 4-4. Methylmercury concentrations vs. $^{15}\delta N$ for biota samples collected through the food web at EFKs 24.5 and 6.3 and the Hinds Creek reference site. (Note: Del-N values are often used as a proxy for trophic level, with a higher value corresponding to a higher trophic level.)

4.2 MERCURY SORPTION STUDIES

4.2.1 Approach for Mercury Sorption by Algal Beads

Algal beads were prepared by mixing 1 g of algal cells with dissolved sodium alginate. The mixture was then introduced to a 0.1 M calcium chloride ($CaCl_2$) solution to create Ca-alginate beads impregnated with algal biomass. The beads were rinsed and then (10 g wet wt.) exposed to two different concentrations of dissolved HgT in 100 mL of DI water (1 mg/L and 1 µg/L) for 5 h. Experiments were conducted in triplicate. Mercury removal was measured by taking 3 mL aqueous samples throughout the experiment. Analysis was done by cold vapor atomic absorption.

4.2.2 Results for Mercury Sorption Studies

Results from sorption experiments starting with aqueous HgT concentrations of 1 mg/L and 1 µg/L are shown in Figure 4-5. Mercury removal was rapid within the first hour of experiments and then leveled off. With an initial aqueous concentration of 1 mg/L, >70% of the initial concentration was removed within the first hour. However, at lower initial concentrations removal was not as efficient, with only 47% of Hg removed by the second hour. In follow-on experiments, algal cell concentration per bead was increased, and the ratio of bead to solution was varied. Sorption and desorption of HgT and MeHg were examined; these results are still pending. These initial experiments were done in batch culture setup; future experiments will use a flow-through system to examine the capacity of algal beads to continually remove Hg.

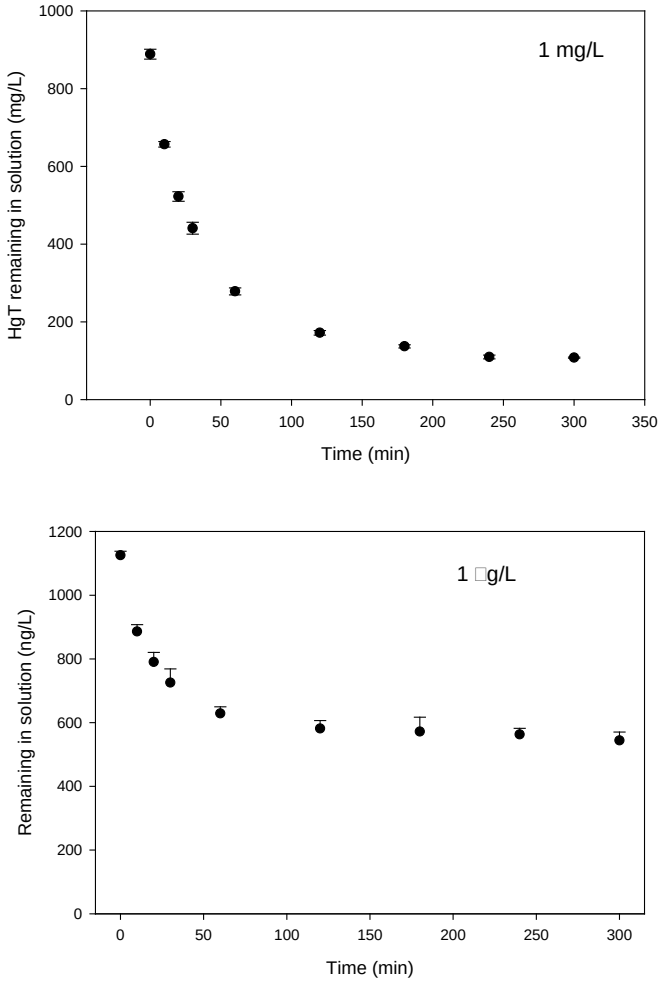

Figure 4-5. Mercury removal from water column over time at different initial aqueous HgT concentrations (1 mg/L and 1 µg/L).

4.3 FOOD CHAIN MODELING

4.3.1 Approach to Food Chain Modeling

Researchers examined Hg bioaccumulation within EFPC as a function of exposure (aqueous concentrations) but also as a function of biodynamics—biological processes that affect Hg concentrations within organisms (e.g., growth, Hg assimilation, and Hg depuration). Researchers used community data available from BMAP studies to examine inventories within the biological compartments of the stream. In particular, they considered somatic growth dilution (SGD) as a way to explain why Hg biomagnification might differ at different sites throughout the creek. The SGD concept is that the concentration of a bioaccumulating contaminant, such as MeHg, becomes more dilute within an organism's body when the organism has a high growth efficiency. Several studies have substantiated the effects of SGD on MeHg concentrations at the individual level, but how SGD affects MeHg concentrations at the population level has not been investigated (Karimi et al. 2007; Ward et al. 2010).

The research team followed previous work in the construction of biodynamic models to place reasonable constraints on unknown parameter values. Table 4-1 shows the contraints used that were adopted from several studies on fish and insect growth (Cain, Croteau, and Luoma 2011; Hawkins 1986; Mason,

Laporte, and Andres 2000; Tsui and Wang 2004). Included are parameters developed for the *Heptageniidae* insect biodynamic model. Constraints were set up and the "solver" function in Excel was used to find the parameter values that minimized the residuals left between the predicted and actual MeHg concentrations. Solver was rerun for each of the five sample sites to produce an individual biodynamic model under the unique conditions present in different sections of the stream.

Table 4-1. Constraints placed on biodynamic model parameters for stonerollers and mayflies, respectively

Species	AE (%)	Ke (d^{-1})	Ku (d^{-1})	IR_c	G multiplier	C_f ratio	Max IR
Campostoma oligolepis	90-100	0.001-0.1	0.5-3.5	0.1-0.9, =IR_c*G	1-3	0.7-1	0.27
Heptageniidae spp.	55-100	0.05-0.058	0.5-3.5	0.1-0.9, =IR_c*G	1-3	0.7-1	0.25

Table 4-2 summarizes the parameters used for the biodynamic models for the five different sample sites. Many of the parameters are at their lower or higher extremities, a sign that the parameters or formula can be altered to be more accurate and provide more variability among the parameters. Additionally, Table 4-3 lists the parameters for the *Heptageniidae* data gathered at two sites.

Table 4-2. Parameters for the stoneroller biodynamic models for each of the five sites studied

Site	AE (%)	K_e (d^{-1})	K_u (d^{-1})	IR_c	G multiplier	C_f ratio	IR_c*G
6.3	90	0.0197	3.5000	0.1000	1.3333	0.7000	0.1000
13.8	90	0.0402	3.5000	0.1000	1.3333	0.7000	0.1000
18.2	90	0.0378	0.5000	0.1000	1.3333	0.7000	0.1000
23.4	90	0.1000	0.5000	0.3036	1.3333	0.9998	0.3036
24.5	90	0.0603	2.5683	0.1000	1.3333	0.7000	0.1000

Table 4-3. Parameters for the mayfly (*Heptageniidae*) biodynamic models for both of the sites studied

Site	AE (%)	Ke (d^{-1})	Ku (d^{-1})	IR_c	G multiplier	C_f ratio	IR_c*G	Max IR
23.4	64.08	0.058	0.5	0.1270	1.33	0.7	0.1270	0.25
13.8	62.05	0.058	0.5	0.1901	1.33	0.7	0.1901	0.25

After the models were developed, researchers applied them to stoneroller population data gathered biannually since 1985. This allowed for development of a historic perspective on MeHg flux through the ecosystem and stoneroller population. Historic data were organized primarily by fish length, which caused issues when analyzing data. The average weight of each age class of fish for every year was known, so length class could be related to age class by comparing the average weights of each. Therefore, age class could be controlled for analyzing relationships between variables. Using the biodynamic models, the MeHg concentration of each size/age class of each sample since 1985 could be calculated.

4.3.2 Growth and Population Dynamics and Impacts on Methylmercury Concentrations

Building biodynamic models required accurately assessing stoneroller growth. Growth was examined across EFPC sites (Figure 4-6) and among age classes (Figure 4-7) by clustering length and weight data and building growth curves.

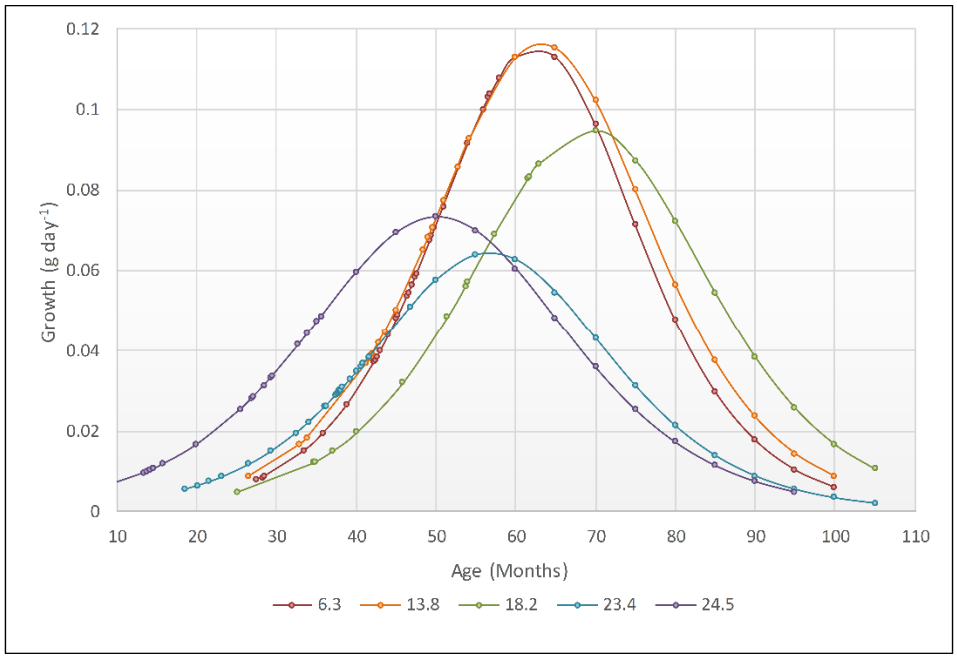

Figure 4-6. Relationships between stoneroller growth and age at each of the five BMAP sites within EFPC.

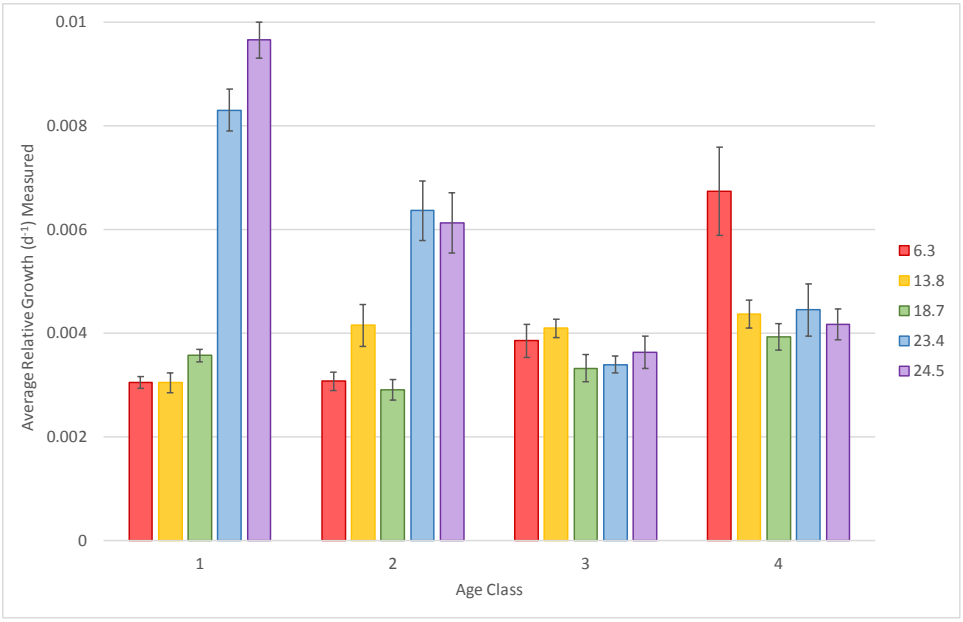

Figure 4-7. Comparisons between measured and biodynamic model-predicted values of average relative growth among each age class at each study site.

Figure 4-6 shows the trends of growth (grams/day) against age for the fish populations. It is evident from this figure that each site has its own unique trend where maximum growth peaks at a certain age. These different growth patterns are, in part, due to different growth rates among age classes (Figure 4-7). In general, EFKs 24.5 and 23.4 have the highest growth rates and individuals attain maximum size at an earlier age (Figure 4-6). Additionally, these sites have very high growth rates for Age 1 and Age 2 classes (Figure 4-7). In comparison, stonerollers at EFKs 6.3 and 13.8 exhibit slower growth but attain larger sizes (Figure 4-6). SGD theories place much importance on relative growth rate as a major factor in diluting contaminants such as MeHg in the bodies of organisms. Directly measuring relative growth in populations is labor intensive, and for this reason, the estimated age classes were developed from length and weight information to allow for prediction of relative growth from parameters that are more easily measured, such as size, weight, and age.

Literature has emphasized the importance of SGD on MeHg concentration in fish; the theory is that more rapid (and assumedly more efficient) growth results in less MeHg accumulating in the fish compared with its additional body mass added (Ward et al. 2010). Consumption of high-quality (high nutrient concentration) food is known not only to increase growth and somatic dilution of MeHg but also to decrease consumption rate and therefore reduce total intake of MeHg (Karimi et al. 2007). Seemingly in accordance with the SGD concept, stoneroller MeHg concentrations appeared to follow general patterns of variation in growth across EFPC sites (Figure 4-8). Sites with the fastest growth (EFKs 24.5 and 23.4) had lower MeHg concentrations, whereas sites with slower growth (EFKs 6.3 and 13.8) had the highest MeHg concentrations. However, this information does not incorporate the effects of dietary levels of MeHg. Researchers evaluate this within the biodynamics model (see the following section).

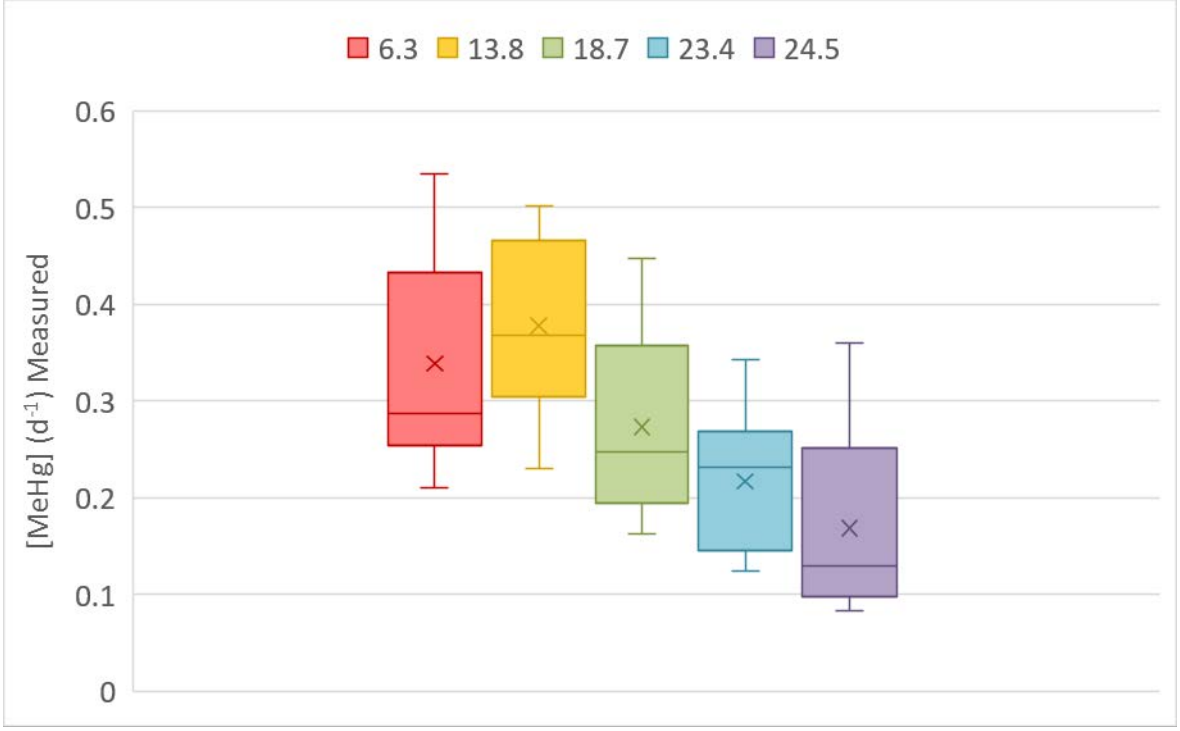

Figure 4-8. Methylmercury whole body concentrations in stonerollers collected from EFPC sites.

4.3.3 Modeling Results

Coarse comparisons of growth among sites yield limited information on the causal factors behind MeHg concentrations. Additionally, results of these comparisons cannot be scaled to evaluate the influence of population dynamics and structure of MeHg storage and flux through upper trophic levels. Thus, a modeling framework, such as the biodynamics concept, is required. As mentioned previously, the biodynamics model takes into account growth and organismal regulation of contaminants as well as the dietary MeHg concentrations.

Researchers applied growth equations to individual stoneroller samples collected along EFPC. Individuals were sorted into age classes to create composite samples. For each sample, an average weight of all individuals was calculated and used to estimate relative growth. The research team then compared estimates of relative growth to the observed MeHg concentrations of stonerollers. Interestingly, the results did not point to rapid growth resulting in lower MeHg levels; in fact, it was quite the opposite (Figure 4-9). Ultimately, stoneroller MeHg concentrations are being driven by differences in MeHg levels in periphyton across EFPC sites (Figure 4-2), not by differences in growth. This suggests that growth likely plays a lesser role in fish MeHg concentrations relative to dietary concentrations and loading to the stream.

Finally, the researchers used the biodynamics model to scale up the total MeHg standing stock within the entire stoneroller populations within EFPC. Using population density data per age from 1986 to 2016, the team applied a calibrated biodynamics model to control for variation in periphyton MeHg concentrations among EFPC sites. Growth equations were used to estimate relative growth for each age class, and negative effects of population density on relative growth (i.e., density dependence) were included. Estimates of MeHg concentrations for individual fish were scaled up to the entire population level. Figure 4-10 shows that the total standing stock of MeHg concentrations is highly driven by population size. This is an intuitive result, but the quantification of total concentrations allows investigators to determine what population sizes, or reduction in population sizes, could result in sufficient declines in total MeHg standing stock in biotic compartments.

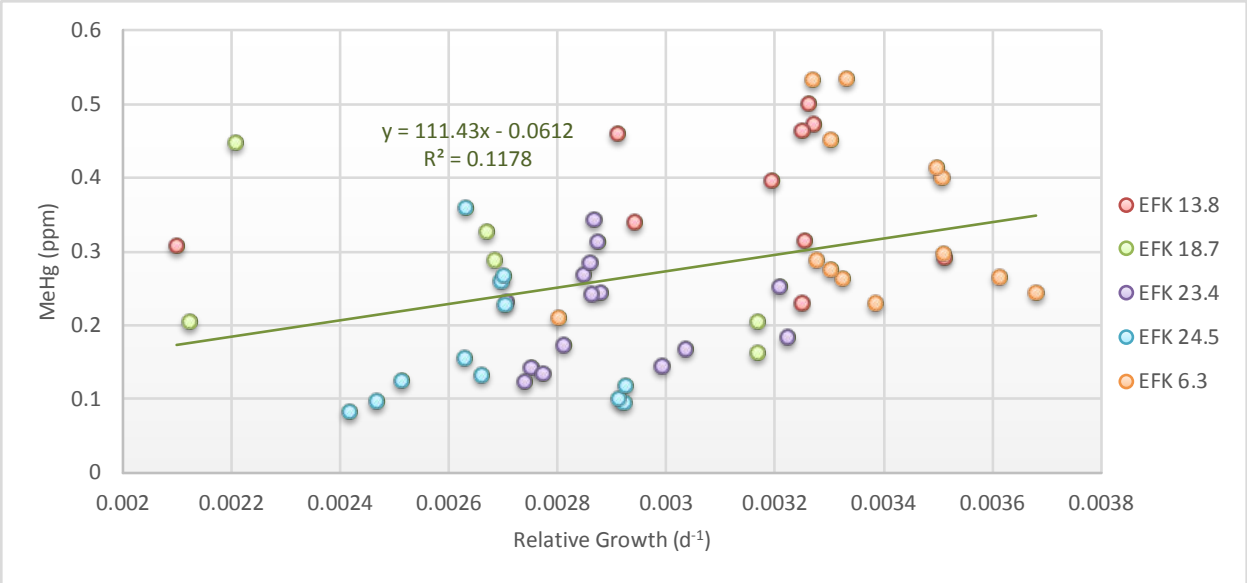

Figure 4-9. Relationship between relative growth in stoneroller minnows and MeHg concentrations across all EFPC sites.

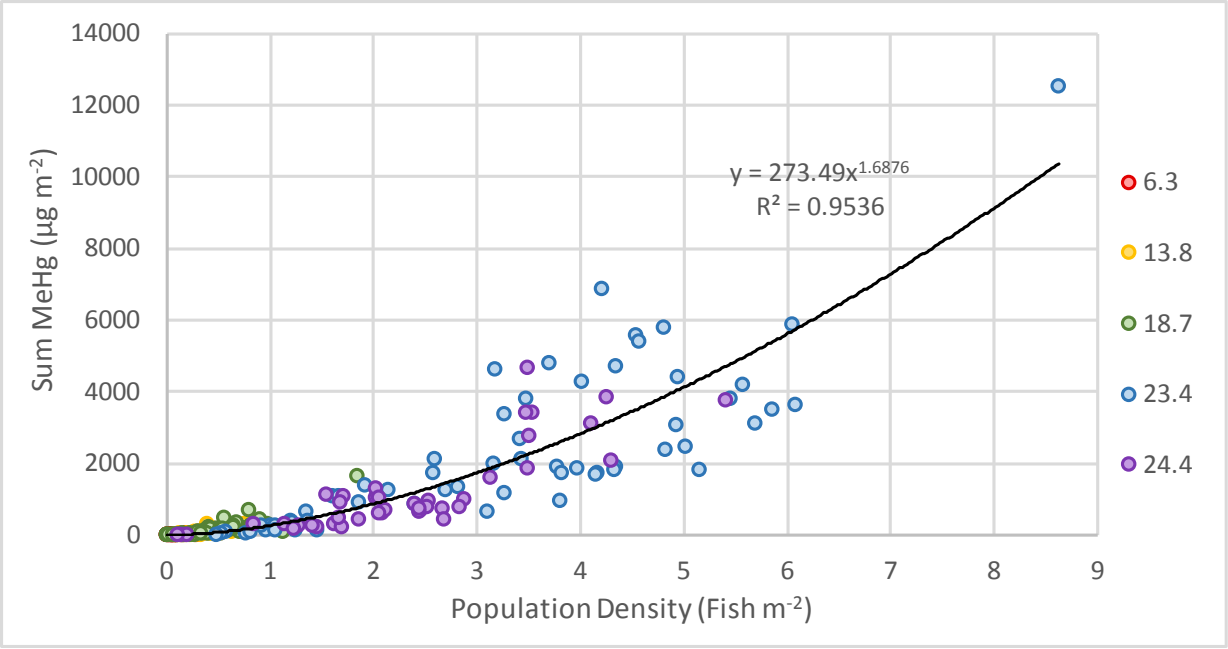

Figure 4-10. Relationship between population density and MeHg standing stock in fish populations across EFPC sites.

4.3.4 Modeling Implications

An accurate biodynamic model was constructed for a stoneroller population in a contaminated stream. The ability to construct a biodynamic model for a primary consumer species is encouraging, as most biodynamic models used currently are for keystone species or final consumers. The ability to adapt models to species earlier in the food chain—such as stonerollers, mayflies, and potentially even algae and periphyton—allows for the generation of a much more comprehensive picture of nutrient/contaminant cycling in ecosystems and a prediction of how population/species changes will affect these cycles.

Additionally, the biodynamic models show promise for use as guides to population management. Figure 4.6 provides site-specific growth rates, which can be used to remove individuals of a given size to minimize MeHg bioaccumulation and trophic transfer. This is analogous to forestry practices, where trees are cut at the point of maximum growth to achieve maximum efficiency. Future work will include applying the mayfly biodynamic back in time to test accuracy. This will also allow estimation of past periphyton and water MeHg levels to increase the accuracy of the fish biodynamic models.

Figure 4-9 illustrates the lack of support for the SGD in stoneroller minnows in EFPC. A reasonable explanation for these results is that MeHg concentrations in periphyton—stonerollers' primary food resource—are driving stoneroller MeHg concentrations. Ultimately, the biodynamics modeling platform allows researchers to examine how varying population size and structure could be used to reduce MeHg standing stock, and eventually fluxes, from biotic compartments.

4.4 TASK 3 FUTURE DIRECTIONS

Important research and TD needs are to quantify the trophic transfer efficiency of Hg through the EFPC food chain and to identify the critical links for Hg transfer to fish. By understanding these critical links, design strategies can be developed to sustainably alter, or manipulate, the aquatic food chain to mitigate Hg transfer to fish. The extensive data collected to date will help inform the modeling efforts. Ultimately,

a modeling tool will be generated for this project that will allow for simulated changes in fish concentrations associated with key ecological manipulations that might be implemented in EFPC.

In FY 2018, information regarding critical food chain links will be coupled with small-scale field and laboratory experiments to better understand Hg methylation and subsequent transfer through the food web in EFPC and to target key ecological manipulations that might have the most benefit to mitigating Hg bioaccumulation. Experiments planned for next year will inform future mesocosm-scale experiments slated to take place in the Aquatic Ecology Laboratory and will potentially inform small-scale field manipulations. Based on current findings, the most promising lines of inquiry include experiments to examine (1) the effect of fish population density and/or species abundance on Hg and MeHg bioaccumulation and (2) the effects of stocking mussels and lower-trophic-level fish on dissolved and particle-associated Hg and MeHg and Hg bioaccumulation.

5. REFERENCES

Aiken, G. R., H. Hsu-Kim, and J. N. Ryan. 2011. "Influence of Dissolved Organic Matter on the Environmental Fate of Metals, Nanoparticles, and Colloids." *Environmental Science and Technology* 45: 3196–3201. doi: 10.1021/es103992s.

Barnett, M. O., et al. 1997. "Formation of Mercuric Sulfide in Soil." *Environmental Science & Technology* 31 (11): 3037–3043.

Bloom, N. S., et al. 2003. "Selective extractions to assess the biogeochemically relevant fractionation of inorganic mercury in sediments and soils." *Analytica Chimica Acta* 479: 233–248.

Bowman, R. S., and J. F. Gibbens. 1992. "Difluorobenzoates as nonreactive tracers in soil and ground water." *Ground Water* 30 (1): 8–14.

Brooks, S., et al. 2017. *Mercury Content of Sediments in East Fork Poplar Creek: Current Assessment and Past Trends. ORNL/TM-2016/578*. Oak Ridge National Laboratory. doi: 10.2172/1338545. doi: 10.2172/1338545.

Cabana, G., and J. B. Rasmussen. 1994. "Modeling Food Chain Structure and Contaminant Bioaccumulation Using Stable Nitrogen Isotopes." *Nature* 372 (6503): 255–257.

Cain, D., M.-N. Croteau, and S. Luoma. 2011. "Bioaccumulation dynamics and exposure routes of Cd and Cu among species of aquatic mayflies." *Environmental Toxicology and Chemistry* 30: 2532–2541. doi: 10.1002/etc.663.

Chung, W. J., et al. 2013. "The use of elemental sulfur as an alternative feedstock for polymeric materials." *Nature Chemistry* 5 (6): 518–524. doi: 10.1038/Nchem.1624.

Crockett, M. P., et al. 2016. "Sulfur-Limonene Polysulfide: A Material Synthesized Entirely from Industrial By-Products and Its Use in Removing Toxic Metals from Water and Soil." *Angewandte Chemie-International Edition* 55 (5): 1714–1718. doi: 10.1002/anie.201508708.

Dickson, J. O., et al. 2015. *Soil Investigation of Lower East Fork Poplar Creek*. ORNL-TM/2015-374, Oak Ridge National Laboratory, Oak Ridge, TN.

Fitzgerald, W. F., C. H. Lamborg, and C. R. Hammerschmidt. 2007. "Marine biogeochemical cycling of mercury." *Chemical Reviews* 107 (2): 641–662. doi: Doi 10.1021/Cr050353m.

Gilmour, C. C., E. A. Henry, and R. Mitchell. 1992. "Sulfate Stimulation of Mercury Methylation in Fresh-Water Sediments." *Environ Sci Technol* 26 (11): 2281–2287.

Gilmour, C. C., et al. 2013. "Activated Carbon Mitigates Mercury and Methylmercury Bioavailability in Contaminated Sediments." *Environmental Science & Technology* 47 (22): 13001–13010. doi: Doi 10.1021/Es4021074.

Gomez-Eyles, J. L., et al. 2013. "Evaluation of Biochars and Activated Carbons for In Situ Remediation Of Sediments Impacted With Organics, Mercury, And Methylmercury." *Environmental Science & Technology* 47 (23): 13721–13729. doi: 10.1021/es403712q.

Haitzer, M., G. R. Aiken, and J. N. Ryan. 2002. "Binding of Mercury(II) to Dissolved Organic Matter: The Role of the Mercury-to-DOM Concentration Ratio." *Environmental Science & Technology* 36: 3564–3570.

Hawkins, C. P. 1986. "Variation in Individual Growth Rates and Population Densities of Ephemerellid Mayflies." *Ecology* 67: 1384–1395. doi: 10.2307/1938694.

Karimi, R., et al. 2007. "Stoichiometric Controls of Mercury Dilution by Growth." *Proceedings of the National Academy of Sciences* 104: 7477–7482.

Kolka, R. K., et al. 2011. "Mercury Cycling in Peatland Watersheds, Chapter 11." In *Peatland biogeochemistry and watershed hydrology at the Marcell Experimental Forest*, edited by R. K. Kolka, et al. Boca Raton, FL: CRC Press: 349–370.

Lepore, B. J., and P. Barak. 2009. "A Colorimetric Microwell Method for Determining Bromide Concentrations." *Soil Science Society of America Journal* 73 (4): 1130–1136. doi: 10.2136/sssaj2008.0226.

Looney, B., et al. 2008. *Recommendations to Address Technical Uncertainties in the Mitigation and Remediation of Mercury Contamination at the Y-12 Plant, Oak Ridge, Tennessee*. WSRC-STI-2008–00212, US Department of Energy, Office of Environmental Management.

Mason, R. P., J. M. Laporte, and S. Andres. 2000. "Factors controlling the bioaccumulation of mercury, methylmercury, arsenic, selenium and cadmium by freshwater invertebrates and fish." *Archives of Environmental Contamination and Toxicology* 38: 283–297.

Mathews, T., et al. 2013. "Decreasing Aqueous Mercury Concentrations to Achieve Safe Levels in Fish: Examining the Water–Fish Relationship in Two Point-Source Contaminated Streams." *Sci. Tot. Environ* 443: 836–843.

Mayes, M. A., et al. 2003. "Transport of multiple tracers in variably saturated humid region structured soils and semi-arid region laminated sediments." *Journal of Hydrology* 275: 141–161. doi: 10.1016/S0022-1694(03)00039-8.

Mayes, M. A., et al. 2009. "Influence of sedimentary bedding on reactive transport parameters under unsaturated conditions." *Soil Science Society of America Journal* 73: 1938–1946. doi: 10.2136/sssaj2008.0317.

Miller, C. L., et al. 2013. "Characterization of Soils from an Industrial Complex Contaminated with Elemental Mercury." *Environmental Research* 125: 20–29.

Peterson, M. J., et al. 2015a. *Mercury Remediation Technology Development for Lower East Fork Poplar Creek*. ORNL/SPR-2014/645, Oak Ridge National Laboratory, Oak Ridge, TN.

Peterson, M. J., et al. 2015b. *East Tennessee Technology Park Biological Monitoring and Abatement Program 2014 Calendar Year Report*. ORNL/SPR-2015/43, Oak Ridge National Laboratory, Oak Ridge, TN.

Peterson, M. J., et al. 2016. *Mercury Remediation Technology Development for Lower East Fork Poplar Creek—FY 2015 Progress Report*. ORNL/TM-2016/48, Oak Ridge National Laboratory, Oak Ridge, TN.

Pham, A. L. T., et al. 2014. "Precipitation of nanoscale mercuric sulfides in the presence of natural organic matter: Structural properties, aggregation, and biotransformation." *Geochimica Et Cosmochimica Acta* 133: 204–215. doi: 10.1016/j.gca.2014.02.027.

Reedy, O. C., et al. 1996. "Quantifying the diffusive mass transfer of nonreactive solutes in columns of fractured saprolite using flow interruption." *Soil Science Society of America Journal* 60 (5): 1376–1384.

Riscassi, A., C. Miller, and S. Brooks. 2016. "Seasonal and flow-driven dynamics of particulate and dissolved mercury and methylmercury in a stream impacted by an industrial mercury source." *Environ. Toxicol. Chem.* 35 (6): 1386–1400. doi: 10.1002/etc.3310.

Southworth, G., et al. 2013. "Sources of Mercury in a Contaminated Stream—Implications for the Timescale of Recovery." *Environmental Toxicology and Chemistry* 32 (4): 764–772. doi: 10.1002/etc.2115.

Stoor, R. W., et al. 2006. "Subsurface sources of methyl mercury to Lake Superior from a wetland-forested watershed." *Science of the Total Environment* (368): 99–110.

Tsui, M. T. K., and W.-X. Wang. 2004. "Maternal transfer efficiency and transgenerational toxicity of methylmercury in Daphnia magna." *Environmental Toxicology and Chemistry* 23: 1504–1511. doi: 10.1897/03-310.

US Department of Energy. 2014. *Mercury Technology Development Plan for Remediation of the Y-12 Plant and East Fork Poplar Creek*. DOE/ORO-2489.

Ward, D. M., et al. 2010. "Rapid, Efficient Growth Reduces Mercury Concentrations in Stream-Dwelling Atlantic Salmon." *Transactions of the American Fisheries Society* 139 (1): 1–10. doi: 10.1577/T09-032.1.

Worthington, M. J. H., et al. 2017. "Laying Waste to Mercury: Inexpensive Sorbents Made from Sulfur and Recycled Cooking Oils." *Chemistry*. doi: 10.1002/chem.201702871.